

AD-A047 096

TEXAS A AND M UNIV COLLEGE STATION DEPT OF OCEANOGRAPHY
GULF OCEANOGRAPHY-GULF STREAM STUDY (GUSS). (U)

F/G 8/3

SEP 77 A D KIRWAN

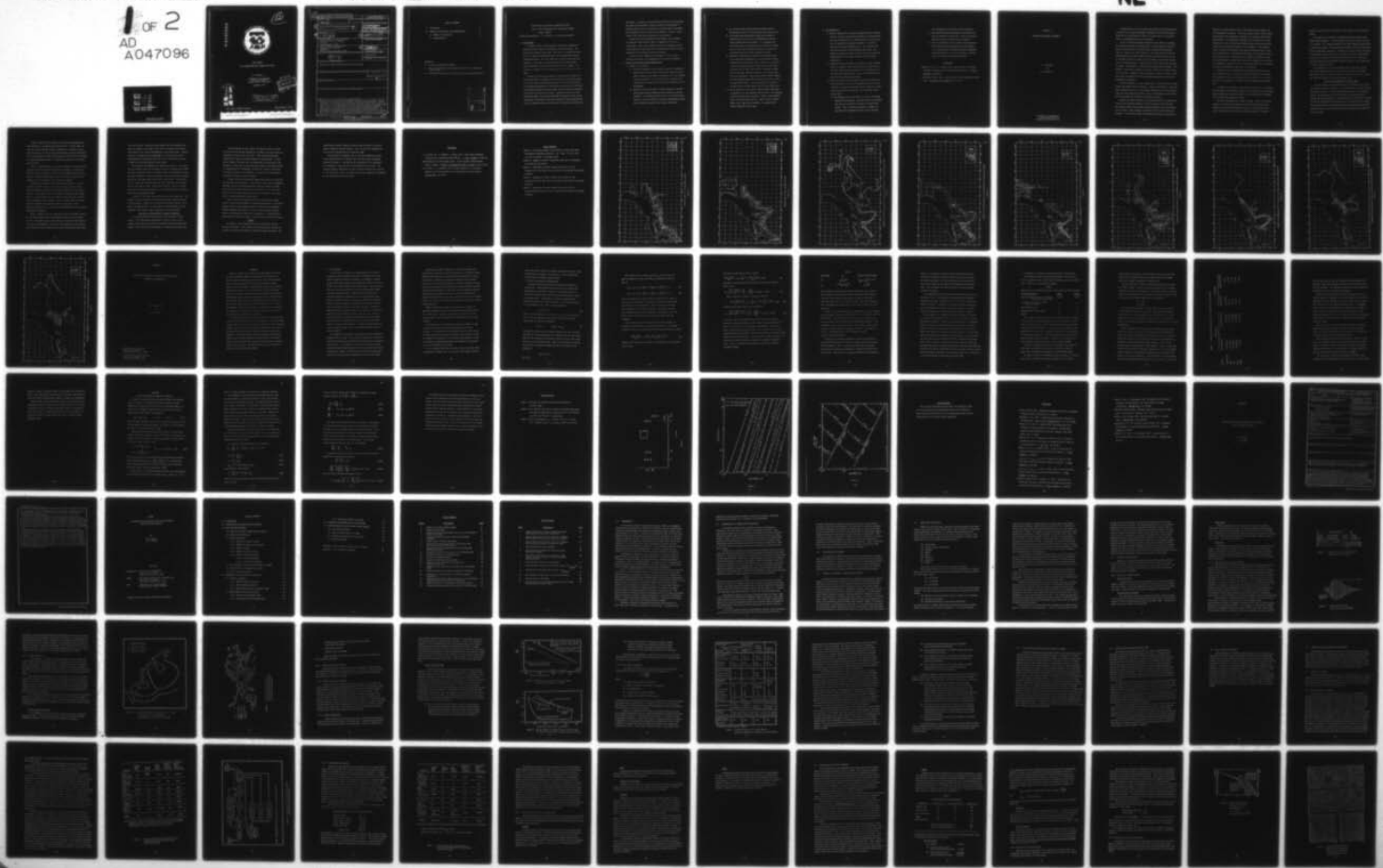
N00014-75-C-0537

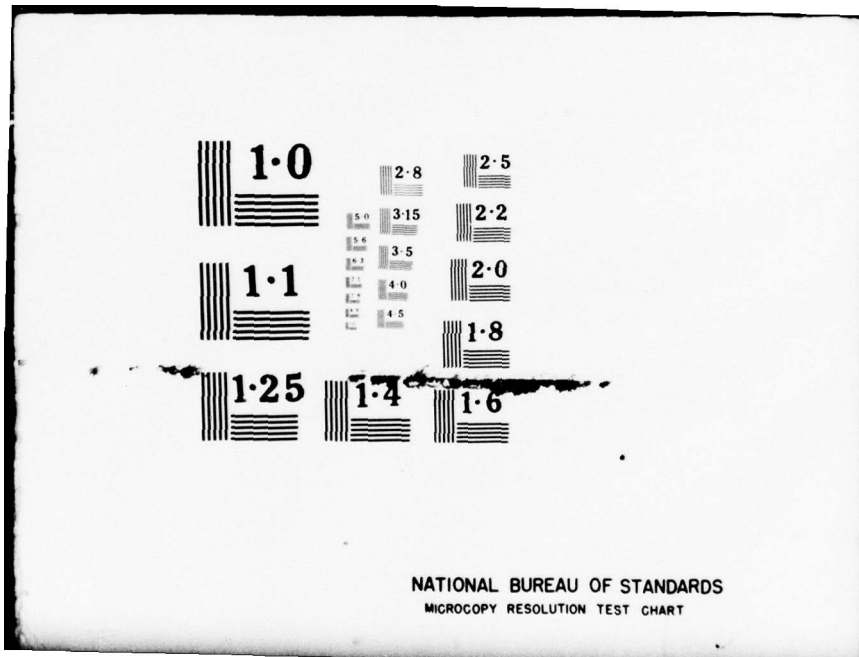
UNCLASSIFIED

TAMU-REF-77-3-F

NL

1 of 2
AD
A047096





AD AU 47096

12
SC



FINAL REPORT

GULF OCEANOGRAPHY-GULF STREAM STUDY (GUSS)

A. D. Kirwan, Jr.

Department of Oceanography
Texas A&M University
College Station, Texas 77843

September 1977

DDC
Received
NOV 22 1977
F
JG

DISTRIBUTION STATEMENT A

Approved for public release;
Distribution Unlimited

AD No. 1
1000 FILE COPY

ONR Contract N00014-75-C-0537

TAMU Reference 77-3-F

TEXAS A&M UNIVERSITY

COLLEGE OF GEOSCIENCES

(14)

SECURITY CLASSIFICATION OF THIS PAGE (Other Data Entered)

TAM

U-REF- REPORT DOCUMENTATION PAGE

READ INSTRUCTIONS
BEFORE COMPLETING FORM

1. REPORT NUMBER 77-3-F	2. GOVT ACCESSION NO.	3. RECIPIENT'S CATALOG NUMBER
4. TITLE (and Subtitle) GULF OCEANOGRAPHY-GULF STREAM STUDY (GUSS)		5. TYPE OF REPORT & PERIOD COVERED 9 1/1/76-5/31/77 Final Report
6. AUTHOR(s) A. D. Kirwan, Jr		7. PERFORMING ORG. REPORT NUMBER 1 Jan 76-31 May 77
8. CONTRACT OR GRANT NUMBER(s) ONR N00014-75-C-0537		10. PROGRAM ELEMENT, PROJECT, TASK AREA & WORK UNIT NUMBERS
9. PERFORMING ORGANIZATION NAME AND ADDRESS Texas A&M Research Foundation FE Box H College Station, Texas		11. REPORT DATE Sept 1977
11. CONTROLLING OFFICE NAME AND ADDRESS Office of Naval Research NORDA/NSTL Bay St. Louis, Mississippi 39520		13. NUMBER OF PAGES 48 (Appendix C - 72)
14. MONITORING AGENCY NAME & ADDRESS (if different from Controlling Office) 12 126p.		15. SECURITY CLASS. (of this report) Unclassified
16. DISTRIBUTION STATEMENT (of this Report) Approved for public release; distribution unlimited.		15a. DECLASSIFICATION/DOWNGRADING SCHEDULE
17. DISTRIBUTION STATEMENT (of the abstract entered in Block 20, if different from Report)		D D C DRAFTED NOV 22 1977 DISTRIBUTED
18. SUPPLEMENTARY NOTES		
19. KEY WORDS (Continue on reverse side if necessary and identify by block number)		
20. ABSTRACT (Continue on reverse side if necessary and identify by block number) This is the final report of a feasibility study of a western boundary current experiment which would use free drifting, drogued buoys (drifters). A pilot experiment in the Kuroshio demonstrated that drifters stay in the strong current region long enough to determine all of the required kinematic parameters. In these regions a theoretical error analysis showed that positions should be determined approximately hourly with an accuracy to within 450 meters. In an investigation of possible position fixing systems that could meet this requirement, it was concluded that the LORAN-C system with a telemetry link through		

TABLE OF CONTENTS

I. Introduction	2
II. Summary of Conclusions and Recommendations	3
A. Summary of Conclusions	3
B. Recommendations	5

Appendices

- A. Tracking the Kuroshio by Nimbus 6
- B. Effect of Sampling Rate and Random Position Error on Analysis of Drifter Data
- C. A Drifting Buoy System for the Study of Western Boundary Currents

ACCESSIONED	
NTIS	Wise Section <input checked="" type="checkbox"/>
DDC	B-ff Section <input type="checkbox"/>
UNANNOUNCED <input type="checkbox"/>	
JUSTIFICATION	
BY	
DISTRIBUTION/AVAILABILITY CODES	
ORIGINATOR'S L. and/or SPECIAL	
A	

Final Report on ONR Contract N00014-75-C-0537

Title: Gulf Oceanography-Gulf Stream Study (GUSS)

Project 3200A-6

Principal Investigator: A. D. Kirwan, Jr., Texas A&M University

I. Introduction

In 1975 the Office of Naval Research initiated a theoretical and observational study of the dynamics of the Gulf Stream. Two phases were planned for the study. The first, or feasibility phase, was to be conducted during 1975-1978 with the observational phase commencing in 1979. The first phase has a technical and scientific component. The former is being conducted by the Charles Stark Draper Laboratory, Inc. under the direction of W. A. Vachon. The scientific component is the responsibility of A. D. Kirwan, Jr. of TAMU.

Because of the successes reported by Kirwan *et al.*, (1976) and Richardson (1976) in tracking the Gulf Stream and Gulf Stream rings, it was felt that the primary observational tool of the study would be Lagrangian measurements of trajectories, velocities, accelerations, differential kinematic properties (DKP) such as horizontal divergence and vorticity and Reynolds stresses. During the first year of the feasibility phase, the A&M group performed an analysis of the errors accruing in calculations of the above quantities from random position error of Lagrangian drifters and the rate from which the position was

determined. In addition, some preliminary field work was undertaken. The Draper group performed a study of position fixing systems to determine which, if any, could meet the accuracy goals as specified by the analyses, and yet still be cost effective. This is a final report of the first years activities on this project.

The details of the preliminary field studies, error analysis, and position fixing study are given in appendices A, B, and C, respectively. Part of the research described in appendices A and B was supported by the Office for the International Decade of Ocean Exploration of the National Science Foundation.

The next section summarizes the findings of each of these studies and presents our recommendations for future developments.

II. Summary of Conclusions and Recommendations

A. Summary of conclusions

- 1) The pilot experiment in the Kuroshio described in Appendix A demonstrated that the drifters stay in the region of strong flowing currents long enough to determine all of the required kinematic parameters. The trajectories and velocities obtained from the drifters are in excellent agreement with the hydrography.
- 2) Appendices B and C show that reliable estimates of the DKP and Reynolds stresses depend upon the accuracy of velocity estimates. For strong currents such as the Gulf Stream and Kuroshio, positions should be determined approximately hourly with a position accuracy of the order of 450 meters.

- 3) The position fixing system should be designed around minimizing the error in velocity rather than acceleration.
- 4) The Random Access Measurement System onboard Nimbus 6 represents the state of the art technology for position fixing systems and data telemetry. It is adequate for describing scales of variability of the order of 24 hours, thus, it can provide reliable estimates of velocity and acceleration but not for DKP and Reynolds stress.
- 5) Appendix C breaks down the problem of specifying a position fixing system adequate for a strong boundary current kinematics into two distinct parts. One part is a specification of the position fixing system based on positional accuracy, rate at which fixes could be determined, weight and cost per buoy, and coverage area. The following systems were considered: RAMS onboard TIROS N, OMEGA, LORAN-C, the Navy Navigation Satellite System, (NNSS) and the Global Position System (GPS). From the standpoint of position accuracy alone, the GPS appears best with the LORAN-C next.
- 6) The second part of the position fixing problem considered in Appendix C was the telemetry and data link. The following telemetry systems were considered: TIROS N, GOES, MARISAT, ATS-5, and an HF telemetry link. Based on power requirements, cost, range, and reliability, it appears that a TIROS N telemetry link is best.

B. Recommendations

- 1) The best combination of position fixing system and telemetry link for a study of small-scale variability in strong boundary currents appears to be a LORAN-C position fixing system with a telemetry link through the TIROS N. The cost is expected to be about \$6,000 per unit. This includes hull costs and batteries for approximately thirty days. The LORAN-C was picked over GPS because of the GPS schedule and uncertainties in user costs, hardware costs, and power consumption.
- 2) Appendix C briefly describes the problem of drogue slippage errors of drifters. The conclusion was that there were no firm data which reliably correlates the buoy motions with the effects of winds and waves. It is recommended that the study of these effects be initiated.
- 3) After the experience with Japanese institutions during the pilot experiment, it is our recommendation that it is cost effective to conduct the boundary current study in the Kuroshio rather than the Gulf Stream. The following reasons dictate this:
 - a) The Japanese have in existence an extensive monitoring program of the Kuroshio. They seem anxious to cooperate with American scientists interested in studying this current. Thus, it would be possible to conduct the experiment with Japanese facilities and no shiptime

cost obligations to the Office of Naval Research.

- b) The extensive monitoring program of the Kuroshio has been in existence for many years. Such an historical data base does not exist for the Gulf Stream.
- c) Once the feasibility of the position fixing and data relay system has been demonstrated to the Japanese, it is expected that the Japan Hydrographic Department would underwrite the cost of the drifters, resulting in further savings to the American effort.

References

Kirwan, A. D., Jr., G. McNally and J. Coehlo, 1976: Gulf Stream Kinematics Inferred from a Satellite-Tracked Drifter. J. Phys. Oceanog., 6, 750-755.

Richardson, Philip, 1976: Tracking a Gulf Stream Ring with an NDBO Buoy. Data Buoy Tech. Bulletin, Vol. 2, No. 4.

Appendix A

TRACKING THE KUROSHIO BY NIMBUS 6

A. C. Vastano

and

A. D. Kirwan, Jr.

Department of Oceanography
Texas A&M University
College Station, Texas 77843

During February, 1977, we had the opportunity of participating with scientists of the Japan Hydrographic Department and the Ocean Research Institute of the University of Tokyo in a pilot study of the Kuroshio. This is a preliminary report of our efforts.

As one of the major Western Boundary Currents (WBC), the Kuroshio has long been an object of intense study. In many respects, the Kuroshio is quite similar to the Gulf Stream, another well-studied WBC. There is, however, one major difference. The Gulf Stream has only one preferred path as it flows along the eastern seaboard of the U.S., but in the region south of the main island of Honshu, the Kuroshio follows one of two possible paths. One path follows quite closely the coastline of Honshu. In the other, a large meander develops south of Honshu. This meander is believed to extend as far south as 30°N or about 300 km from the other path. Examples of these two paths are shown in figure 1 which were taken from bulletins that are distributed regularly by the Japan Hydrographic Department.

When the Kuroshio is in its meander mode, a cold water mass develops between the meander and the coastline. South of the meander, a warm core eddy is believed to exist. This meander circulates some of the Kuroshio water with the subtropical counter current system (Rikiishi and Yoshida, 1974) and perhaps the Kuroshio itself south of Kyushu.

Because the strong currents of the Kuroshio have such a significant effect on the shipping industry, and the intrusion of the cold water mass greatly affects the fishing industry and weather over the northern part of Honshu, Japan expends a considerable effort in monitoring the Kuroshio. This includes almost continuous ship surveys by such diverse

agencies as Japan Fisheries Agency, Japan Meteorological Agency, and the Hydrographic Department. These ship surveys include closely spaced XBT stations, some hydrographic stations, and continuous underway GEK measurements. The Hydrographic Department is responsible for assimilating all of the data from these diverse sources and producing a bulletin on the location and intensity of the Kuroshio. This bulletin comes out every other Saturday and includes observations made as late as the previous day. Figuring conservatively, over six-hundred days of ship time per year are allocated by the Japanese government for monitoring the Kuroshio. Despite this effort, the Japanese feel that there are significant scales of motion of the Kuroshio which are not detected by either the frequency or the scale of the surveys.

Because one of us had previously successfully tracked the Gulf Stream (Kirwan, et al., 1976) by the Nimbus 6 satellite, the Japanese were anxious to test this technique with the Kuroshio. Thus, we were invited to participate in a cooperative pilot experiment in February, 1977.

We deployed four drifters, each drogued at 100 m by a 9.2 m personnel parachute, off the island of Kyushu. The deployments were made from the R/V TAKUYO which was made available by the Hydrographic Department of the Marine Safety Agency of Japan.

This pilot experiment had a number of goals. First, we wished to compare the results of the drifter tracks and velocities with that obtained by GEK and the hydrographic surveys. The second goal was to verify the existence of the cold and warm water eddies. The third

objective was to study the variability of the currents in the extension region.

The drifters are tracked by the Random Access Measurement System (RAMS) onboard Nimbus 6. A brief summary of the way the system operates is as follows: The transmit terminal in the buoy transmits approximately 1 second every minute. The transmission contains a four-digit identifier and four eight-digit data words. Actually, the system has the capability of transmitting eight data words, four words in alternate transmissions. The data are recorded by the satellite during the fly-by (~ 20 min.). The buoy positions are determined by Doppler shifts of the transmissions occurring during the fly-by.

The satellite is in a sun-synchronous polar orbit which crosses the equator northward bound at local noon and southward at midnight. The orbital period is about 107 minutes. Each orbit crosses the equator 27° longitude further west than the previous orbit.

Discussion of Trajectories West of 140° E

The four drifters were deployed along a line normal to the axis of the Kuroshio just east of Honshu. The trajectories up to Julian day 110 are shown in figure 2. Drifter 106 was deployed just to the landward side of the high speed core of the Kuroshio as determined by GEK. Drifter 130 was deployed just to the seaward side of this core. Drifters 307 and 341 respectively were deployed out on the flank of the current. The deployment scheme was selected with the expectation that 106 would break off into the cold core eddy and that 341 would peel off into the warm core eddy.

Figure 2 shows that the drifters all moved at approximately the same velocity (2 - 2½ knots) until Julian day 54. At that time, 341 took off to the southeast along the meander axis. However, as indicated in figure 2, it did not leave the Kuroshio as we had anticipated. At the other extreme was 106, which from day 56 to day 60 was entrained in a small anticyclonic eddy. It rejoined the main flow of the Kuroshio on day 62.

This is a puzzling result. The model of White and McCreary (1976) suggests that 106 should have undergone the greatest acceleration as the flow enters the meander and that 341 would exhibit the least acceleration. Instead, there appears to be an area of stagnation on the northern part of the Kuroshio as it starts the meander.

Examination of figure 2 shows that the trajectories of all four drifters, along the eastern flank of the meander, are quite close, even though there is as much as eleven days difference in the time of traverse. This supports the view of Japanese scientists that during days 47 - 59 the meander was in an extreme western position, and that it was beginning to move eastward. Thus, in eleven days the western part of the current could have moved 20 km to the east. Such east-west migrations of the meander are well documented in the Japanese oceanographic literature.

Figure 3 compares the four trajectories with the Japanese analysis of the current location and the temperature field at 100 m for days 47 - 59. The dashed lines in these figures are areas in which there is a paucity of hydrographic or GEK data. The agreement with the current chart generally is quite good with only minor discrepancies where there

is a lack of data. Note that on the western leg of the meander, two days are missing in the track of 307, thus the straight line between date points is not a good representation of the actual track. Finally, there is no evidence in the hydrographic or current charts of the anticyclonic eddy detected by 106, but it is of such small scale that it might not have been detected by the survey.

Data from days 60 through 74 are compared in figure 4. Up to the time the drifters reach the Izu Ridge, which runs southward along 140°W , the 100 m temperature field, the current chart, and trajectories are in excellent agreement. It was encouraging to note that 307 went straight through the Izu Ridge right in the core of the current. The track of 130 as it peels off from the main flow east of the ridge is also indicated in the current chart. Drifter 341, after it reaches the ridge, enters an anticyclonic eddy which is not inconsistent with the surface flow field as determined by GEK.

For days 75 - 90, only 106 and 341 remain in the survey area. The latter is seen in figure 5 to be following the main current axis east of the Izu Ridge. Drifter 341 drifted slowly southward (about .1 kt.) until it reached $30^{\circ} 30'$. At this point it turned eastward and then northward. This track is quite consistent with the GEK survey.

Discussion of Trajectories in Kuroshio Extension

It is well known that the flow east of the Izu Ridge is quite complex. Data from numerous hydrographic surveys indicate a very complicated structure of the dynamic topography with rapid large-scale changes. Ocean fronts and large eddies are conspicuous features here.

The trajectories in this region (see figure 2) attest to this.

Drifters 307 and 130 came through the Izu Ridge at the same point but separated in time by about five days. Their initial tracks upon departing the ridge are nearly identical to latitude 148° . At this point, however, 130 broke off in a large warm core eddy north of the Kuroshio. Drifter 307, on the other hand, follows a wave-like pattern to approximately 151° longitude, at which time it did an about-face and started flowing to the southwest. On day 95 it turned abruptly northward and then on day 105 eastward.

Drifters 106 and 341 have been moving slowly just to the south of the mean axis of the Kuroshio. They arrived in this area by completely different routes; 341 having performed an end run around the ridge, while 106 came shooting through the gap at $33^{\circ} 30'$. Since day 109, however, 341 has been following closely the trajectory of 307, except that it looped much further to the north.

A more detailed interpretation of these tracks cannot be made without concurrent hydrographic or infrared satellite data. The hydrographic data is being obtained through the North Pacific Experiment (NORPAX) TRANSPAC XBT program. It will be several months, however, before it is available to make such a comparison. It should also be noted that data from the drifters is still being received from ~~Nimbus~~ 6.

Summary

To summarize, the agreement between the trajectories and the surveys is excellent. Main features of the Kuroshio such as path and velocity are duplicated in both the drifter and survey data sets. The

trajectories, however, failed to detect either the warm or cold core eddies associated with the meander. Also, it was quite remarkable to find that 130 pinched off into a warm core ring.

From the Navy's standpoint, one of the most significant results is the demonstration of a (nearly) real time data return capability provided by Nimbus 6. The RAMS on this satellite has the capability of returning not only position but environmental data as well. The transmit terminal electronics are very reliable and draw very low power so that long-term, remote, and inexpensive sensing capability is possible now for operational use by the fleet.

References

A. D. Kirwan, Jr., G. McNally, J. Coehlo, 1976: Gulf Stream Kinematics
Inferred from a Satellite-Tracked Drifter. J. Phys. Oceanog. 6, 750-755.

Kunio Rikiishi and Kozo Yoshida, 1974: On the Kuroshio Countercurrent
South of Honshu. Records of Oceanographic Works in Japan, 12 (2), 31-43.

W. B. White, J. P. McCreary, 1976: On the Formation of the Kuroshio
Meander and its Relationship to the Large-Scale Ocean Circulation.
Deep-Sea Res., 23, 33-47.

Figure Captions

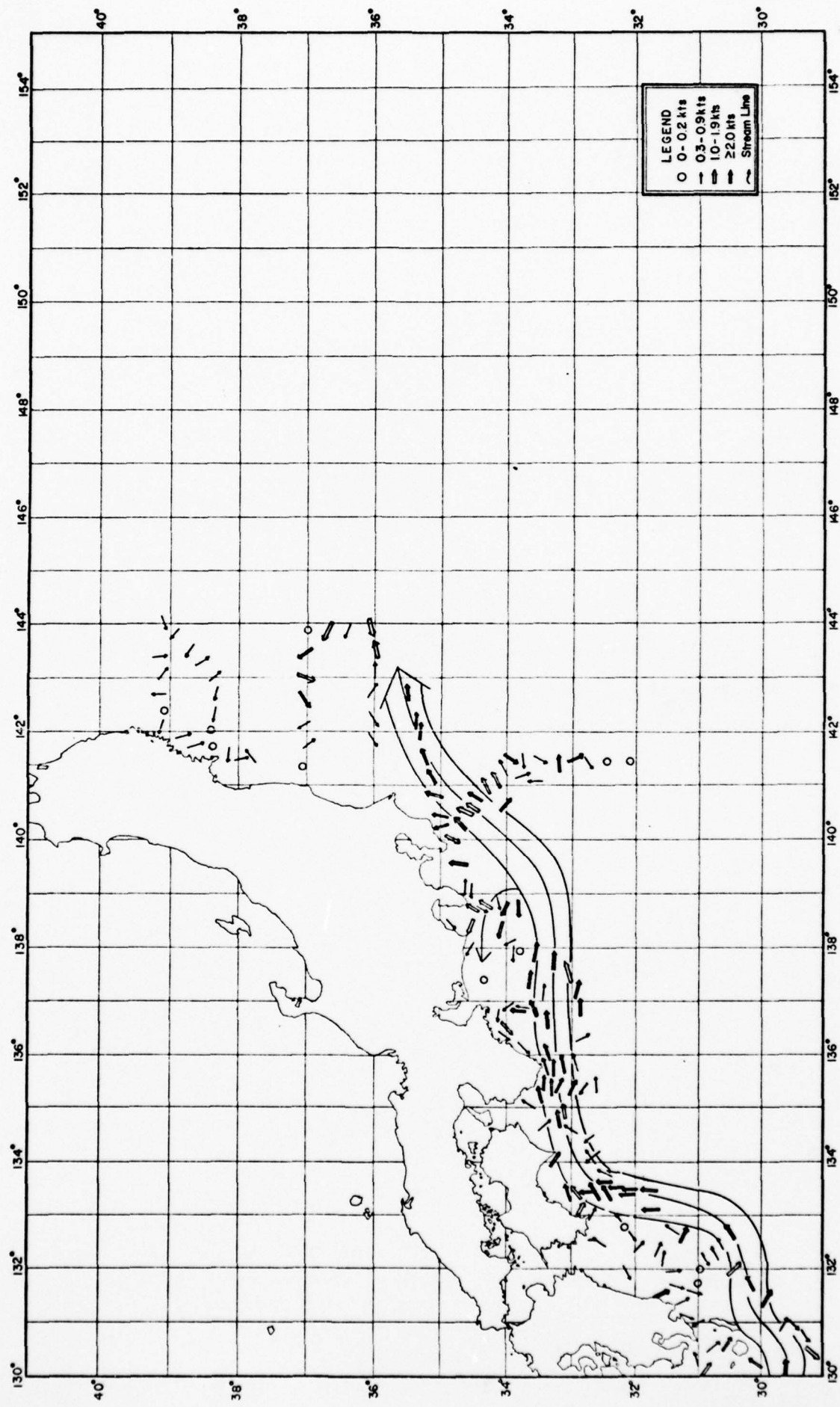
Figure 1 - Two possible paths of the Kuroshio as shown from Japan Hydrographic Department bulletins: (a) 1 June - 17 June, 1975
(b) from 1 December - 15 December 1975.

Figure 2 - Summary of drifter trajectories from time of deployment to Julian day 125 of 1977.

Figure 3 - Comparison of drifter tracks with current (a) and temperature (b) for days 47-59 as provided in Hydrographic Department bulletin.

Figure 4 - Comparison of drifter tracks with current (a) and temperature (b) for days 60-74 as provided in Hydrographic Department bulletin.

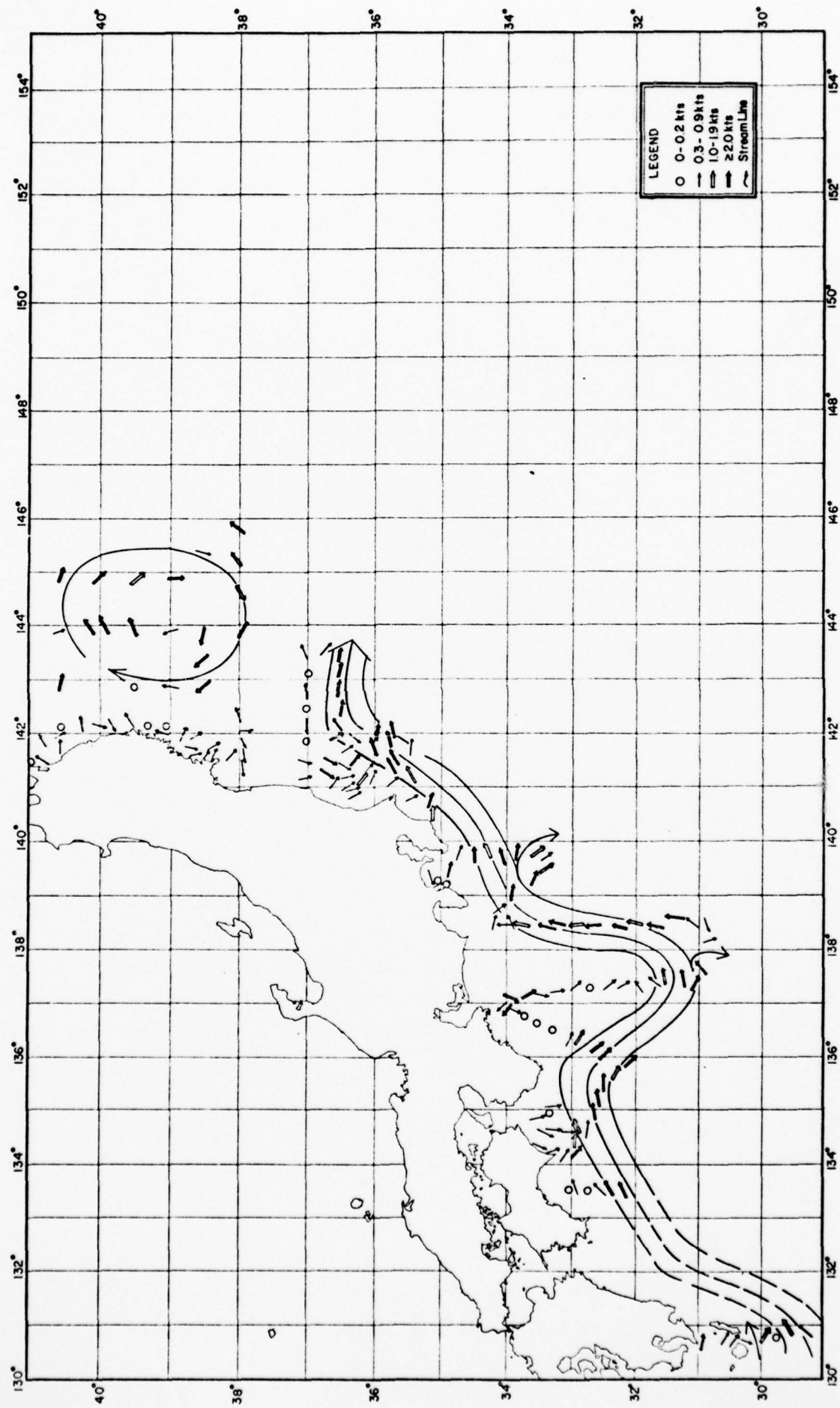
Figure 5 - Comparison of drifter tracks with current (a) and temperature (b) for days 75-90 as provided in Hydrographic Department bulletin.



A-10

Coastline path of the Kuroshio Current

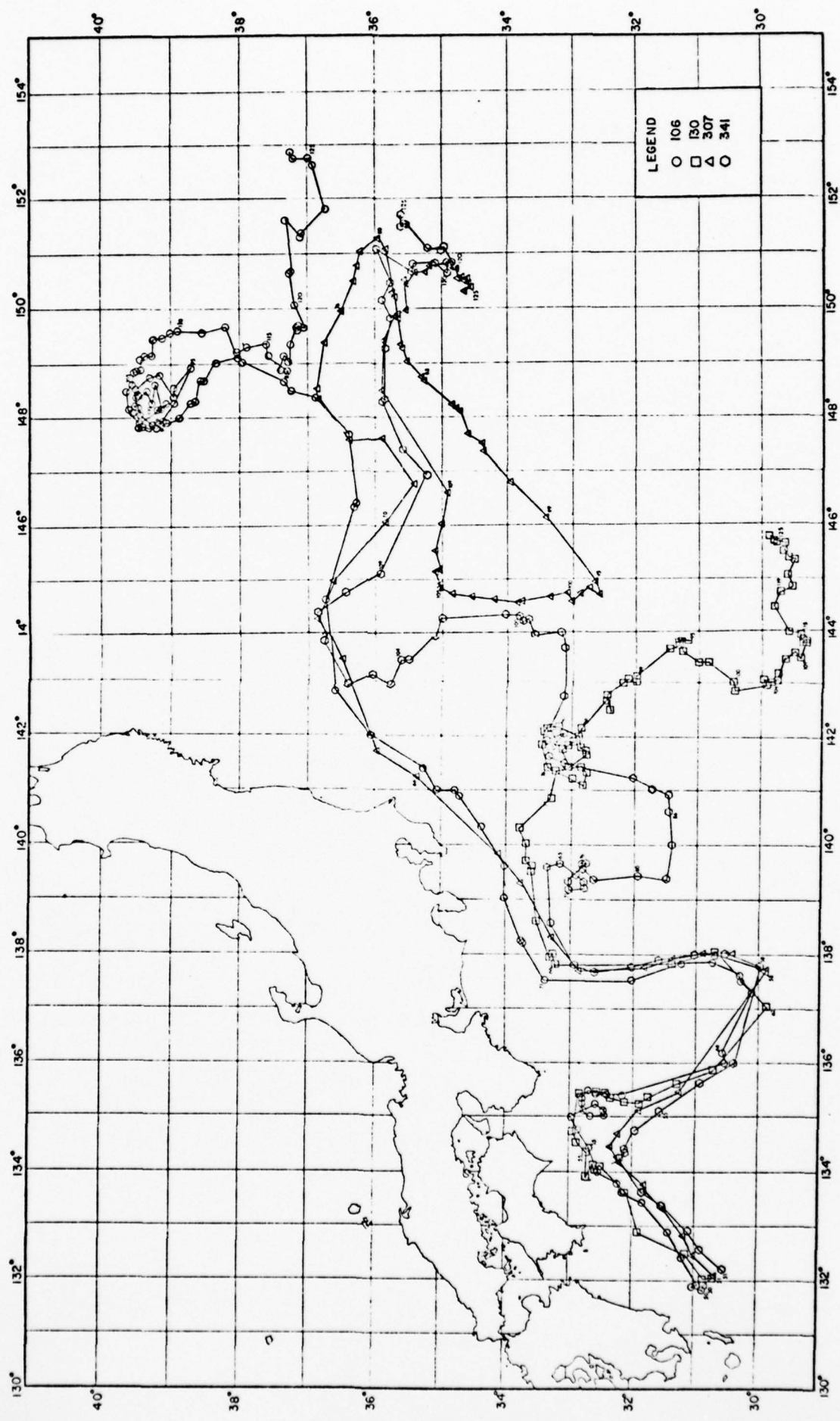
Figure 1A



A-11

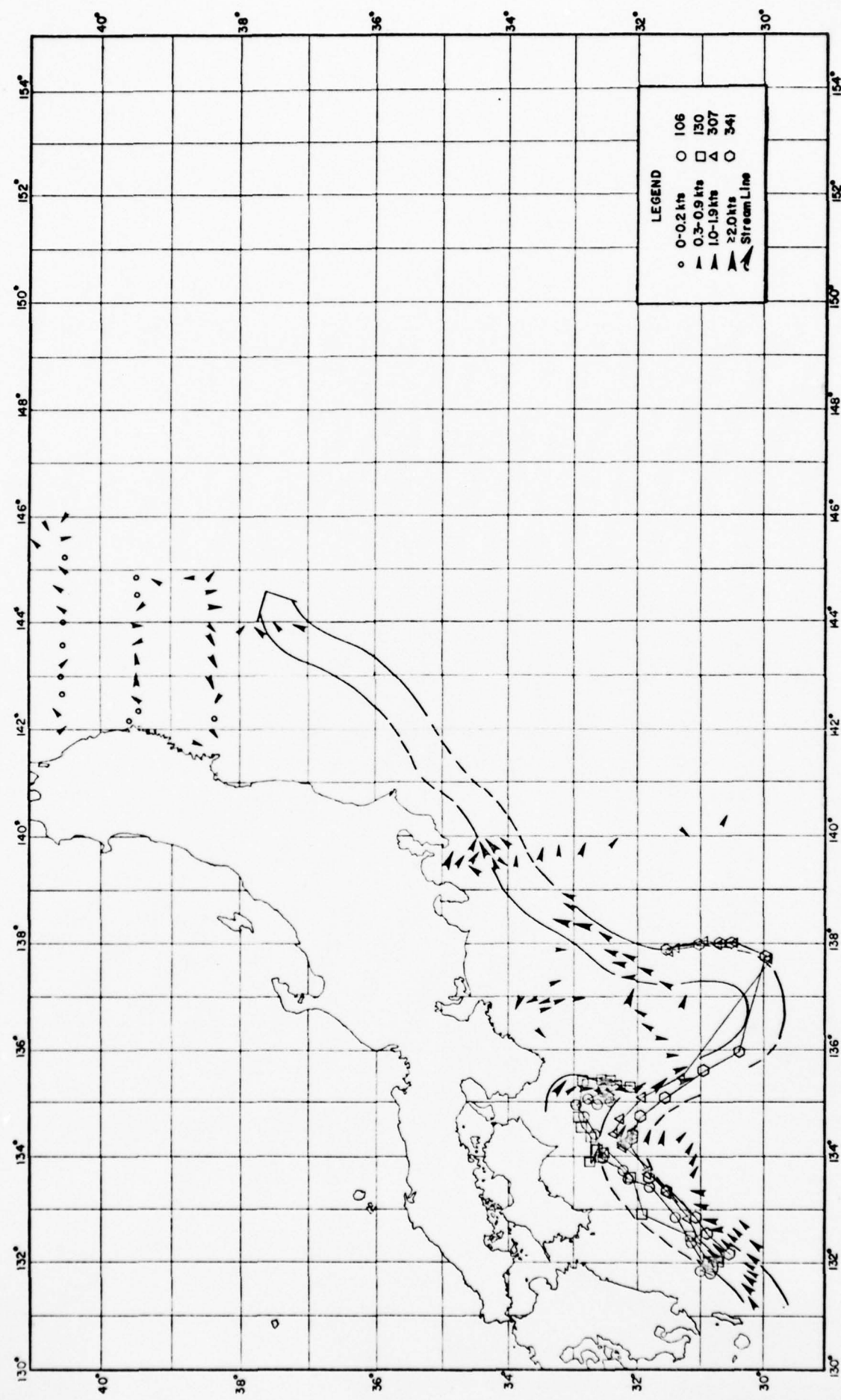
Meander path of the Kuroshio Current

Figure 1B



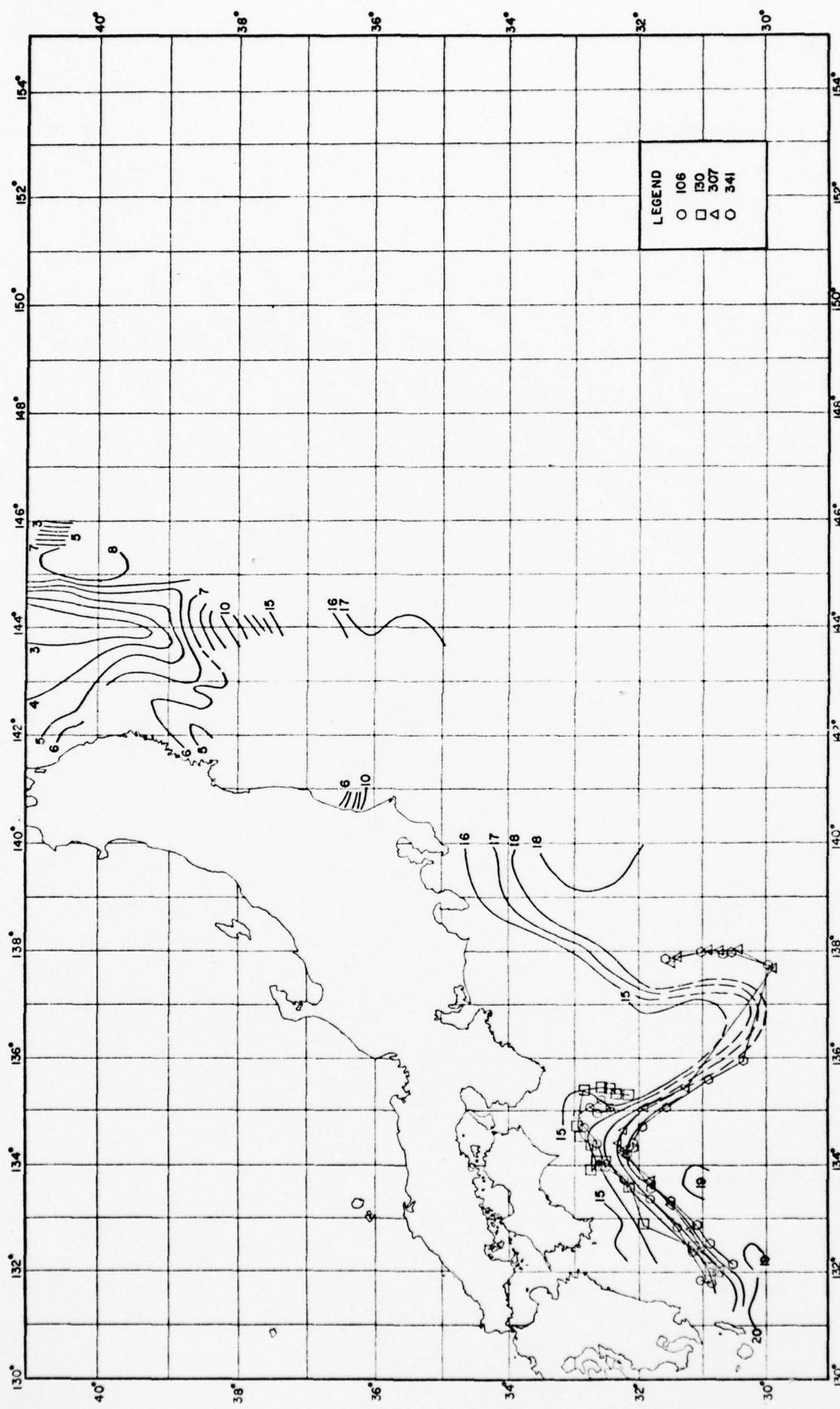
Summary of drifter trajectories from time of deployment to Julian day 125 of 1977

Figure 2



Summary of surface current for the time period Julian day 47 to 59.

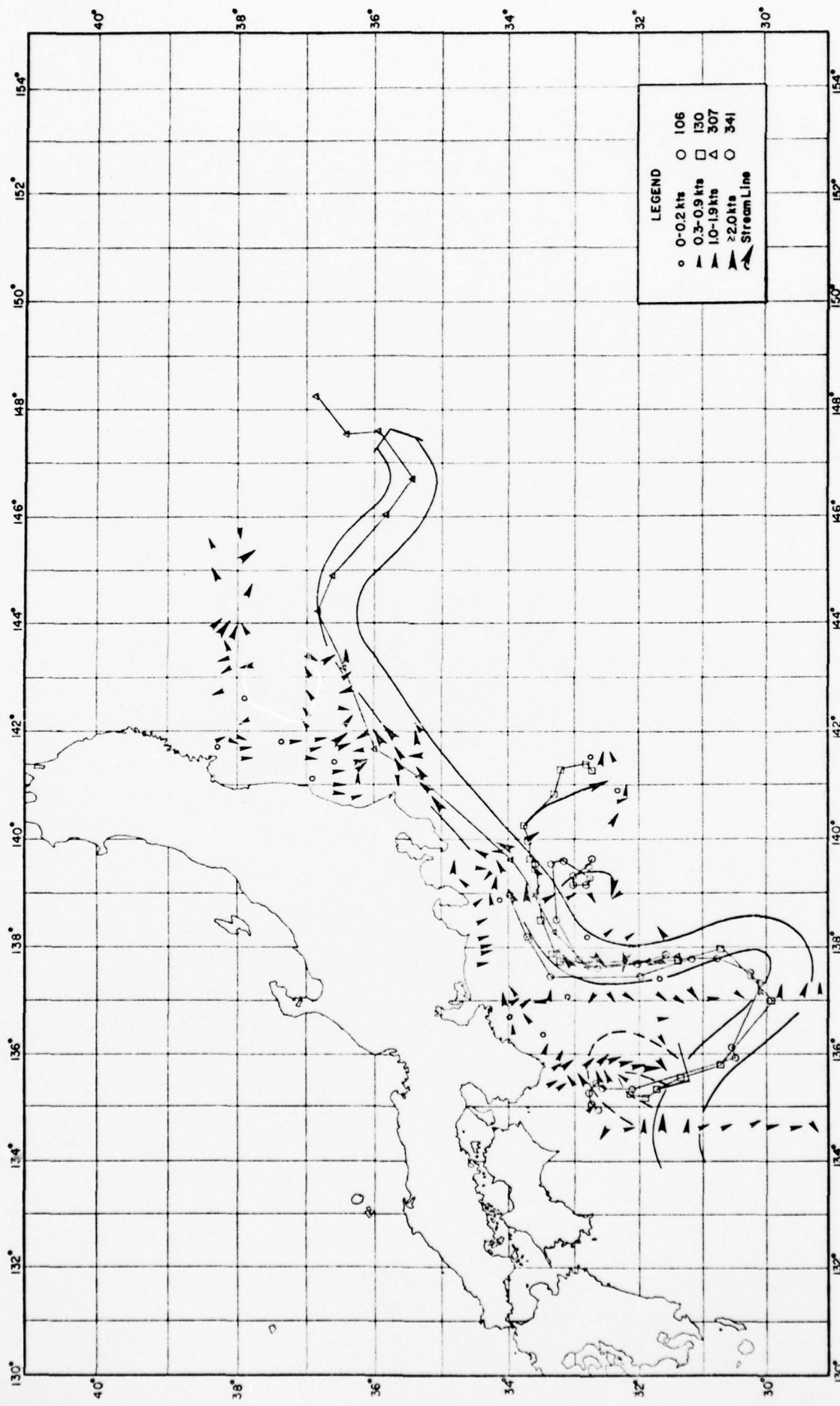
Figure 3A



Summary of temperature (°C) at 100m for the time period Julian day 47 to 59.

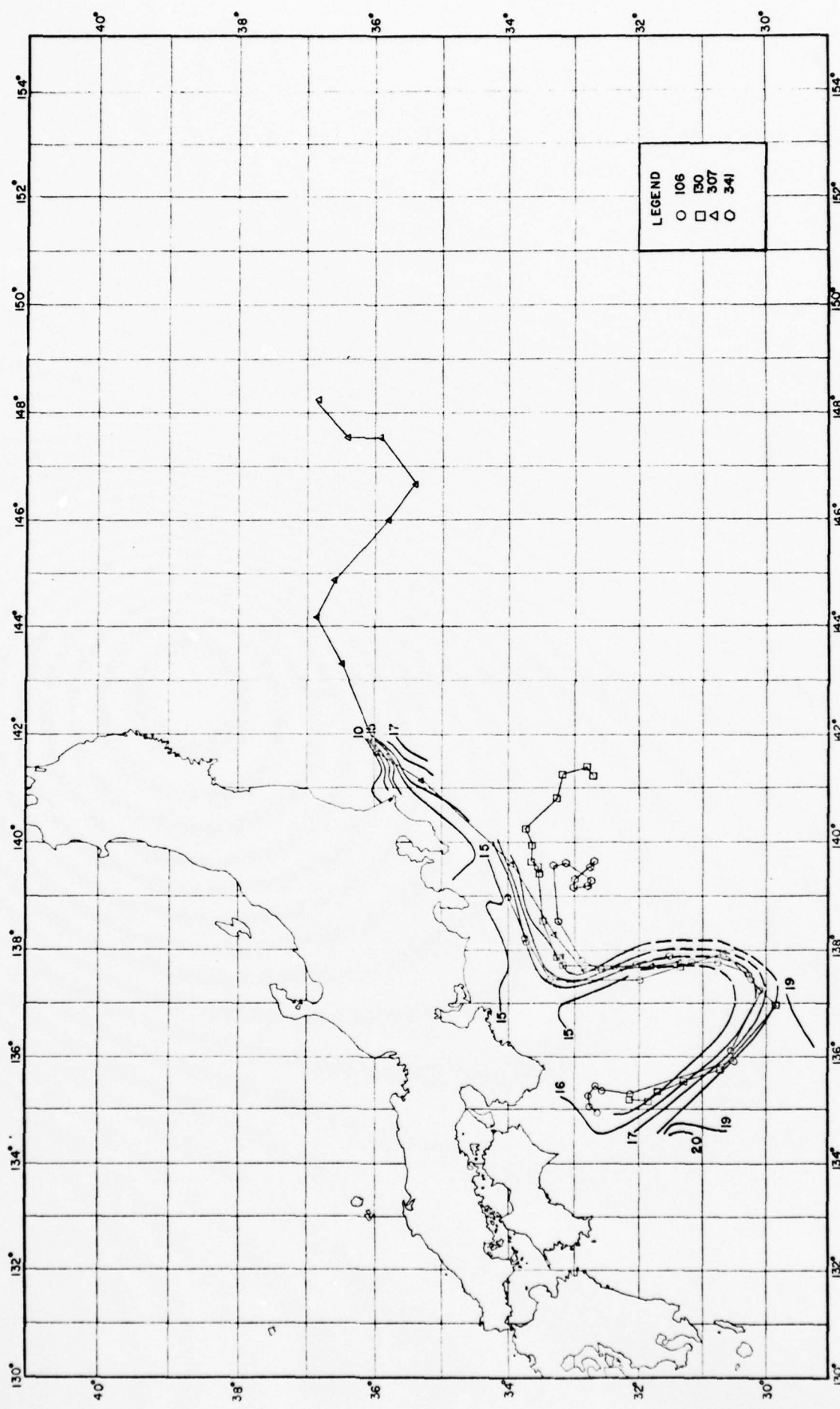
Figure 3B

A-14



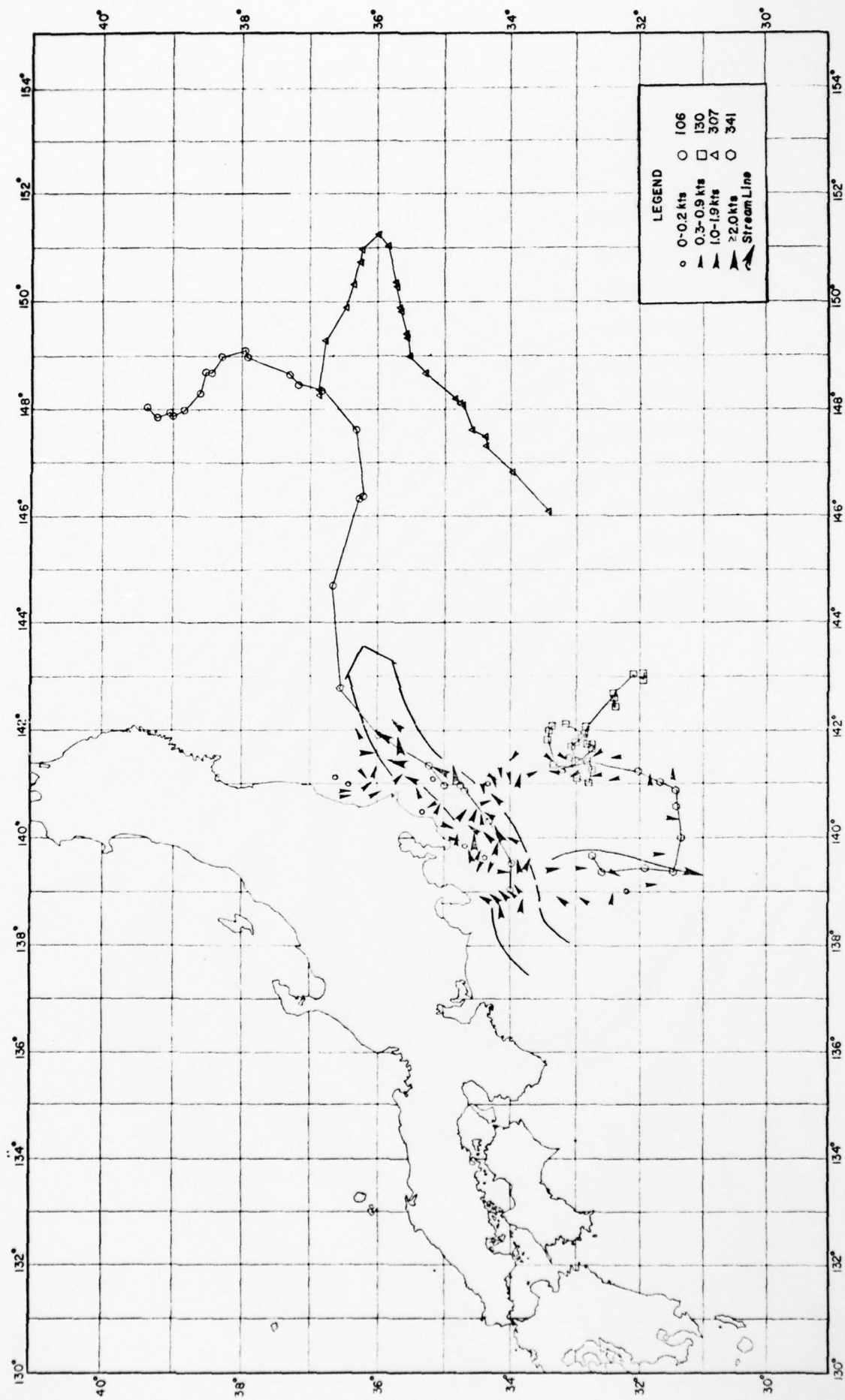
Summary of surface current for the time period Julian day 60 to 74.

Figure 4A



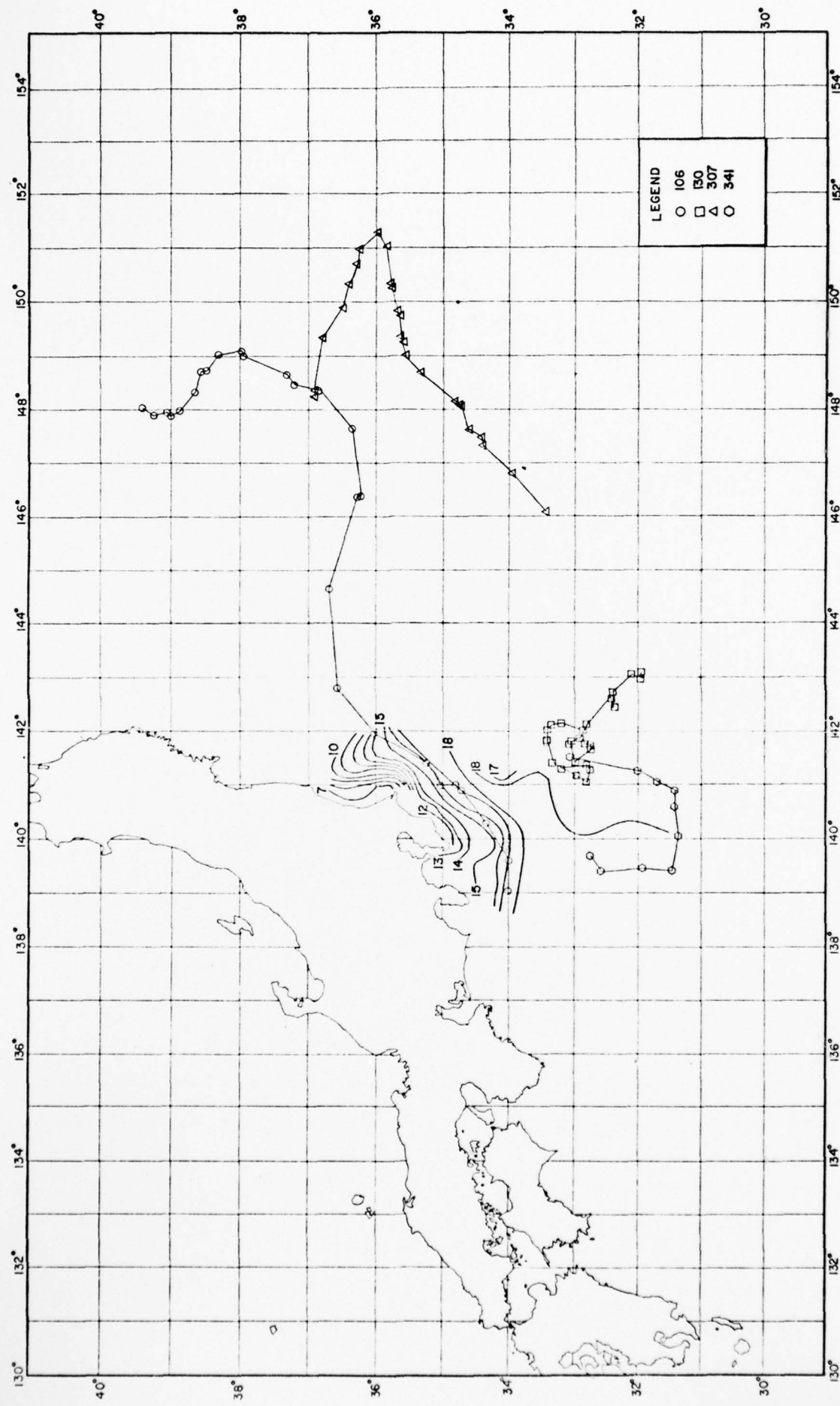
Summary of temperature (C°) at 100 m for the time period Julian day 60 to 74.

Figure 4B



Summary of surface current for the time period Julian day 73 to 90.

Figure 5A



Summary of temperature (°C) at 100m for the time period Julian day 73 to 90.

Figure 5B

Appendix B

EFFECT OF SAMPLING RATE AND RANDOM POSITION ERROR ON
ANALYSIS OF DRIFTER DATA

A. D. Kirwan, Jr.¹

and

M.-S. Chang²

1 Department of Oceanography
Texas A&M University
College Station, Texas 77843

2 Naval Ship Systems Research and
Development Center
Carderock, Maryland 20084

ABSTRACT

This is a report of the effect of random position error and the rate of position fixing on the inference of velocity and acceleration from drifter trajectory data. The analysis focuses on the relation between these two system parameters and the natural ocean time scales. Direct effects of ocean space scales, however, are ignored. It is shown that for a given time scale there is an optimum combination of position fixing sampling rate and position error. As intuitively expected, the limiting factor for sampling rates higher than the optimum is position error. A more serious problem arises when the sampling rate is less than the optimum. Then it is shown that the limiting effect on errors in velocity and acceleration is aliasing by ocean motions with time scales less than the sampling rate.

The analysis results are used to evaluate four position fixing systems previously reported in the literature, as well as the ARGO system, which will be in use during the First Garp Global Experiment (FGGE). This shows the Over the Horizon Radar (OHR) system to be the least effective and local tracking by radar to be the most effective. The Random Access Measurement System (RAMS) and Eole appear to be reasonable compromises between these two extremes; however, there are some ocean time scales which cannot be investigated by these systems. The ARGO system will be a significant advance over these last two systems.

1. Introduction

A recent area of interest in oceanography has been the description of the horizontal scales of the velocity field of the ocean through observations of drifters. For example, Freeland et al. (1975) have presented some intriguing results of deep flow in the western North Atlantic from Sofar floats. Earlier work in this area has been performed by Swallow and Worthington (1961) and Rossby and Webb (1971). Dickson and Baxter (1972) and Cresswell (1976) have reported some current observations from satellite-tracked drifters. Kirwan et al. (1976) and Richardson (1976) also have employed this technique for studying the Gulf Stream and cyclonic eddies in the North Atlantic. Kirwan and McNally (1975) used Stanford Research Institute Over the Horizon Radar (OHR) for studying the North Pacific Current. Molinari and Kirwan (1975) determined the differential kinematic properties (DKP) in the vorticity balance in the Yucatan Current by the use of radar-tracked drifters. A similar technique has been used by Stevenson et al. (1974) in studying upwelling off the coast of Oregon.

The studies cited above have determined a number of kinematic properties of the ocean. These include trajectories, velocities, Coriolis and inertial accelerations and the DKP such as divergence and vorticity. The sampling rate and position accuracy of the position fixing systems employed in the cited studies have varied tremendously. However, an analysis of how these characteristics affect the accuracy of the calculations has not yet been made.

Kirwan et al. (1976) estimated the accuracy of estimates of velocity and acceleration from the Random Access Measurement System (RAMS) by regarding successive position measurements as a random time series in which the position uncertainty σ is the standard deviation of the position measurement. Standard deviations for velocity and acceleration were obtained by familiar formulas for differencing random variables. Obviously, such an approach cannot be applied to flow in which there may be significant natural and regular variability whose time scales are comparable to the sampling period. An example is sinusoidal flow whose period is less than the sampling period.

Okubo and Ebbesmeyer (1976) have investigated a number of theoretical problems involved in estimating kinematic quantities from drifter data. However, the effects of position error and sampling rate on the calculations were outside the scope of their analysis.

The purpose here is to extend these last two studies so that effects of position error and sampling period are assessed properly. It is hoped that the analysis will result, not only in a better feel for the accuracy of previous calculations, but also as a guide for the design of new position fixing systems, as well as criteria for planning experiments to determine the horizontal scales of variability in the ocean.

It is recognized that there are other factors which may affect the quality of drifter data. For example, with surface drifters,

winds and surface currents can produce considerable errors in the trajectories and, perhaps, the velocities. These problems are treated elsewhere (Kirwan, et al., 1975).

2. Errors in velocity and acceleration

The basic kinematic information obtained from drifters is trajectories. Other kinematic properties such as velocity and acceleration are inferred. Typically, the trajectory data is obtained at discrete times with each position observation subject to a random error. A schematic of a typical trajectory with position error bars is shown in Figure 1. The observed position at t_i is denoted as X_i . This is decomposed into

$$X_i = Z_i + r_i \quad (1)$$

Here Z_i is the expected or true position, and r_i is the position error. For our purposes the position error will be taken as random with the following properties:

$$\overline{r_i} = 0, \quad \overline{r_i r_j} = \sigma^2 \delta_{ij} \quad (2)$$

Equation (2) asserts that the random position error has zero mean and that it is uncorrelated with the position error at other times. However, the variance of the position error at any one time is the same as it is at any other time. Also, for convenience it will be assumed that the position sampling interval is constant and is denoted by

$$t_{i+1} - t_i = \Delta$$

for all i .

The true position at times t_{i+1} and t_{i-1} can be given as a Taylor's Expansion in time about the true position at time t_i . This is

$$z_{i+1} = A_i + v_i \Delta + \frac{1}{2} A_i \Delta^2 + \frac{1}{3!} \dot{A}_i \Delta^3 + \frac{1}{4!} \ddot{A}_i \Delta^4 + \dots \quad (3)$$

$$z_{i-1} = z_i - v_i \Delta + \frac{1}{2} A_i \Delta^2 - \frac{1}{3!} \dot{A}_i \Delta^3 + \frac{1}{4!} \ddot{A}_i \Delta^4 + \dots \quad (4)$$

In these equations v_i is the velocity of the drifter at time t_i , and A_i is its acceleration. \dot{A}_i and \ddot{A}_i are the first and second derivatives of the acceleration. They are termed respectively jerk and quake. All of these quantities are evaluated at the true position (z_i) and not the observed. In practice, only estimates of these quantities at the observed positions (x_i) are available.

First consider the errors associated with the estimates of velocity and accelerations from individual drifters. A velocity estimate at time t_i is obtained from the centered difference formula

$$\frac{x_{i+1} - x_{i-1}}{2\Delta} = \frac{z_{i+1} - z_{i-1} + r_{i+1} - r_{i-1}}{2\Delta} \quad (5)$$

Equation (5) represents the average of the velocity in the interval t_{i-1} to t_{i+1} .

Inserting (3) and (4) into (5), we obtain

$$\frac{x_{i+1} - x_{i-1}}{2\Delta} = v_i + \frac{\dot{a}_i}{3!} \Delta^2 + \frac{r_{i+1} - r_{i-1}}{2\Delta} + 0(\Delta^4) \quad (6)$$

Squaring and averaging this last result gives the mean square velocity error:

$$E_v = \left(\frac{x_{i+1} - x_{i-1}}{2\Delta} - v_i \right)^2 = \frac{\dot{a}_i^2 \Delta^4}{(3!)^2} + \sigma^2/2\Delta^2 + 0(\Delta^6) \quad (7)$$

The acceleration estimate at time t_i is given by

$$\frac{x_{i+1} - 2x_i + x_{i-1}}{\Delta^2} \approx a_i + \frac{\ddot{a}_i}{12} \Delta^2 + \frac{r_{i+1} - 2r_i + r_{i-1}}{\Delta^2} + 0(\Delta^4) \quad (8)$$

Squaring and averaging this last result yields

$$E_a = \left[\frac{x_{i+1} - 2x_i + x_{i-1}}{\Delta^2} - a_i \right]^2 = \left(\frac{\ddot{a}_i}{12} \right)^2 \Delta^4 + 6\sigma^2/\Delta^4 + 0(\Delta^6) \quad (9)$$

It is seen from (7) and (9) that for small sampling periods the position error term dominates, and the errors are proportional to Δ^{-2} and Δ^{-4} for velocity and acceleration, respectively. This is the error assumed by Kirwan *et al.* (1976). On the other hand, for large sampling periods, the position error term is small, but the higher order terms in (3) and (4) dominate. Thus, for large Δ both errors go as Δ^4 . In both cases then there are Δ 's which give a minimum mean square error. Table 1 summarizes the optimum Δ 's, denoted Δ_m , and the associated errors.

Table 1

<u>Statistics</u>	<u>Δ_m</u>	<u>Minimum Value of Error</u>
E_v	$(3\sigma/\dot{A}_i)^{1/3}$	$3[\dot{A}_i\sigma^2/3!]^{2/3} 4^{-2/3}$
E_a	$6^{1/8} [12\sigma/\ddot{A}_i]^{1/4}$	$\sigma\ddot{A}_i/\sqrt{6}$

These formulae show that Δ_m is determined solely by the variance of the position error, which is a position fixing system characteristic, and the higher order nonlinear terms in the Taylor's expansion, which is an ocean characteristic. The table also shows that the minimum rms error increases with the increasing rms position error.

Figure 2 is a plot of σ vs Δ_m for both velocity and acceleration. In this graph \dot{A} is varied from 10^4 to 10^{-1} km dy $^{-3}$ and \ddot{A} from 10^5 to 10^{-2} km dy $^{-4}$. (We have found it convenient to use km and dy as space and time scales for large scale oceanographic problems. The conversion to these units from m and s for velocity, acceleration, jerk (\dot{A}), and quake (\ddot{A}), respectively, are $1\text{ ms}^{-1} = 86.4\text{ km dy}^{-1}$, $1\text{ ms}^{-2} = 7.46 \cdot 10^6\text{ km dy}^{-2}$, $1\text{ ms}^{-3} = 6.45 \cdot 10^{11}\text{ km dy}^{-3}$, $1\text{ ms}^{-4} = 5.57 \cdot 10^{16}\text{ km dy}^{-4}$.)

The Δ_m 's are especially significant in that they represent a natural division between two types of analyses that can be made on the observations. For $\Delta > \Delta_m$ the finite difference algorithms given above are efficient techniques for estimating velocity and acceleration. However, for $\Delta < \Delta_m$ these formulae are not adequate.

Rather, it is better to employ specially designed filters for calculating velocities and accelerations from the observations. Of course, knowledge of σ^2 and other statistical properties of the position error can be used in the construction of such filters. Such techniques can reduce the error to less than that specified by the Δ_m .

The algorithms yield velocity and acceleration estimates as a function of time. From the Eulerian standpoint, the nonrandom variability in these estimates is the result of both spatial and temporal effects. By adhering to a purely Lagrangian description here the difficult question of relating the effects of position error and sampling rate to horizontal variability is avoided.

At this point it is logical to question the effect that position error and sampling period have on the calculations of the DKP from drifter clusters. Viewed in the abstract this is a formidable problem because the equations from which the DKP are calculated involve ratios of velocity moments with respect to the center of mass of the array and second order position moments. However, with the stipulation that the estimated center of mass can be replaced by the true, then it can be shown that the DKP are merely linear functions of the velocities. From this it follows (Cramer, 1966) that the mean square errors (arising from position uncertainty and sampling period) in the DKP are proportional to the mean square velocity errors. The appendix gives details of this derivation along with a discussion of the ramifications of the simplifying assumption.

3. Assessment of existing and proposed position fixing systems

The different position fixing systems reported in the literature, or planned, cover a broad range of position error and sampling rate. Table 2 is a representative sample.

Table 2

Position error and sampling rate for various position fixing systems

<u>System/Investigator</u>	<u>σ(km)</u>	<u>Δ(day)</u>
Local Radar/Stevenson <u>et al.</u> (1974) Molinari and Kirwan (1975)	$5 \cdot 10^{-2}$	10^{-2}
Eole/Dickson and Baxter (1972) Cresswell (1976)	1	.5
RAMS/Kirwan <u>et al.</u>	1	.5
OHR/Kirwan and McNally (1975)	25	3
ARGOS/	1	.1

Eole, RAMS, and ARGOS are all polar orbiting satellite systems. The first has been phased out, the second is operational, and the last is scheduled to be in 1978. ARGOS differs in two significant ways from the previous systems. First, its position accuracy will probably be less than 1 km. Secondly, it will have two satellites in orbit rather than one. This will greatly increase the number of fixes available from this system. Moreover, these fixes will be more uniformly spaced in time than in the previous systems.

Since the satellite systems are polar orbiting, the number of fixes vary tremendously with latitude. The numbers given in table 2 are conservative estimates for a mid-latitude region.

In order to assess the capability of these systems, it is necessary to have estimates of the jerk and quake of ocean motions.

Unfortunately, calculations of these higher order derivatives from current meter or drifter data may be contaminated by measurement errors and, perhaps, insufficient sampling rates.

This obstacle can, in part, be overcome by prescribing the flow by a simple model. Such an approach is desirable in that extreme situations are easily investigated. To this end, consider a periodic velocity field specified by a frequency ω and scale velocity U . The jerk and quake are readily found to be of the order of

$$\dot{A} \sim U\omega^2$$

$$\ddot{A} \sim U\omega^3$$

Two cases are of interest. For the "fast" ocean case, take U as $8.64 \cdot 10 \text{ km dy}^{-1}$ and ω as $2\pi \text{ rad dy}^{-1}$. This might correspond to a daily cycle in a strong current such as the Gulf Stream. At the other extreme is the "slow" ocean as typified by a mesoscale eddy whose scale velocity and period of rotation are 8.64 km dy^{-1} and 20 dy , respectively.

Table 3 summarizes the velocity and acceleration Δ_m 's for these two cases for each of the position fixing systems mentioned above. Inspection of this table shows that for both the fast and slow ocean cases, the velocity Δ_m will always be less than the acceleration Δ_m . This means that if the position fixing system Δ is close to the velocity Δ_m , the acceleration is "over sampled". This is a desirable situation because special filtering techniques can be used to provide better estimates of the acceleration than would be available if the system Δ was the acceleration Δ_m . Note that this is a system characteristic which applies only when the Δ is close to the Δ_m . If the Δ 's

Table 3 Velocity and Acceleration Δ_m 's for Position Fixing Systems

System	Δ_m (velocity)	Fast Ocean		Slow Ocean	
		Δ_m (acceleration)	Δ_m (velocity)	Δ_m (acceleration)	Δ_m (acceleration)
Local Radar	$3.5 \cdot 10^{-2}$ dy	$9.1 \cdot 10^{-2}$ dy	$5.6 \cdot 10^{-1}$ dy	1.5 dy	
RAMS	$1.6 \cdot 10^{-1}$ dy	$2.9 \cdot 10^{-1}$ dy	2.6 dy	4.9 dy	
OHR	$2.8 \cdot 10^{-1}$ dy	$4.3 \cdot 10^{-1}$ dy	4.4 dy	7.3 dy	
Eole	$9.6 \cdot 10^{-2}$ dy	$1.9 \cdot 10^{-1}$ dy	1.5 dy	3.2 dy	
ARGOS	10^{-1} dy	$1.9 \cdot 10^{-1}$ dy	1.52 dy	1.39 dy	

are less than the Δ_m 's and the velocity spectrum decreases with frequency, then the acceleration spectrum will be whiter than the velocity spectrum. For comparable accuracy this would require an acceleration Δ to be less than the velocity Δ .

Figure 3 is a plot of ratio of the rms velocity error to the velocity scale as a function of Δ . This figure was constructed by specifying the jerk and quake from the fast and slow ocean cases. This shows the two error regimes mentioned above. The solidus, with a slope of 4, to the right of the minimum is the region in which the ocean variability effects (jerk and quake) are the dominant error sources. If the position fixing system Δ intersects this portion of the curve, there is little that can be done to reduce the error.

Such is not the case if the system Δ intersects the dashed lines whose slope is -2 which is to the left of the minimum. This is the region in which the error indicated in the figure can be significantly reduced by filtering the data.

It is stressed that the error ratio given in figure 3 is the worst case estimate in that the true velocity was taken as sinusoidal. In reality, there is frequently a significant steady or nonsinusoidal component. Incorporation of a steady component in the true velocity will reduce the error accordingly.

The calculations described above suggest that RAMS is not suitable for investigating diurnal oscillations of the Gulf Stream.

However, it could certainly be used to study longer period phenomena there. Note that figure 3 shows that the Δ for this system makes it ideal for investigating mesoscale eddies or longer period phenomena.

Neither RAMS, Eole nor the OMR is likely to be adequate for calculating DKP unless a large number of drifters are used. To achieve a reasonable accuracy it may be necessary to use Δ 's significantly less than the Δ_m 's. A position fixing system Δ of the order of .1 a day and σ of 10^{-1} km might suffice for this. The ARGOS system approaches this.

Appendix

Errors in Differential Kinematic Properties

In order to analyze the effect of position error and sampling rate on the DKP, it is necessary to indicate both the X and Y components of position as well as the time and drifter number. To this end the coordinates relative to the center of mass of the cluster for the m^{th} drifter are denoted as

$$x_{im} = z_{im} + r_{im} \quad i = 1, 2; \quad m = 1, \dots, n \quad (A-1)$$

Here the first subscript refers to the coordinate direction (X or Y) and the second to the drifter number. As before, the true position is z and r is the random position error.

Following Molinari and Kirwan (1975) and Okubo and Ebbesmeyer (1976), the velocity components of the m^{th} drifter of a cluster of n drifters can be expressed as a Taylor's Expansion (in space) about the cluster center of mass. Thus

$$u_m = u_o + \frac{\partial u}{\partial x_i} x_{im} + \dots \quad (m = 1, \dots, n; \text{sum on } i = 1, 2) \quad (A-2)$$

$$v_m = v_o + \frac{\partial v}{\partial x_i} x_{im} + \dots$$

In (A-2) u_m and v_m can be calculated by the algorithms given above while the coefficients u_o , v_o , $\frac{\partial u}{\partial x_i}$ and $\frac{\partial v}{\partial x_i}$ can be determined by least squares provided there are three or more drifters (Molinari and Kirwan, 1975; Okubo and Ebbesmeyer, 1976).

The aim here is to determine how the position error and sampling rate affect the accuracy of the estimates of u_o , $\partial u / \partial x_i$, etc. For

this it is only necessary to consider the U component equation.

The assumption is now made that the expansion given by (A-2) is valid relative to either the observed or true center of mass if the true coefficients are used. For many applications this is not a severe restriction. The variance of the difference between these two position is σ^2/n . Thus, the estimated center of mass will be within one standard deviation of the true. Moreover, it can be made as close to the true as desired by increasing the number of drifters. One a-priori condition on how close the estimated to the true should be is that it should be less than the rms relative displacements of the drifters from the estimated.

With this assumption it is seen that only the left hand side of (A-2) need now be considered as random. Thus, the problem is reduced to that of multiple regression with nonrandom independent variables (see Cramer, 1966).

The following nonrandom functions are introduced:

$$P_{ij} = \sum_{m=1}^n (x_{im} - \bar{x}_i) (x_{jm} - \bar{x}_j) \quad i, j = 1, 2$$

$$\bar{x}_i = \frac{1}{n} = \sum_{m=1}^n x_{im} \quad (A-3)$$

$$P = \det \{P_{ij}\} \quad (A-4)$$

$$M_{ij} = i^{\text{th}}, j^{\text{th}} \text{ cofactor of } P_{ij} \quad (A-5)$$

along with the random vector

$$s_i = \sum_{m=1}^n (U_m - \bar{U}) (x_{im} - \bar{x}_i) \quad (A-6)$$

Here \bar{U} is the expected value of the X component of the center of mass velocity.

The use of (A-3) through (A-6) allows us to express the least squares estimates of U_o , $\frac{\partial U}{\partial X_1}$, and $\frac{\partial U}{\partial X_2}$ as

$$\hat{U}_o = \frac{1}{n} \sum_{m=1}^n U_m \quad (A-7)$$

$$\frac{\partial \hat{U}}{\partial X_1} = \{s_1 M_{11} + s_2 M_{12}\}/P \quad (A-8)$$

$$\frac{\partial \hat{U}}{\partial X_2} = \{s_1 M_{21} + s_2 M_{22}\}/P \quad (A-9)$$

Note from (A-7) through (A-9) that each of these coefficients is a linear function of the drifter velocities which are random. In such cases it is readily shown that the expected values of the estimates are merely the same linear functions of the expected values of the velocities. From (A-2) it is seen that the latter involves the true values of the coefficients. By inserting (A-3)-(A-6) into (A-8) and (A-9), it is found that

$$\overline{\frac{\partial \hat{U}}{\partial X_i}} = \frac{\partial U}{\partial X_i}, \quad \overline{\hat{U}_o} = U_o \quad (A-10)$$

A second aspect of the linear relation is that the covariance matrix of the estimates are given by

$$\overline{(\hat{U}_o - U_o)^2} = \epsilon^2/n \quad (A-11)$$

$$\left(\overline{\frac{\partial \hat{U}}{\partial X_i}} - \frac{\partial U}{\partial X_i} \right) \left(\overline{\frac{\partial \hat{U}}{\partial X_j}} - \frac{\partial U}{\partial X_j} \right) = \epsilon^2 L_{ij}/nL, \quad (i,j = 1,2) \quad (A-12)$$

Here the maximum likelihood estimate of ϵ^2 is

$$\hat{\epsilon}^2 = \frac{1}{n} \sum_{m=1}^n \left[U_m - U_o - \frac{\partial \tilde{U}}{\partial X_i} X_{im} \right]^2 \quad (\text{sum on } i = 1,2) \quad (A-13)$$

Eq. (A-10) says that the expected value of the estimates of the center of mass velocity and the velocity gradients are the true values. Eqs. (A-11) and (A-12) show that the variance of the center of mass velocity and the velocity gradient covariance are proportional to the regression variance. From (A-13) this is seen to be composed of the mean square velocity error (velocity variance) and quadratics involving the estimated velocity gradients. The last set of terms may be assumed to be independent of the sampling rate (Molinari and Kirwan, 1975). Thus, the covariances are all proportional to the mean square velocity error, and their dependency on Δ is the same, except for a displacement along the ordinate.

Figure Captions

Figure 1 Schematic of drifter trajectory data obtained at discrete times.

Figure 2 Plot position error versus velocity and acceleration Δ_m 's. Jerk (Δ) and quake ($\ddot{\Delta}$) are varied from 10^{-1} to 10^4 km dy $^{-3}$ and 10^{-2} to 10^{-5} km dy $^{-4}$, respectively.

Figure 3 Plot of normalized rms velocity error as a function of Δ . Position error σ is varied from 10^{-2} km to 10 km.

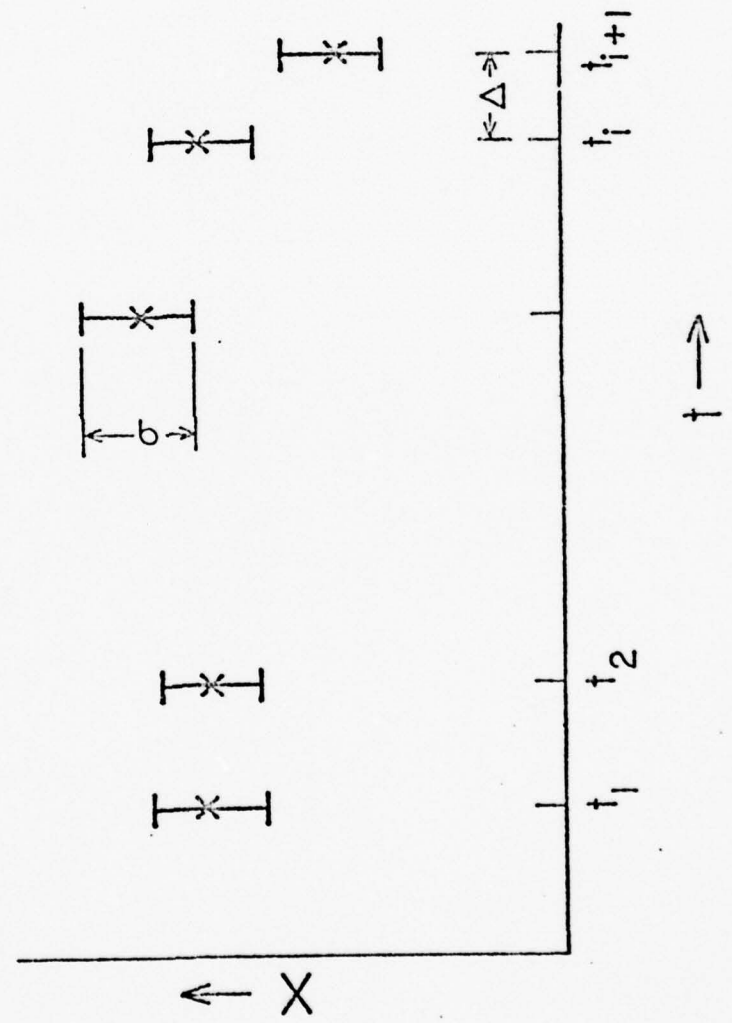


Figure 1

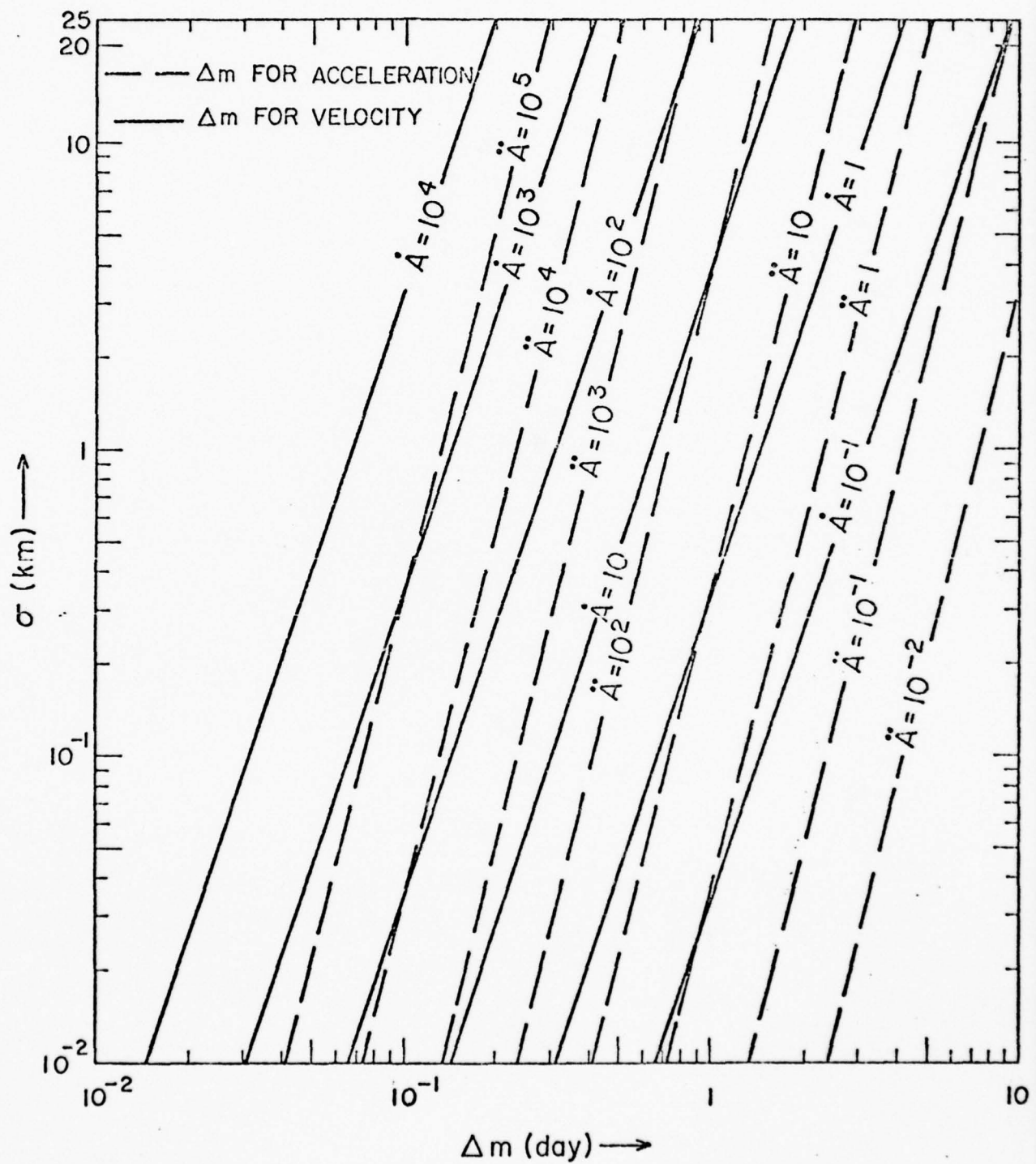


Figure 2

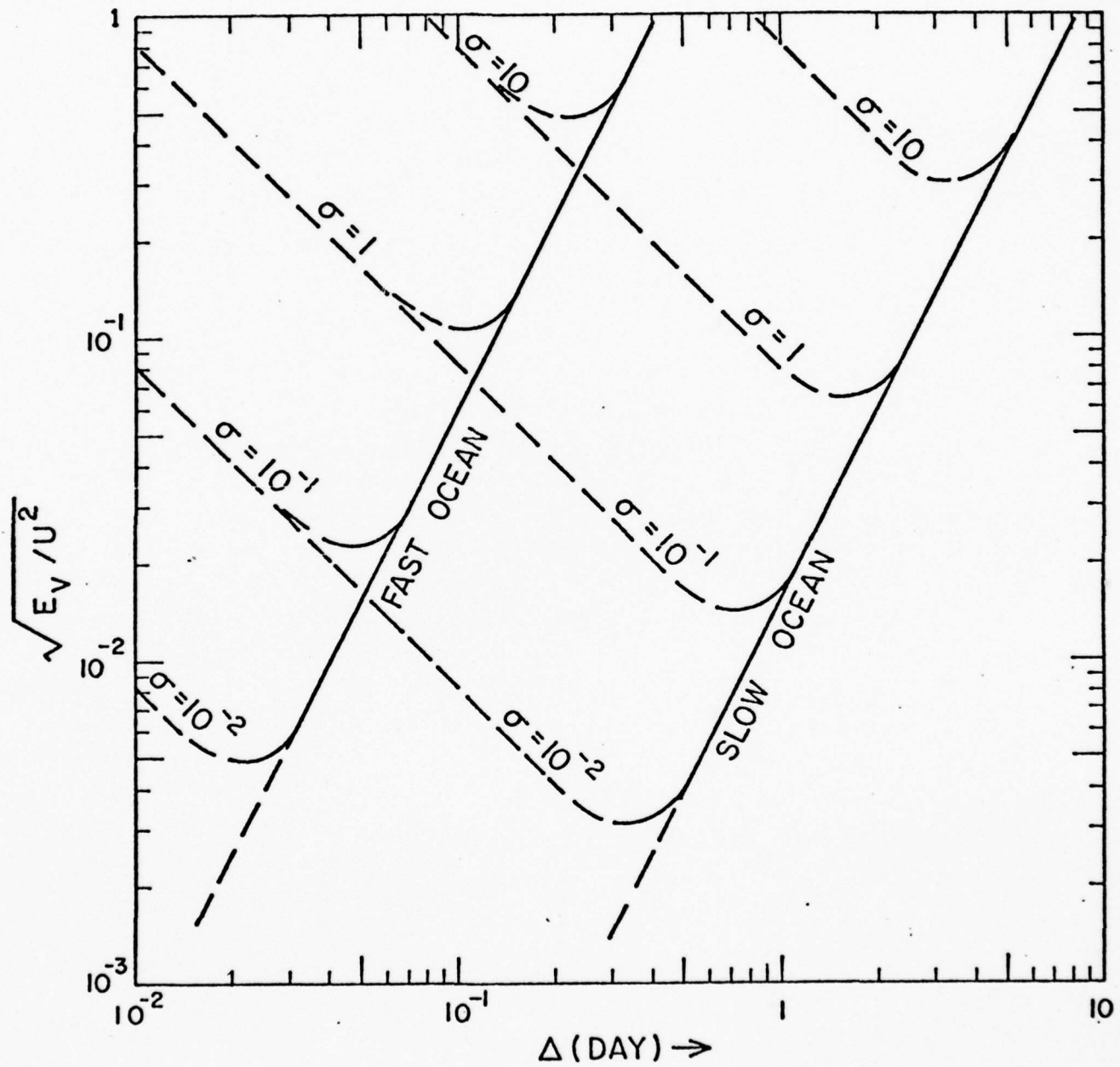


Figure 3

Acknowledgments

The research culminating in this report was sponsored in part by the Ocean Sciences and Technology Division of the Office of Naval Research and the Office of the International Decade of Ocean Exploration of the National Science Foundation.

References

Cramer, Harold, 1966: Mathematical Methods of Statistics, Princeton University Press, Princeton, N.J., 574 pp.

Cresswell, G. R., 1976: A drifting buoy tracked by satellite in the Tasman Sea. Aust. J. Mar. Freshwater Res., Vol. 27, 251-262.

Dickson, R. R. and G. C. Baxter, 1972: Monitoring deep water movements in the Norwegian Sea by satellite. International Council for the Exploration of the Sea, Committee Manuscript, Mimeo, 9 pp. + 8 figs.

Freeland, H. J., P. B. Rhines and T. Rossby, 1975: Statistical observations of the trajectories of neutrally buoyant floats in the North Atlantic. J. Mar. Res., 33, 383-404.

Kirwan, A. D. Jr., G. McNally, 1975: A note on observations of long-term trajectories of the North Pacific Current. J. Phys. Oceanog., 5, 188-191.

_____, _____, M.-S. Chang and R. Molinari, 1975: The effect of wind and surface currents on drifters. J. Phys. Oceanog., 5, 361-368.

_____, _____, and J. Coehlo, 1976: Gulf Stream kinematics inferred from a satellite-tracked drifter. J. Phys. Oceanog., 6, 750-755.

Molinari, Robert and A. D. Kirwan, Jr., 1975: Calculations of differential kinematic properties from Lagrangian observations in the western Caribbean Sea. J. Phys. Oceanog., 5, 483-491.

Okubo, A. and C. C. Ebbesmeyer, 1976: Determination of vorticity, divergence and deformation rates from analysis of drogue observations. Deep-Sea Res., 23, 349-352.

Richardson, Philip, 1976: Tracking a Gulf Stream ring with an NDBO buoy. Data Buoy Tech. Bulletin, Vol. 2, No. 4.

Rossby, T. and D. Webb, 1971: The four month drift of a Swallow float. Deep-Sea Res., 18, 1035-1039.

Stevenson, M. R., R. W. Garvine and Bruce Wyatt, 1974: Lagrangian measurements in a coastal upwelling zone off Oregon. J. Phys. Oceanog. 4, 321-336.

Swallow, J. C. and L. V. Worthington, 1961: An observation of a deep countercurrent in the western North Atlantic. Deep-Sea Res. 8, 1-19.

Appendix C

**A Drifting Buoy Positioning System for the Study of
Western Boundary Currents**

W. A. Vachon

D. R. Yoerger

REPORT DOCUMENTATION PAGE		READ INSTRUCTIONS BEFORE COMPLETING FORM
1. REPORT NUMBER R-1094	2. GOVT ACCESSION NO.	3. RECIPIENT'S CATALOG NUMBER
4. TITLE (and Subtitle) A Drifting Buoy Positioning System for the Study of Western Boundary Currents		5. TYPE OF REPORT & PERIOD COVERED Final Report April 1976 - May 1977
		6. PERFORMING ORG. REPORT NUMBER
7. AUTHOR(S) William A. Vachon Dana R. Yoerger		8. CONTRACT OR GRANT NUMBER(S) Subcontract No. S-102(3200A-6 Prime: #N00014-75-C-0537
9. PERFORMING ORGANIZATION NAME AND ADDRESS Charles Stark Draper Laboratory, Inc. 555 Technology Square Cambridge, Mass. 02139		10. PROGRAM ELEMENT, PROJECT, TASK AREA & WORK UNIT NUMBERS
11. CONTROLLING OFFICE NAME AND ADDRESS NORDA NSTL Station Bay St. Louis, MS 39529		12. REPORT DATE June 1977
14. MONITORING AGENCY NAME & ADDRESS (if different from Controlling Office) Texas A & M Research Foundation FE Box H College Station, Texas 77843		13. NUMBER OF PAGES 72
		15. SECURITY CLASS. (of this report) Unclassified
		15a. DECLASSIFICATION/DOWNGRADING SCHEDULE
16. DISTRIBUTION STATEMENT (of this Report) Approved for public release; distribution unlimited		
17. DISTRIBUTION STATEMENT (of the abstract entered in Block 20, if different from Report)		
18. SUPPLEMENTARY NOTES		
19. KEY WORDS (Continue on reverse side if necessary and identify by block number) Drifting buoys, Lagrangian drifters, drogued drifters, buoy positioning systems. Lagrangian oceanographic buoys, western boundary currents.		
20. ABSTRACT (Continue on reverse side if necessary and identify by block number) A study is conducted to examine the feasibility of tracking the higher frequency meanders of western boundary with remotely-positioned Lagrangian drifters. The study compares the utility of using various off-the-shelf positioning systems and means of data telemetry. It is concluded that a low cost automatic IORAN-C microprocessor receiver with on-board memory is the best means of acquiring the desired position data. It is further concluded that the best means of transmitting position and other ancillary data such as		

Non-classified

SECURITY CLASSIFICATION OF THIS PAGE (When Data Entered)

water temperature, is by a TIROS-N satellite transmitter. The total cost of a drifting buoy positioned by LORAN-C, telemetering data by the TIROS-N satellite is under \$6,000. each.

The utility of using single-sideband (SSB) suppressed carrier high-frequency (HF) telemetry is examined. It is concluded that frequency shift keying (FSK) modulation of a single 4.1 MHz carrier twice per day is a useful means of telemetering the desired data out to a distance of about 1500 km. from the receiver. It is shown that at 4.1 MHz, a ground-wave propagation mode is relied upon during daylight hours and skywave at night. The lower reliability and increased complexity of the HF link make it less desirable than a satellite link.

Estimated drogued buoy trajectory error bounds are compared with the positional accuracy of LORAN-C for the nominal case of a Nova buoy reporting one buoy position per hour. It is found that reliable wind field data must be employed for estimating buoy trajectory errors for winds above 10 knots. With such data, it appears possible to keep a knowledge of trajectory errors per hour within the overall accuracy limits of a LORAN-C system up to wind speeds of approximately 30 knots even if the drogue is not working as desired. Above this wind speed the trajectory data are suspect until better correction models are available. For overall drogue slippage correctability a bi-planar crossed vane is recommended until more hard data are available on parachute and window shade drogue performance.

SECURITY CLASSIFICATION OF THIS PAGE (When Data Entered)

R-1094

A Drifting Buoy Positioning System for the Study of
Western Boundary Currents

by

W. A. Vachon
D. R. Yoerger

June 1977

Submitted to: Department of Oceanography
Texas A & M University
College Station, Texas 77843

From: The Charles Stark Draper Laboratory, Inc.
555 Technology Square
Cambridge, Massachusetts 02139

For: Subcontract No. S-102 (3200A-6)
Prime Contract #N00014-75-C-0537

Approved for public release; distribution unlimited

TABLE OF CONTENTS

1.0	INTRODUCTION	1
2.0	OCEANOGRAPHIC AND SYSTEM DESIGN OBJECTIVES	2
3.0	BUOY POSITIONING SYSTEMS	3
3.1	TIROS N (or NIMBUS 6)/RAMS Satellite System	3
3.2	OMEGA Radio Positioning	4
3.3	LORAN-C Navigation	6
3.3.1	Operation of LORAN-C Chains	6
3.3.2	LORAN-C Accuracy and Repeatability	7
3.3.3	LORAN-C Coverage	9
3.3.4	LORAN-C System Availability	12
3.3.5	LORAN-C Receiving Equipment	12
3.3.5.1	Power Requirements	12
3.3.5.2	Net Power Consumption	15
3.4	Navy Navigation Satellite System (NNSS) or TRANSIT	19
3.5	NAVSTAR Global Positioning System (GPS)	20
3.6	Other Positioning Systems	21
4.0	TELEMETRY OF BUOY POSITION AND SENSOR DATA	22
4.1	Satellite Telemetry	22
4.1.1	TIROS-N Satellite Telemetry	22
4.1.2	GOES Satellite Telemetry	26
4.1.3	Other Satellite Data or Telemetry Links	28
4.2	High Frequency (HF) Data Telemetry	31
4.2.1	Ground Wave HF Telemetry Link	33
4.2.2	Ionospheric Wave HF Telemetry Link	34

4.2.3 Skywave-Groundwave Interaction	46
5.0 SUMMARY AND RECOMMENDED SYSTEM CONFIGURATION	47
6.0 ESTIMATED BOUNDS ON DROGUED BUOY SLIPPAGE ERRORS	53
6.1 Buoy Wind Drag Forces	53
6.2 Drag on Wetted Portions of a Buoy	57
6.3 Comparison with Measured Slippage Data	60
6.4 Drogue Performance	60
Appendix A - Word Structure and Date Rate Description	64
Appendix B - HF Transmission Equipment	66

LIST OF FIGURES

<u>Figure</u>	<u>Description</u>	<u>Page</u>
1	Example of Received LORAN-C Signal	8
2	Typical LORAN-C Pulse	8
3	LORAN-C Positional Repeatability for 0.1 μ sec TD Variation on East Coast Chain	10
4	LORAN-C Groundwave Coverage: Existing and Proposed Worldwide	11
5	LORAN-C Signal Variation with Range	14
6	LORAN-C SNR as Function of Search and Settling Time for the Micrologic ML-200 Receiver	14
7	Block Diagram of LORAN-C/TIROS-N Hybrid Drifting Buoy Positioning System	25
8	Ground Wave Field over the Sea for 1 kw Radiated Power	35
9	Typical Noise Chart for HF Radio Waves	36
10	HF Skywave Propagation Modes	38
11	Maximum and Minimum Absorption Index	38
12	Signal Field as a Function of Frequency and Absorption Index (A)	39
13	Signal Field as a Function of Distance for 1 kw Radiated Power	39
14	Critical Frequency for F_2 -Layer Ionospheric Reflection	41
15	Definition of Incident Angle ϕ for One-Hop F_2 -Layer Propagation	41
16	Expected Signal-to-Noise Ratios (db) for 4.1 mHz Groundwave Propagation from a Gulf Stream Drifting Buoy	42
17	Modular Concept of a Drifting Buoy Positioning System	52
18	Estimated Cross-Sectional and Drag Areas of Drifting Buoys	55

LIST OF TABLES

<u>Table</u>	<u>Description</u>	<u>Page</u>
1	Summary Comparison of Leading LORAN-C Receivers Adaptable to Drifting Buoy Applications	16
2	Typical Power Budget and Unit Cost for a LORAN-C/ TIROS-N Hybrid Drifting Buoy Positioning System	24
3	Typical Power Budget and Unit Cost for a LORAN-C/ GOES Hybrid Drifting Buoy Positioning System	27
4	HF Transmitter Data Word Structure	32
5	Drifting Buoy Positioning and Data Acquisition System Cost Summary	48
6	Comparative Engineering Data and Hardware Cost Summary for 2-year Program to Monitor a Western Boundary Current	50
7	Estimated Wind Forces on Drifting Buoys	54
8	Estimated Nova Buoy Slip with No Shear Present, $(C_D)_{drogue} = 2.0$	56
9	Estimated Nova Buoy Slip with No Shear, $(C_D)_{drogue} = .5$	56
10	Nova Minibuoy Estimated Wetted Drag Characteristics	57
11	Current Forces on Nova Buoy	58
12	Maximum Buoy Forces and Drogue Slippage for Sum of Wind and Wind-Induced Current Forces	59

1.0 INTRODUCTION

At the present time the Buoy Transmit Terminal (BTT) of the NIMBUS-6 satellite has demonstrated the simplicity, reliability and cost effectiveness of deriving oceanographic data from satellite-tracked drifters (Kirwan, 1977 and Richardson et al, 1977). Employed in an expendable mode, these buoys have measured useful data for periods of over one year in such places as the North Pacific at Latitudes to 45°N. The satellite positioning system has provided a position fix and enabled the transmission of on board sensor data at frequencies of 2 to 8 times per day, with 2 transmissions assured when the satellite is nearly overhead twice per day. The positional accuracies reported from controlled tests are approximately \pm Km, 90% of the time when the satellite is overhead twice per day and less when passing near the horizon.

In planning an experiment, an investigator can really only plan on position data every 12 hours. At this rate there is a risk that energy at the diurnal or shorter periods may be aliased (i.e., Nyquist frequency of 1 cycle/day = $1/2\Delta t$, Δt = sample period). As a result, the existing NIMBUS-6 (to be succeeded by the TIROS-N satellite in 1978) satellite is useful in the study of slowly changing phenomenon and large scale circulation.

Dr. A. D. Kirwan of Texas A. & M. University (TAMU) has chosen to measure the motions of western boundary currents in general and the Gulf Stream and Kuroshio currents in particular. Because of the extent of such currents and cost considerations the method of investigation will be by remotely-positioned, expendable, drogued drifting buoys. It has, however, been found by Robinson et al (1974) and others that one of the dominant energy modes for Gulf Stream meanders is at approximately the diurnal period. The buoy transmit terminal (BTT) of either the NIMBUS-6 or TIROS-N satellite is therefore an inappropriate method of directly deriving sufficient buoy trajectory data. The classical manner of handling aliasing in dynamic systems is to sharply attenuate energy at frequencies above the Nyquist frequency by electronic or mechanical filters. Drifting buoy motion cannot be filtered in a like manner, nor would it be desirable. This is the very information being sought.

Alternative schemes for economically measuring buoy position at a higher rate than a BTT will be explored in this writing. In addition, the

trade-offs of buoy positional accuracy, frequency of position, and drogue current locking accuracy (i.e., slippage) will be discussed.

2.0 OCEANOGRAPHIC AND SYSTEM DESIGN OBJECTIVES

The highest frequency energy reported for Gulf Stream Motions (Robinson et al, 1974) was at a period of approximately 24 hours. They also indicate that there is an appearance of energetic small scale structure (period ~2-4 days) which may possibly disappear into large scale structures (period ~1 day). Because their detailed data were limited to a 180-km swath along the Gulf Stream axis, it was not possible to trace the smaller scale disturbances over a wide enough area to document behavior conclusively. There is even very limited evidence in their data of structure at periods of less than one day.

Sampling theory indicates that position data should be recorded at least twice per shortest period in order to record unaliased trajectory data at this frequency. In general, though, it is desirable to have at least 5-10 data points for the shortest period. Therefore, a nominal design goal will be to acquire a position data point every hour. For economy of onboard buoy power it will be initially assumed that the $\pm 3\sigma$ error footprint of a buoy position fix does not overlap the footprint of a subsequent fix. If it was later found that there was an overabundance of power and data capability, fixes could be taken more frequently and averaging done. With the above assumption, the maximum tolerable positioning error for useful measurements is given by the relation:

$$\epsilon = \frac{V}{2f} \quad (1)$$

where V is the minimum expected velocity, f the sampling frequency (assumed at 1 hr^{-1}), and ϵ the 3σ bound of an error footprint in the direction of buoy travel. For western boundary currents such as the Gulf Stream or the Kuroshio the near-surface velocity is generally greater than 0.5 knots (i.e., .9 km/hr) which dictates a positional accuracy of $\pm 450 \text{ m}$ for hourly position fixes.

The planned lifetime of the system electronic design is 30 days. This value is based on an estimate of the longest period of time that a buoy would remain within the current regime of interest. All power budget figures which follow can be linearly scaled about this nominal lifetime while confidence on the acquisition of certain radio signals varies with buoy location with respect to stations.

It is poor judgment to place a sophisticated, precise, radio positioning system aboard a drifting buoy for the purpose of monitoring currents when

the buoy itself may have drogue slippage between position fixes which is in excess of the positional accuracy. In such cases the derived trajectory data can be meaningless in light of the defined goals. On the other hand, it is recognized that even for the best design, under certain extreme weather conditions, highly erroneous data can arise and should be discounted. This writing will attempt to bound the slippage error as a function of the particular buoy design and environment by applying existing data and analytic approaches to estimating buoy forces and drogue slippage. Lastly, suggestions will be made as to required parameters to be measured and means by which first order corrections can be made for drogue slippage.

3.0 BUOY POSITIONING SYSTEMS

The problem of automatically determining the position of a drifting buoy breaks down into two parts - the position determination and the means of reporting the position. This section will address the various means of position determination (both present and future), many of which also provide a means of automatically reporting the data. The next section will cover the existing schemes for the telemetry or otherwise reporting buoy position.

3.1 TIROS-N (or NIMBUS-6) / RAMS Satellite System

As mentioned in the introduction, the Random Access Measurement System aboard either the NIMBUS-6 satellite (presently orbitting but working only half-time every other day) or the TIROS-N satellite (mid 1978 launch date) would not be an appropriate method of deriving buoy position data because of the infrequent reliable fixes. Furthermore, section 2 also shows that its positional accuracy does not meet the design requirements. The RAMS system could, however, provide a means of resolving positional ambiguities or receiver error problems in a LORAN C positioning system. For example, occasionally a LORAN C receiver, which normally tracks the third cycle crossing in a pulse, may erroneously track the second cycle crossing, leading to an error of 10 microseconds or approximately a 3 km error. If the RAMS system were used as the means for LORAN C data transmittal such errors could be revealed. Otherwise the RAMS system by itself is not useful as a prime buoy positioning system.

3.2 OMEGA Radio Positioning

OMEGA is a very long range, hyperbolic radio positioning system that works in the Very Low Frequency (VLF) range. Lines of position are generated by phase-difference measurements of a composite three-frequency, time-shared system from each of eight stations giving worldwide coverage. When fully operable the eight stations will be at the following locations which exhibit up to 8,000 to 10,000 Km baseline distances:

- (1) North Dakota
- (2) Reunion Island, Indian Ocean
- (3) Trinidad
- (4) Norway
- (5) Japan
- (6) Australia
- (7) Argentina
- (8) Hawaii

At present all but the Australian station are operable.

Each station transmits each of the following frequencies for approximately one second (continuous wave) every ten seconds in a prescribed format at a 10 kw power level:

$$f_1 = 10.200 \text{ kHz}$$

$$f_2 = 11.333 \text{ kHz}$$

$$f_3 = 13.600 \text{ kHz}$$

The particular timing format of a given transmitter allows its unique identification. The time synchronization between stations is maintained by atomic clocks.

The composite or three-frequency format is helpful for two reasons:

- (1) increased lane widths
- (2) increased knowledge of signal phase propagation

As stated earlier, a complete OMEGA receiver monitors the phases of three pulsed, continuous waves from each transmitter. If a single frequency

receiver were employed it would find that the signal phase relationship along a station baseline would be the same every $\lambda/2$ (λ = wavelength). For the 10.2 kHz signal alone this would occur every 15 km (i.e., the single frequency lane width). Therefore, if a sudden ionospheric disturbance (SID) should occur, arising in a matter of minutes from a solar flare, the accompanying ionospheric lowering could result in as much as a 40 centicycle (i.e., 40 CEC = .4 cycle) change in signal phase for an all-daylight path (Research Triangle Institute, 1973). Furthermore, as the solar terminator passes across the path between transmitter and receiver as much as a 25 CEC change can occur at the receiver over a period of 30 minutes (Beukers, 1973). Such rapid occurrences might easily lead to loss of lane count if constant signal monitoring were not maintained.

In an effort to artificially widen the lanes, in order to lessen the amount of position monitoring required, three frequencies were introduced. In essence the larger lane widths are now determined by the difference or beat frequencies between the transmitter frequencies. Therefore, the difference frequency between the 10.200 and 11.333 kHz signals dictates a lane width of 133 km.

The second reason for using the composite OMEGA system is that by taking advantage of the available phase information at more than one frequency it is possible to enhance computerized predictions of signal phase propagation. Such a potential arises from the fact that phase perturbations at VLF are to some extent frequency-dependent (Pierce, 1972).

Without any corrections at all, the positional accuracy of an OMEGA receiver can be on the order of 10 to 15 km. By estimating errors introduced by diurnal variations such as variable propagation velocities as a function of solar angle and variable ground conductivity it is possible to increase the accuracy to better than ± 2 km (daytime) and better than ± 3.5 km (nighttime) (Research Triangle Institute, 1973). This accuracy is not good enough for the drifting buoy program envisioned nor does it perform any better than the positional accuracy of the BTT/RAMS package which is on the NIMBUS-6 or TIROS-N satellite system.

The accuracy of the OMEGA system only approaches an acceptable level when it is used in the differential mode. That is, a monitor station should

be mounted at a fixed location and its recorded positional changes subtracted from that of the buoy. For buoy-monitor ranges (i.e., correlation distances) of less than 20 km the positional accuracy can be as good as ± 450 m (i.e., 3 CEC) for data which are instantaneously updated. If, however, the correlation distance exceeds 400 km, positional errors approaching 4.5 km (i.e., 30 CEC) can be expected (Beukers, 1973). Because buoys tracking western boundary currents can be expected to be on the order of hundreds of kilometers from land masses it does not seem possible to employ differential OMEGA. On the other hand it does not even seem economically feasible to think of employing monitoring stations unless they were already installed for other reasons. It will, however, be mentioned later that it is hoped that the OMEGA system might fit into a multi-purpose modular drifting buoy positioning system that could be taken anywhere in the world.

3.3 LORAN-C Radio Navigation

LORAN-C is a high-accuracy radio navigation system which appears to be the best choice for tracking drifting buoys in the Gulf Stream. The system provides accuracy of greater than 500 m at a range of 2000 km. The system is also highly reliable and there is a large amount of commercial receiving equipment available.

3.3.1 Operation of LORAN-C Chains

Lines of Position

A position fix is obtained using LORAN-C by determining the time difference between the arrival of a pulse from a master station and each of two slave stations. Each time difference defines a hyperbolic line of position (LOP). The intersection of two LOPs corresponds to the position.

Group Repetition Interval

All transmitters operate at 100 kHz and transmit groups of pulses at an interval known as the Group Repetition Interval (GRI). The GRI is expressed in tens of microseconds and varies from 4000 to 9999. Each chain (a master and up to 4 slaves) has its own GRI.

Coding Delay

Slaves are positioned such that at least two can be received throughout the desired coverage area. To prevent ambiguity between slaves, each slave transmits after the master by a time interval known as the coding delay. Coding delays are chosen such that throughout the coverage area, pulses will always be received in the same order, that is Master, Slave x, Slave y, Slave z, etc. This is shown in Figure 1.

Blink Code

Each group of pulses consists of 8 pulses, with the exception of the Master, which transmits 9 pulses. The extra pulse serves to identify the Master. Additionally, this ninth pulse in the Master group may be switched on and off to inform users of a transmitter malfunction. Different on-off patterns are used to tell which transmitter is malfunctioning. This is known as the blink code.

3.3.2 LORAN-C Accuracy and Repeatability

High accuracy of LORAN-C is obtained by taking the time of arrival to be the zero-crossing at the end of the third cycle of the groundwave, as shown in Figure 2. The shape of the pulse allows this third cycle zero-crossing to be identified. Groundwave propagation is stable with respect to time of day, year, sunspot cycle, and ionospheric conditions in general. Skywaves, reflected off different levels of the ionosphere, will arrive between 35 μ sec and 1000 μ sec after the corresponding groundwave. The earliest case will not interfere, as the measurement is made 30 μ sec after the beginning of the pulse. Therefore, the groundwave signal can't be contaminated by its own skywave. However, a pulse may be contaminated by the skywave of the previous pulse if the skywave delay approaches 1000 μ sec. Automatic receivers can identify these delayed pulses, since the phase of the 100 kHz carrier is changed in each pulse in a group according to a prearranged sequence known as the phase code.

The accuracy of the LORAN-C system is a function of the receiver location within the coverage area as well as time measurement noise, earth conductivity changes, atmospheric refraction (for cases of skywave interference), and system synchronization. The accuracy as a function of location, referred to as geometric dilution of position (GDOP), can become rather large for hyperbolic systems, especially in regions of transmitter baseline-extension.

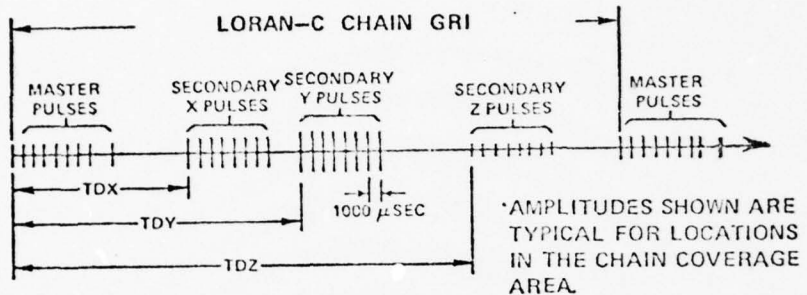


Figure 1 - Example of Received LORAN-C Signal
(from LORAN-C User Handbook)

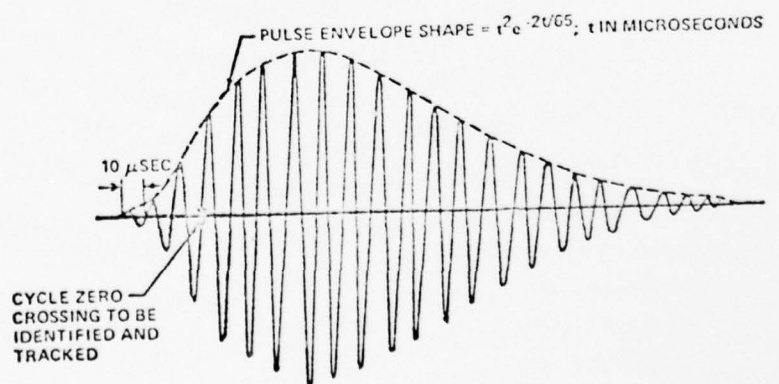


Figure 2 - Typical LORAN-C Pulse
(from LORAN-C User Handbook)

In general, the overall system accuracy is within 500 meters, 95% of the time; with a relative or repeatability error of 15 to 100 meters - depending on the above conditions (Fried, 1974). In practice, the measured time differences at the same spot will vary by about 0.1 μ sec. This time difference variation results in positional variations which depend on the location of the receiver, master, and slaves. Figure 3 shows this positional variation in meters for the region of the United States East Coast Chain (Micrologic Inc., 1975).

3.3.3 LORAN-C Coverage

The existing U. S. East Coast Chain provides adequate coverage for a Gulf Stream monitoring experiment out to a position north and east of Bermuda. Additionally, coverage is available in many other parts of the world, as shown in Figure 4. All chains transmit on the same frequency (100 kHz), but generally should not interfere with each other, as all chains have different GRIs. Therefore, the same receiving equipment could be used with any existing chain.

When the Coast Guard has completed installation of the newest stations, new LORAN-C chains will be created, leading to increased coverage as shown in Figure 4. This change will mean that in a few locations such as the southern part of the U. S. east coast there are potential interference problems between chains operating at different GRIs. This close proximity of different chains could lead to a cross-rate interference problem if a LORAN-C receiver front end were not properly designed.

It is additionally possible to install one's own LORAN chain by the rental of small (1 kw) portable transmitters similar to the LORAN-D tactical system. This allows a LORAN-C chain to be set up anywhere in the world at moderate cost. Transmitters are available from Megapulse, Inc. of Bedford, MA and have a range of about 400 mi.

Effect of Distance on SNR

The usefulness of a received signal is expressed as the signal-to-noise ratio (SNR). This ratio is primarily dependent on distance from the transmitter, however it is also affected by other factors such as:

Slave Station Key

1. Jupiter, Florida
2. Carolina Beach, N.C.
3. Nantucket, Mass.

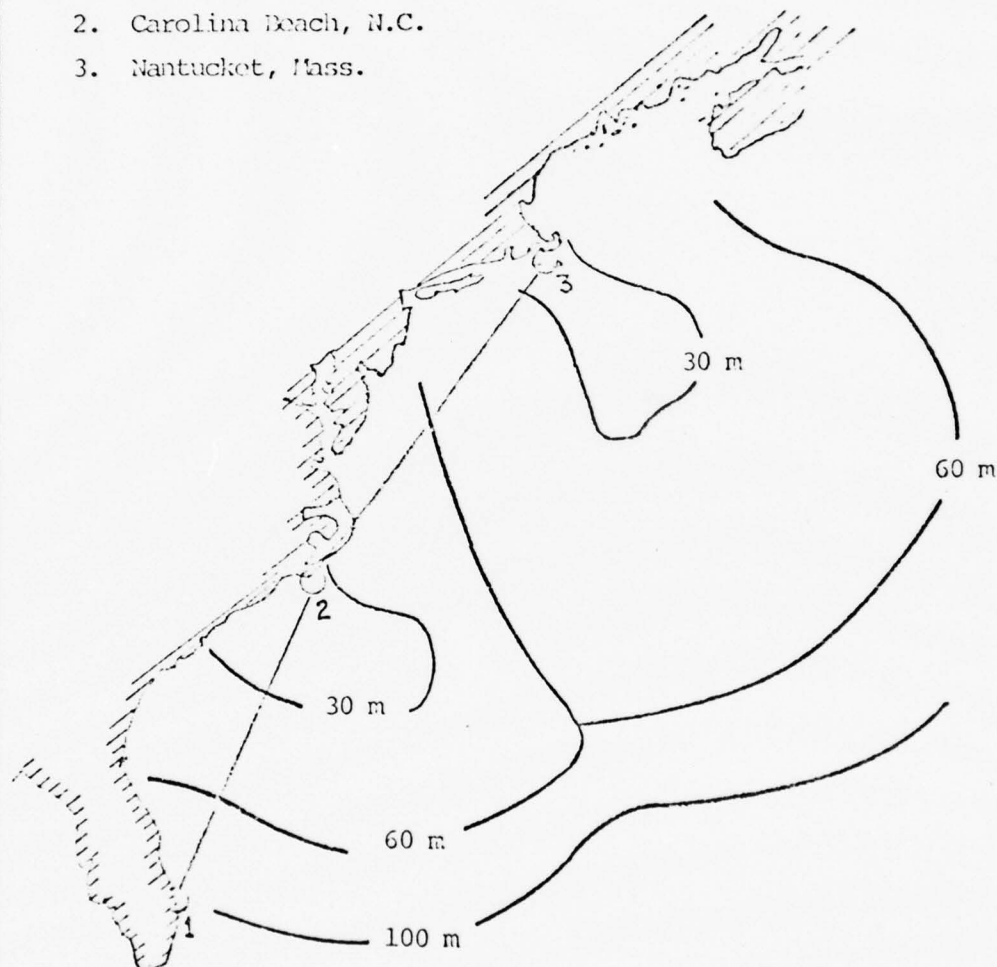


Figure 3 - LORAN-C Positional Repeatability for 0.1 μ sec
TD Variation on East Coast Chain
(from Micrologic Inc. Operators Manual)



Figure 4 - LORAN-C Groundwave Coverage:
Existing and Proposed Worldwide
(from LORAN-C User Handbook)

- reflectivity of earth's surface (different for land, sea water, fresh water)
- time of day and year
- distance from the equator

Using the average values of all these factors, Figure 5 shows SNR as a function of distance.

3.3.4 LORAN-C System Availability

The LORAN-C system has maintained a 99% availability (Roland, 1973). If scheduled maintainance is not included, the figure becomes 99.7%. Presently, new equipment is being developed which will permit more on-air maintainance, which will improve service even more.

3.3.5 LORAN-C Receiving Equipment

The new generation of LORAN-C receivers currently on the market are ideally suited to an automatically positioned drifting buoy application. Using microprocessors, the receivers automatically search for the LORAN-C signals, lock on to the third cycle crossing, and compute time differences. Such receivers generally monitor the SNR and check for blink code messages. As described earlier, LORAN-C has provisions for sorting out groundwaves from skywaves, and this is done by all fully automatic receivers. Some manufacturers have even provided a frequency shift keying (FSK) option on the output such that the time difference words are converted to signals that can modulate a higher frequency data return link. This option is presently available on both the Teledyne and Internav microprocessor LORAN-C receivers.

3.3.5.1 Power Requirements

Power consumption for automatic receivers, with displays eliminated, varies from 15 watts to 38 watts. In either case, it would be impractical to leave the receiver on during the entire experiment. Because a receiver can

automatically acquire and track LORAN-C signals, it is possible to turn on the receiver for only a short time for each sample. After the receiver has searched, settled, and computed a pair of time differences, the two time difference words could be immediately transmitted or stored in a random access memory and the receiver shut down until the next sample is to be taken. The total power consumption for only the acquisition of time difference information is therefore dependent on the sampling rate, the amount of power drawn by the receiver, as well as the amount of time required for the receiver to determine the two time difference words. This is called search and settle time.

Search and Settle Time

Search and settle time varies with the receiver design and is dependent on SNR. Figure 6 shows search and settle time as a function of SNR for four leading manufacturers of LORAN-C receivers. The great disparity in receiver performances, seems to vary with the sampling techniques on the front end and efficiency of use in the microprocessor. The Northstar 6000 receiver made by Digital Marine Electronics in Bedford, Mass. appears to be outstanding on this point plus field reports on this system are glowing. The Internav LC-123 is too new to know much about it and thus the dashed curve in the low SNR region of Figure 6. The Teledyne 701 data derived from the manufacturer are felt to be somewhat optimistic in light of test data derived by the Coast Guard on this unit. The Micrologic ML-200 data are felt to be realistic upper time bounds for power budget estimates for the case of a Gulf Stream study for the following reasons:

- (1) The U. S. Coast Guard Electronics Research Lab in Wildwood, New Jersey, which has been testing LORAN-C receivers which were marketed up to about 1-year ago, indicate that reliable master and slave station lock-on can only be obtained under low SNR conditions by the longer times shown in Figure 6.

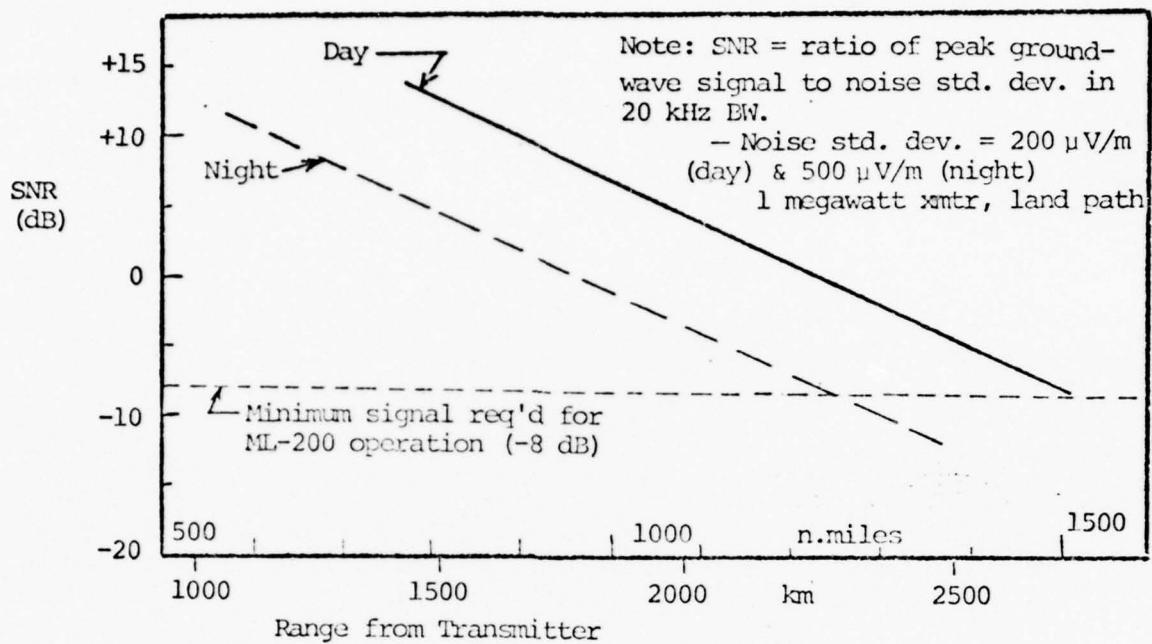


Figure 5 - LORAN-C Average SNR Variation with Range over Land (Micrologic Inc., 1975)

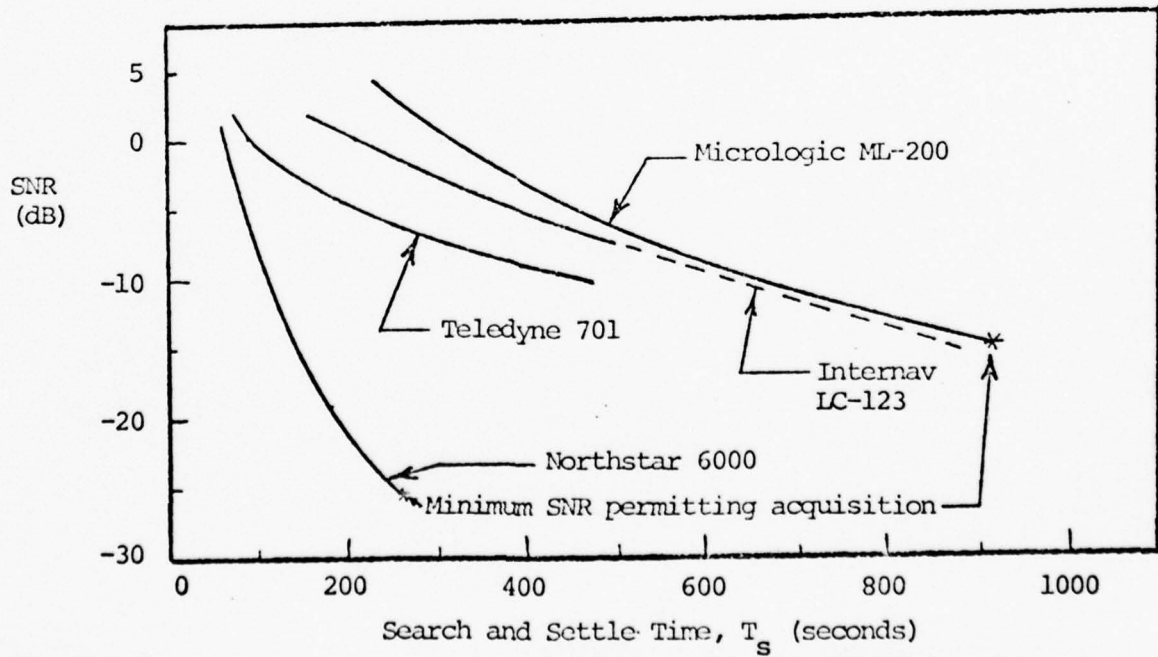


Figure 6 - SNR as Function of Average Search and Settle Time for Four Different LORAN-C Microprocessor Receivers

(2) With the addition of 2 new East Coast LORAN-C chains in 1978, the cross-rate interference problem between chains of different GRIs may make search plus settle times greater than originally measured by some receivers.

The cross-rate interference problem may not be present in tracking the Kuroshio (only one LORAN-C chain) but conservative time estimates must be used in the calculations.

3.3.5.2 Net Power Consumption

The amount of battery energy which must be stored to power the receiver over the entire 30-day experiment may be expressed as:

$$E = \frac{D S I P T}{3600} \quad (2)$$

where

E = energy storage required (watt-hr)

D = number of days of experiment = 30 (nominal)

S = no. samples/day

I_P = power drawn by receiver (watts)

T_S = average search and settle time (sec)

It can be seen that the amount of batteries required will be directly dependent on receiver power, sampling rate, and search and settle time. Thus, both power and speed of search and settle must be considered in order to determine how much energy a receiver will require.

Table 1 is a summary of the 30-day energy requirements as well as other pertinent parameters for four leading manufacturers of LORAN-C receivers that could be employed in a drifting buoy application. The details of the power budget calculation, and the sensitivity to sampling interval, are given in Appendix A. The receiver SNR employed in the calculations (i.e., 0 dB) is that of a typical night-time SNR (lower than daytime) at a distance of approximately 1850 km (1000 miles) from the station. This is felt to be

Manufacturer and Model Parameter	Micrologic ML-200	Digital Marine Electronics Northstar 6000	Internav (SIMRAD) LC-123	Teledyne Model 701
<u>Power Functions:</u>				
Power Drain	15.25 w.	38 w.	~18 w.	20.4 w.
T _s @ 0 dB SNR	~310 sec	~60 sec.	~240 sec.	~90 sec.
DC powered	yes	yes	yes	yes
Voltages	12/24/32vdc	10-40 vdc	12/32 vdc	12 vdc
<u>Front End Filters</u>				
No. Fixed Notches	4	0	None	0
Variable Notches	4	4	None	2
<u>Processing</u>				
Microprocessor	Intel 4004	Intel 8080	Intel 8080	Rockwell pps-4
Logic	TTL	TTL	Low pwr Schottky	TTL
Slaves Tracked	5	5	4	4
Blink Code	yes	yes	no	no
SNR Tracking	yes	yes	no	yes
Memory Avail.	extra cost	extra cost	extra cost	yes (option.)
FSK Output	no	no	yes (option)	yes (option.)
Field Experience	Fishing boats - very good	Commercial boats - excellent	New system ---- little experience	Considerable ---- very good results
Price: (*)				
Single:	~\$2600. (GSA)	\$3,200 (GSA)	~\$2450. (GSA)	~\$2900. (GSA)
Lot qty: (10+)	~\$1925. (GSA)	\$3200. (GSA)	\$2340. (GSA)	~\$2900. (GSA)
30-Day Energy Budget (1 pt/hr) (watt-hrs)	946.	456.	864.	367.

* Includes antenna coupler (~\$200.)

Table 1 - Summary Comparison of Leading LORAN-C
Receivers Adaptable to Drifting Buoy Applications

representative of a maximum distance found while tracking a western boundary current such as the Gulf Stream. The large deviations in the estimated search (i.e., signal acquisition) and settle (i.e., cycle selection) times of the various receivers seems to arise from design differences in the receiver front end. It appears that both the Northstar 6000 and the Internav LC-123 designs have placed a special emphasis on this aspect by achieving high signal power gains while maintaining linearity. In so doing it appears that more power may be dissipated in this portion of their units than with other designs. This front end signal conditioning may be especially important on a drifting buoy that would be retransmitting an HF or UHF signal through an adjacent antenna that may create a "noisy" environment.

The estimated prices shown in Table 1 were derived in a somewhat different manner for the Micrologic ML-200 system than for the other units. The ML-200 list price is based on a breakdown of prices for the key system elements: digital computer board (\$1566.), LORAN-C receiver (\$830.), antenna coupler (\$192.), and antenna (~\$100.). The prices of the other three units are estimates for a full system, including case, display lights, buttons, and antenna coupler, because that is the simplest manner by which they can sell systems and estimate price. The equivalent GSA list price on the Micrologic ML-200 is \$3775. (\$3104 for 10 or more). It would be a task for the system fabricator to remove the case and disconnect the lights. Perhaps this pricing aspect would change favorably for such systems as the Northstar 6000 if a more serious price quotation were sought on a quantity purchase. It should also be mentioned that approximately \$100. should be added to the costs given in Table 1 to account for an 8' LORAN-C whip antenna.

Many other manufacturers' catalogs were consulted but, at the time of this writing, their products were deemed to be not fully automatic enough for buoy operation. For example, some units required visual LORAN-C cycle matching with a cathode ray tube; while others did not contain a microprocessor for acquiring and tracking the LORAN-C signal. In the future, if the design suggested were to be implemented, the available units should be resurveyed because of the extremely competitive and rapidly-changing market for such systems. A few factors make for both a technical and marketing volatility for LORAN-C systems:

- (1) The advent of microprocessors and their lowering price and expanding capabilities.
- (2) The expanded capability on the LORAN-C system will bring in more land-based users.
- (3) The impending shut-down of the LORAN-A navigation system in approximately 1981 forcing fishermen and small boat owners to use LORAN-C.
- (4) The new 200-mile fishing limit and its patrol - possibly necessitating foreign vessels to employ automatic LORAN-C to be assured of compliance.

It does not appear as though any LORAN-C receiver manufacturer will build a new receiver employing low power CMOS (complimentary metal oxide semiconductor) logic. There are three very good reasons for not doing such:

- (1) CMOS logic, including even the more reliable ceramic encapsulated version, has not proven to be sufficiently reliable under the environmental conditions to which the average LORAN-C receiver would be subjected at sea. The average market, which is being addressed by the manufacturers, is that of fishing vessels and larger ships on which the receiver is installed in the pilot house - subjected to the hazardous environment of humidity, vibration, and salt air.
- (2) There is no strong, compelling reason to reduce the power consumption of the receiver from a range of 40 to 75 watts (including display lights) to approximately 20 or 30 watts (again including lights) when vessel power in these ranges is readily available.
- (3) There are not as many desirable design components available employing CMOS logic.

If a CMOS version of the stripped-down receivers described in Table 1 (i.e., no display lights) were implemented, the power dissipations would drop to the 3-5 watt range - consumed primarily in the front end receiver and antenna coupler.

3.4 Navy Navigation Satellite System (NNSS) or TRANSIT

The Navy Navigation Satellite System (NNSS), often referred to as the TRANSIT System, has been in existence since 1964. It consists of 5 polar-orbitting satellites (1.8 hour orbital period) which permit a position fix approximately every hour and one-half to an accuracy of .04 km to 2 km depending on the receiver sophistication and knowledge of receiver velocity. In order to obtain the highest accuracy a user, such as a large ocean-going ship, generally uses a receiver which costs over \$20,000. It has been suggested by Westerfield (1972) that a simplified TRANSIT receiver be installed aboard a drifting buoy for the acquisition of trajectory data only, anywhere in the world. Such a receiver would cost approximately \$5,000 (in quantity), give an accuracy of the order of 2 km, a fix approximately every 1.5 hours, and require approximately 660 watt-hours of electrical energy over a 30 day mission. Such power consumption would necessitate approximately 40 pounds of alkaline cells. The suggested system provides no capability for sending additional ancillary data such as a drogue indicator, wind speed, or barometric pressure. Because many of the above factors do not meet the system objectives the TRANSIT system was rejected at present. It is, however, possible that in the future a low power-consuming receiver may be efficiently manufactured in quantity with adequate accuracy such that it may become more competitive with other systems described. In light of the fact that the Global Positioning System (GPS) will replace the function of TRANSIT in the 1980's it is felt that such a TRANSIT receiver will not be made.

3.5 NAVSTAR Global Positioning System (GPS)

The Global Positioning System (GPS) is a high accuracy satellite positioning system being designed primarily for the U. S. Military under Air Force sponsorship. Until recently both the Navy and Air Force were pursuing designs of similar systems - the Navy system being called Timation was destined to be the successor to TRANSIT. For efficiency all efforts have recently been channeled into the GPS effort only. The GPS system is expected to exhibit an overall positional accuracy (including all error sources) of approximately 10-15 meters independent of vehicle velocity with positions provided on command. TRANSIT, on the other hand, is inherently velocity sensitive (unless very costly equipment is used) and only provides fixes on a periodic basis while requiring a total 20-minute pass in order to acquire a fix.

The GPS system will eventually consist of 20 polar-orbiting satellites (12 hour period) such that 4 satellites are always in view at any time. The present schedule calls for a 2-dimensional GPS capability to be ready in 1980 (good for surface oceanography) and a 3-dimensional system ready by 1984 (Dennis, 1975). The satellites will transmit 2 carrier frequencies - one signal coded in a jam-resistant manner for the military and another coded in a well-defined manner for all types of use. It appears that the accuracy of the non-military channel may be poorer than that described already but still more than adequate for the needs of drifting buoys.

At present it appears that one manufacturer may try to come out with a "Spartan" GPS receiver which they will attempt to market for approximately \$2000. There is no word yet on power drained from such a unit. Lastly, although the GPS system may be available for general usage there may be a use charge associated with it which should be factored into system cost analysis.

In summary it appears that the GPS system has many features which are appealing for a drifting buoy positioning system of the future. Because of its schedule and unknowns associated with buoy system costs and power, the system cannot be fully examined at present.

3.6 Other Positioning Systems

Other drifting buoy remote positioning systems are available but are generally of such low accuracy or limited range that they are inapplicable for the study of higher frequency motions of western boundary currents. For example, Kirwan and McNally (1975) tracked drifting buoys in the North Pacific with over-the-horizon (OTH) radar receiving signals from a transmitter on the buoy. The buoys were tracked to ranges of approximately 3000 km. with a positional accuracy of approximately ± 8 km. In addition, Whelan et al (1975) of the ITT Electro Physics Lab designed, built, and marketed a low cost drifting buoy positioning system using an HF transmitter. A $\pm 1/2^\circ$ azimuth resolution was claimed on the HF direction-finding system. The limited range and accuracy of such a system (~ 300 km, max.), problems with night-time HF radio interference, plus the cost of manning two shore stations for signal triangulation, were factors making the system unuseful for the purposes described.

4.0 TELEMETRY OF BUOY POSITION AND SENSOR DATA

The telemetry of data from the buoy is the major problem associated with the given design. There are only two means for the transmittal of buoy data - high frequency (HF) radio signals employing frequency shift keying (FSK) or the use of satellite transmitters. There is a choice of two relatively low cost satellite systems for the expected buoy deployments of 1979-1980, the TIROS-N or the GOES satellite. Each system of data return has its positive and negative aspects and will be described in this section.

4.1 Satellite Telemetry

The TIROS-N and GOES satellites are the only real candidate satellites for drifting buoy applications because of their low system cost and power consumption. Other systems, available or projected for the transmittal of data, are possible candidates, but their system or usage costs (or both) are too high. These systems will be mentioned in Section 4.1.3.

4.1.1 TIROS-N Satellite Telemetry

The TIROS-N Buoy Transmit Terminal (BTT) is a low cost transmitter (~\$1600. with antenna, single qty) that employs a reliable telemetry system with considerable experience derived from its progenitors, the BTT/NIMBUS-6 system and the IRLS (Interrogation, Recording and Location Subsystem) aboard the NIMBUS II and III satellites. The TIROS-N satellite should be launched and available for use in mid-1978. NASA, Goddard Space Flight Center, who operates the NIMBUS and TIROS satellites, promises only one position and telemetry link per day, from each satellite at \pm 5km (i.e., 3σ data) accuracy, but investigators have been deriving data at frequencies of 2 to 8 times per day from a single NIMBUS-6 satellite. These positions are accurate to approximately \pm 1-2 km with repeatabilities of less than \pm 1 km (i.e., 3σ limits). There will be 2 sun-synchronous, polar-orbitting TIROS-N satellites with a 108-minute orbital period. Each satellite should be visible at least twice per day. Because only one satellite will be operable for a while, awaiting the launch of the second, and because one satellite may become inoperable at a future date, the TIROS-N data telemetry link will be conservatively based

on a single satellite. If the 2 satellite systems were analyzed the design would vary little.

It will be assumed that a half-redundant data point, with the word structure for each data point as shown in Appendix A, will be radioed up to the satellite every 12 hours. The 4 least significant digits of a LORAN-C TD (including tenths of microseconds) are coded as 12-bit words.

A strawman LORAN-C/TIROS-N hybrid buoy positioning system is described in Figure 7. A typical power budget and cost for such a system is given in Table 2 based on the Micrologic ML-200 microprocessor LORAN-C receiver described in Table 1. This receiver is chosen because of its adequate performance and low cost. The key features of the system which make it more complex and yet very flexible are the system sequencing logic and on-board memory - both of which are necessarily powered all of the time. Because of their low power drains, the temperature and barometric pressure sensors as well as the drogue indicator are assumed to be powered up all of the time. The memory is assumed to be necessary because the LORAN-C TD's must be stored between periodic position fixes, awaiting telemetry to the satellite. The high power requirements of the present microprocessor LORAN-C receivers require that, between position fixes, the unit be powered down. If such were not the case the receiver energy consumption would increase 15-fold from its already burdensome 946 watt-hours for hourly fixes.

Wherever possible CMOS logic is employed in order to conserve power. Special care should be taken in order to employ high reliability, ceramic-encapsulated components. The estimated prices reflect single unit purchases (except for the LORAN-C receiver) after developmental or design work is completed on the timing and memory circuitry. Care will be taken not to require alteration of the manufacturer's microprocessor functions and programs. Certain elements in Figure 7 are eliminated for simplicity. For example, it is assumed that the signal from the existing off-the-shelf microprocessor receiver is readily inputted to a random access memory (RAM) or to a simple first-in, first-out buffer memory. These signals will in most cases have to first be converted to the proper form (parallel-to-serial conversion, etc.) for acceptance by the memory. In like manner, the signal from the memory to the satellite transmitter may require changes in order to interface properly. These additions add very little to the system cost, because components are inexpensive, but do complicate the engineering somewhat. The next section will indicate a design that is much simpler but more expensive.

Component	Current Drain (ma)	Voltage (Volts)	Power Drain (Watts)	Energy/30 days @ 1 fix/hr (watt-hrs)	Component price after Development
LORAN-C μ-proc. rcvr and antenna	1270	Assume +12	15.25	946	~\$2100.-
Clock* & Sequencing Functions	10 ma.	+5	.05	36.	\$80.-
CMOS* Memory	.000020	+5	.0001	.07	\$10.-
Water Temperature	.00024	+12	.003	2.2	~\$100.-
Barometric [†]	1.0	+12	.012	8.6	~\$500.-
Drogue Indicator	nil	+12	nil	nil	~\$100.-
TIROS-N XMTR + Antenna	550	+12	6.6 (max)	83.9	\$1600.-
TOTALS	1831	-	21.92	1076.8	\$4490.-

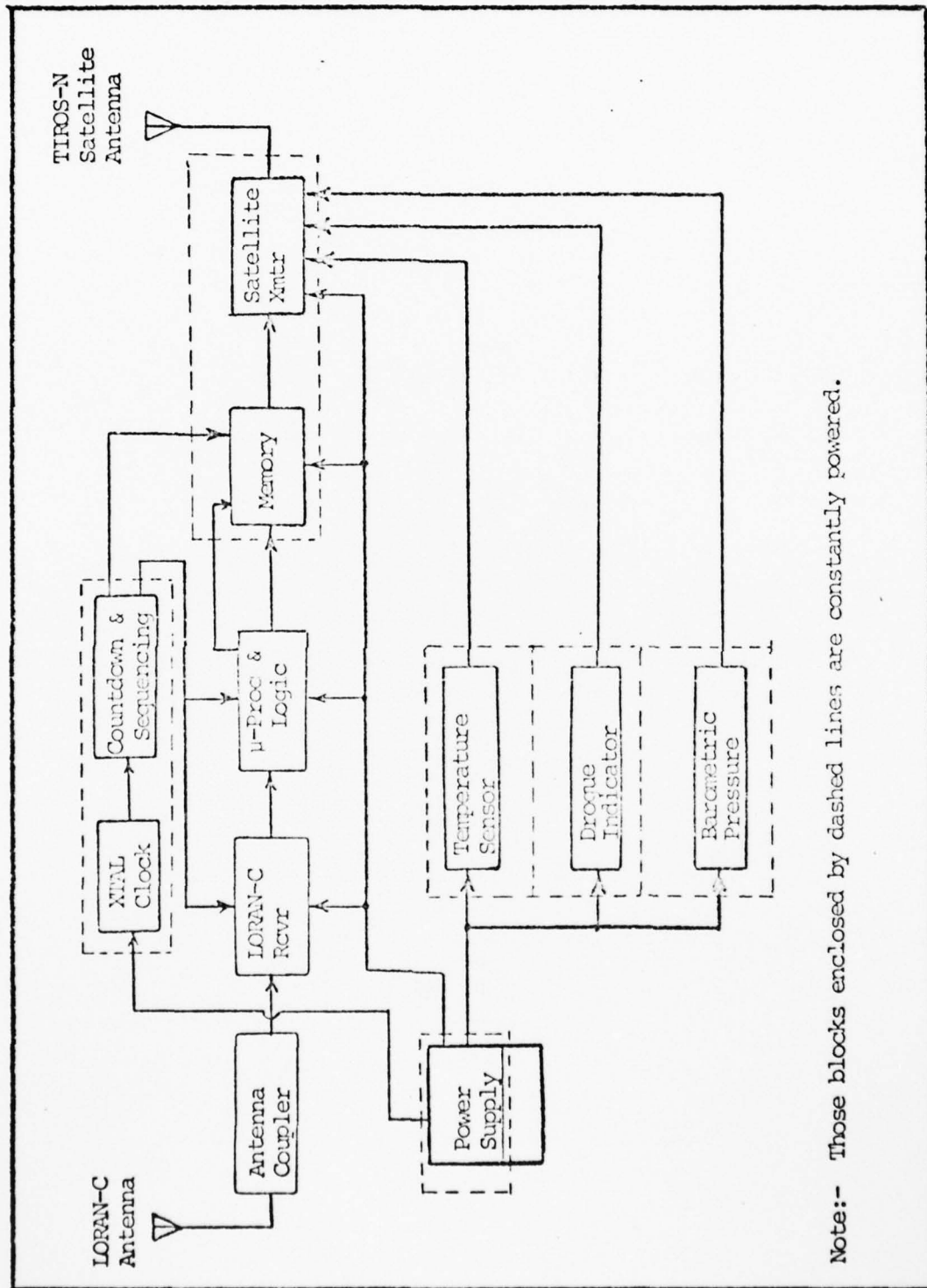
Note:- Estimated power drains include power supply voltage regulation.

-*Asterisks indicate required design work - others off-the-shelf.

-†Dunker-Ramo (NCAR) barometric pressure all assumed.

ξFor Northstar 6000 unit: 586 w-Hrs, \$5690. (tot.)

Table 2 - Typical Power Budget and Unit Cost for a
LORAN-C/TIROS-N Hybrid Drifting Buoy
Positioning System



Note:- Those blocks enclosed by dashed lines are constantly powered.

Figure 7 Block Diagram of LORAN-C/TIROS-N Hybrid Drifting Buoy Positioning System

4.1.2 GOES Satellite Telemetry

Because the GOES satellites are synchronous over the equator (75° w. long, 100° w. long, and 135° w. long) a drifting buoy positioning itself by LORAN-C can immediately get access to GOES for data transmittal. In this way the system does not require an on-board memory capability. The design problem is reduced to mainly that of a clock/sequencing function for the LORAN-C microprocessor and proper data handling (see Figure 7). The power budget and costs for such a system (single qty) are summarized in Table 3. This nominal power budget assumes a pair of 12-bit LORAN-C TD's; one 12-bit measurement of barometric pressure and water temperature, and a 4-bit drogue indicator word - totalling 52 bits of data transmitted every hour. The timed acquisition of the TD's is governed by the clock and sequencing circuitry. As soon as these data are ready (after search and settle time) they are fed directly to the GOES in a BCD format. They are immediately transmitted along with the P_{baro} , T_{water} , and drogue indicator; which are instantaneously sampled and digitized within the GOES transmitter.

The GOES transmitter telemeters up to 16 words per transmission at 100 bits/sec in the following general format:

GOES Timing Format (Hourly Data Transmissions)

Carrier Enable:	5.0 sec
Manch-Coded bit sync	2.5 sec
15-bit (max.) sequence	.15 sec
31-bit command word	.31 sec
52-bit data word	.52 sec
<hr/>	
Total Time:	8.48 sec

The transmitter consumes .05 watts (quiescent) between transmissions and 40-watts during the above estimated transmission period. This leads to a 30-day energy budget of 108.8 watt-hours as shown in Table 3. The resulting total energy requirement for the LORAN-C/GOES hybrid system is estimated to be 857.7 watt-hours - requiring approximately 45-pounds of alkaline cells.

Component	Current Drain (ma)	Voltage (Volts), DC	Power Drain (Watts)	Energy/30 days @ 1 fix/hr (watt-hrs)	Component Price after Development
LORAN-C -proc. rcvr and antenna	1270	12	15.25	702	~\$2100.-
Clock and Sequencing Functions	10 ma	+5	.05	36.0	\$80.
CMOS Memory	.00002	+5	.0001	.07	\$10
Water Temperature	.00024	+12	.003	2.2	~\$100
$P_{\text{barometric}}^+$	1.0	+12	.012	8.6	~\$500.
Drogue Indicator	mil	+12	mil	nil	~\$100.
GOES ξ Satellite Transmitter + Antenna	3300 (max) .04 (quiescent)	+12	40 (max) .05 (quiescent)	103.8	\$3300.-
TOTALS:	4581 (max)	-	55.3 (max)	857.7	\$6190.-

+ Assume Bunker-Ramo (NCAR) P_{baro} sensor

ξ Assuming 52 bits/hr (i.e., 2 TD's, p, T, drogue indicator)

Table 3 - Typical Power Budget and Unit Cost for a LORAN-C/GOES Hybrid Drifting Buoy Positioning System

The GOES energy estimate is very comparable to that of the LORAN-C/TIROS-N hybrid system which might require 1076.8 watt-hours. The GOES system would, however, cost approximately \$1700. more per buoy than the TIROS-N hybrid, but engineering development costs associated with implementing the TIROS-N memory would somewhat offset this cost difference. The original proposal called for the deployment of six expendable drifting buoys every three months for two years or a total of 48 buoys. At a differential cost per buoy of \$1700. this amounts to a total cost difference of \$81,600. over the 2-year life of the experiment. If the LORAN-C/TIROS-N system shown in Figure 7, were designed and implemented the memory costs shown in Table 2 are negligible (i.e., ~\$10. per buoy). The engineering and test costs associated with implementing the memory and timing interfaces to the TIROS-N transmitter are conservatively estimated to be less than \$20,000. The overall battery-pack costs and reliability of each system in terms of longevity and data quality are felt to be equivalent. Therefore, it is estimated that the LORAN-C/TIROS-N hybrid design would cost approximately \$60,000. less than the LORAN-C/GOES system over the 2-year life of the planned experiment.

4.1.3 Other Satellite Data or Telemetry Links

There are numerous other satellites which are useful for either military purposes, earth monitoring programs, or data and voice communications from sea. This section will briefly describe some of the most frequently-mentioned systems to varying levels of detail.

MARISAT

A communications satellite operated by Comsat General Corporation for the U. S. Navy and private use. It provides ship-to-shore and shore-to-ship telegraph and telephony service working in the GHz (private use) and UHF (U. S. Navy) frequencies. It requires a 1.2-meter diameter gimballed (stabilized) antenna. Systems generally find usage on offshore oil rigs and exploration vessels. Costs for purchase, rental, and use are high compared to the guidelines in this report.

GEOS

A geodetic earth observation satellite with no communication or location capabilities. This type of satellite is still being launched by the multi-nation European Space Agency.

LANDSAT (formerly ERTS)

LANDSAT is the new name for the NASA Earth Resource Technology Satellites (ERTS) which contain multi-spectral scanners for earth monitoring. There are no on-board communication or location capabilities on LANDSAT.

SEASAT-A

SEASAT-A is part of the NASA applications satellite program. To be launched in mid 1978, it will carry a radar altimeter, capable of measuring sea surface topography (including currents and tides); a radar scatterometer in order to measure surface winds by their effect on capillary waves; a scanning multi-frequency microwave radiometer for the measurement of sea surface temperature; and a synthetic aperture radar, capable of providing data on ocean waves, coastal regions, and sea ice (personal communication).

Estimates of the locations of currents can be inferred through measurements of sea surface topography and temperature. The temperature resolution of the multi-frequency radiometer will vary from 0.34 to 1.09°C , depending on the frequency used. This temperature resolution represents an average over a footprint whose smallest size is 21×14 km. The temperature resolution would be potentially adequate for the study of boundary currents but the spatial resolution is too coarse. An additional modest visual and infrared imaging instrument will be aboard SEASAT-A but it will only be capable of a 1°C resolution with a surface resolution of 9 km - again too coarse.

The performance and data from SEASAT-A should be closely followed as a strong adjunct to near-surface studies of not only western boundary currents but such areas as rings and internal waves. The capability to remotely monitor temperature, sea state, and wind field data may provide the necessary data base for more accurately assessing the quality of Lagrangian drifter data (i.e., slippage estimation).

ATS-5

The NASA Applications Technology Satellites allow the transmittal of voice, teletype, facsimile, and coded data to shore via geostationary satellites. Positions to an average accuracy of approximately 2.0 km are also available. The systems are finding increased use aboard ocean research vessels to effectively link the vessel to shore-based computers. The system would be inappropriate for a drifting buoy application because it requires a directional or steered antenna on the buoy.

4.2 High Frequency (HF) Data Telemetry

The feasibility of using frequency shift keying (FSK) single sideband (SSB) high frequency telemetry has been examined. High frequency telemetry enables the experimenter to know the buoy's position immediately after the LORAN-C coordinates have been transmitted, without the delay and possible cost required for satellite services or the costs and problems involved in using a privately-purchased TIROS-N ground station interrogation unit. It is not possible to use the LORAN-C pulses to directly modulate an HF carrier because of HF bandwidth limitations. It might be possible to use a hard-limited LORAN-C signal (i.e., square-wave) for modulation, but timing delays in HF propagation would seriously degrade the LORAN-C accuracy.

A buoy mounted HF transmitter is cheaper and more flexible than a satellite system, but monitoring stations would have to be maintained and reliability would not be as good as with a satellite system (Livingston et al, 1977).

The system considered here is very simple in order to remain within the economic constraints. A multi-frequency system such as that described by Livingston et al (1977) or that in the report by the Intergovernmental Oceanographic Commission (1967) could be employed in order to increase reliability, but system costs and power consumption would increase beyond the design guidelines. A single frequency system, besides being simple, avoids problems of antenna detuning and radiating inefficiency, while employing an on-board timer, data memory and ionospheric predictions in order to optimize the quality of transmission.

In order to increase the data reliability of a single frequency system it will be assumed that transmissions are made at local noon and midnight. Each transmission will contain the data from the previous 24 hours, with each transmission repeated three times. This format results in each data point being transmitted six times - three times at noon and three times at midnight. Later discussion will show that around midnight a particular frequency choice will lead to the maximum probability of reliable skywave data transmittal on a year-round basis while maximizing noon-time ground-wave propagation. This frequency could be changed to optimize predictions for a particular time of year - but only within allotted frequency bands. The transmissions from the system should be self-timed with an output power of 100 watts to an 8-foot whip antenna. The nominal data rate is conservatively assumed to be 100 bits/sec.

Power

Supplying power to the transmitter is a primary consideration. Although the transmitter draws a large amount of power, transmissions are short enough such that the total power consumed over a 30-day experiment is not impractical. The total amount of time that the transmitter must be on is determined by the total amount of data to be transmitted each 12 hours. Based on a nominal one position sample/hour, (i.e., 2, 12-bit TD's) with water temperature, barometric pressure, and the drogue indicator being sampled every 12 hours, the data format shown in Table 4 is assumed (see also Appendix B).

Table 4

HF Transmitter Data Word Structure

Parameter	Bits/Word	Max. Words/12 hr	Total Bits
LORAN-C, TD ₁	12	12	144
LORAN-C, TD ₂	12	12	144
Water Temperature	12	1	12
P _{baro}	12	1	12
Drogue Indicator	4	1	4
			<hr/>
		data bits recorded/12 hrs. :	316
		data bits transmitted/12 hrs :	632

Assuming that 632 data bits must be transmitted every 12-hours results in an HF transmission time computed as follows:

Transmit Format

- (1) Warm-up 5.0 sec
- (2) Carrier enable and bit sync (from Picquenard (1974)) 7.5 sec
- (3) 632 bits/100 bits/sec 6.3 sec

Total Transmitter On-Time: 18.8 sec

It is assumed that six such transmissions are made each day with approximately 100-watts of power to the antenna while consuming approximately 200 watts total. As a power safety margin it is assumed that during the warm-up time the transmitter is also consuming 200 watts. During the "off" time there is no standby power consumption because the system is assumed to be fully activated by a low power clock in the same manner as the LORAN-C receiver. The above power profile leads to a total 30-day energy consumption computed as follows:

$$\bar{E}_{HF} = 30 \text{ days} (6 \text{ transm/day}) (18.8 \text{ sec/trans}) \frac{(200 \text{ w.})}{3600}$$

or:

$$\bar{E}_{HF} = 188 \text{ watt-hours}$$

This amount of energy could be provided by approximately 10-pounds of alkaline batteries.

Frequency

A frequency in the 4.1 mHz oceanographic band (i.e., 4.1625 to 4.1660 mHz) was chosen for this analysis. This choice was made to allow a large portion of the Gulf Stream to be covered using reliable ground-wave propagation. While this choice of frequency eliminates the possibility of long range skywave propagation during the day, adequate skywave propagation can be expected at night.

Signal Strength

The foremost problem associated with high frequency telemetry is predicting the signal-to-noise ratio for different times of day, year, and sunspot cycle. High frequency waves are propagated by many modes, and the background noise is also highly variable. If frequency shift keying (FSK) modulation is used, a shore-based received signal-to-noise ratio of 10 db would be required according to Picquenard (1974).

4.2.1 Ground Wave HF Telemetry Link

The most reliable propagation mode available is the ground wave. No ionospheric reflection is required, so this mode is less subject to the cyclic variations which dominate the other modes.

The most likely frequency for ground-wave use is 4 mHz. The ITT handbook entitled "Reference Data for Radio Engineers" indicates that atmospheric noise increases by about 55 db/decade below 4 mHz. Above 4 mHz, ground-wave propagation losses increase by about 23 db/decade. Additionally, above 5 mHz scattering and ground-wave/skywave interaction degrade ground-wave propagation.

The ground-wave field over sea water, for 1 kw of radiated power, appears in Figure 8, taken from Picquenard (1974). The atmospheric noise level was also computed from figures in Picquenard's book. Figure 9 is an example of such a table. The noise data, nominally presented in db above 1 watt, have been converted to db above $1\mu\text{v}/\text{m}$ (see Picquenard, p.212) for compatibility with the ground-wave field data. Fluctuations and uncertainty margins are included in order to make the noise data valid for 95% of the time at the worst time of year. Calculations are shown in Appendix B.

Antenna gain is the remaining factor needed in order to predict receiver signal-to-noise-ratios for the ground-wave mode. The following conservative assumptions will be made:

Receiving antenna gain 0 db

Transmitting " " -15 db

Additionally, $10 \log \frac{100}{1000} = -10$ db must be added to the curves for field strength, as those curves are for 1 kw radiated power while the system described employs 100 watts. Combining field strength, power, antenna gain, and noise yields the receiver SNR.

If a receiving antenna with high gain is used (a certainty if military receiving stations are used), the antenna gain can be added to the S/N ratios obtained.

4.2.2 Ionospheric Wave HF Telemetry Link

Ionospheric waves are capable of propagation over much longer distances. However, conditions vary greatly with time of day, year, and sunspot cycle. Additionally, many modes of propagation exist in the high frequency band. Consequently, performance is much more difficult to characterize than with ground-waves.

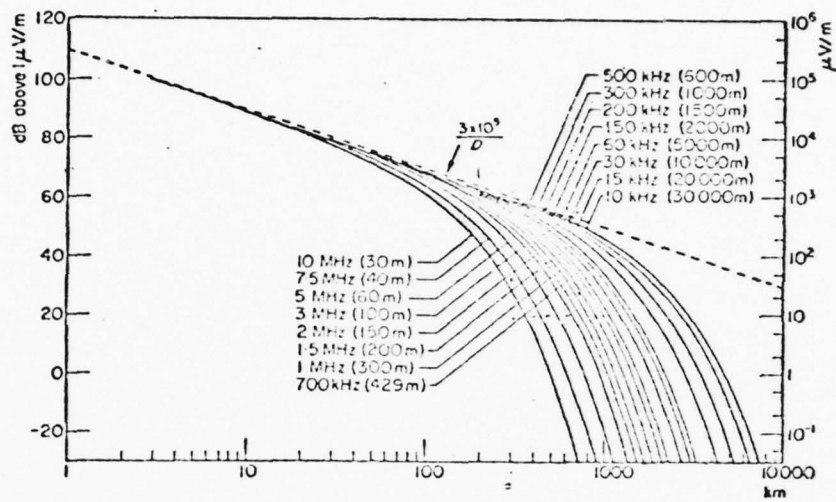


Figure 8 - Ground-Wave Field Over

The Sea for 1 Kw of

Radiated Power,

$$\sigma = 4 \Omega^{-1} \text{m}^{-1}, \epsilon = 80$$

(from Picquenard, p. 220)

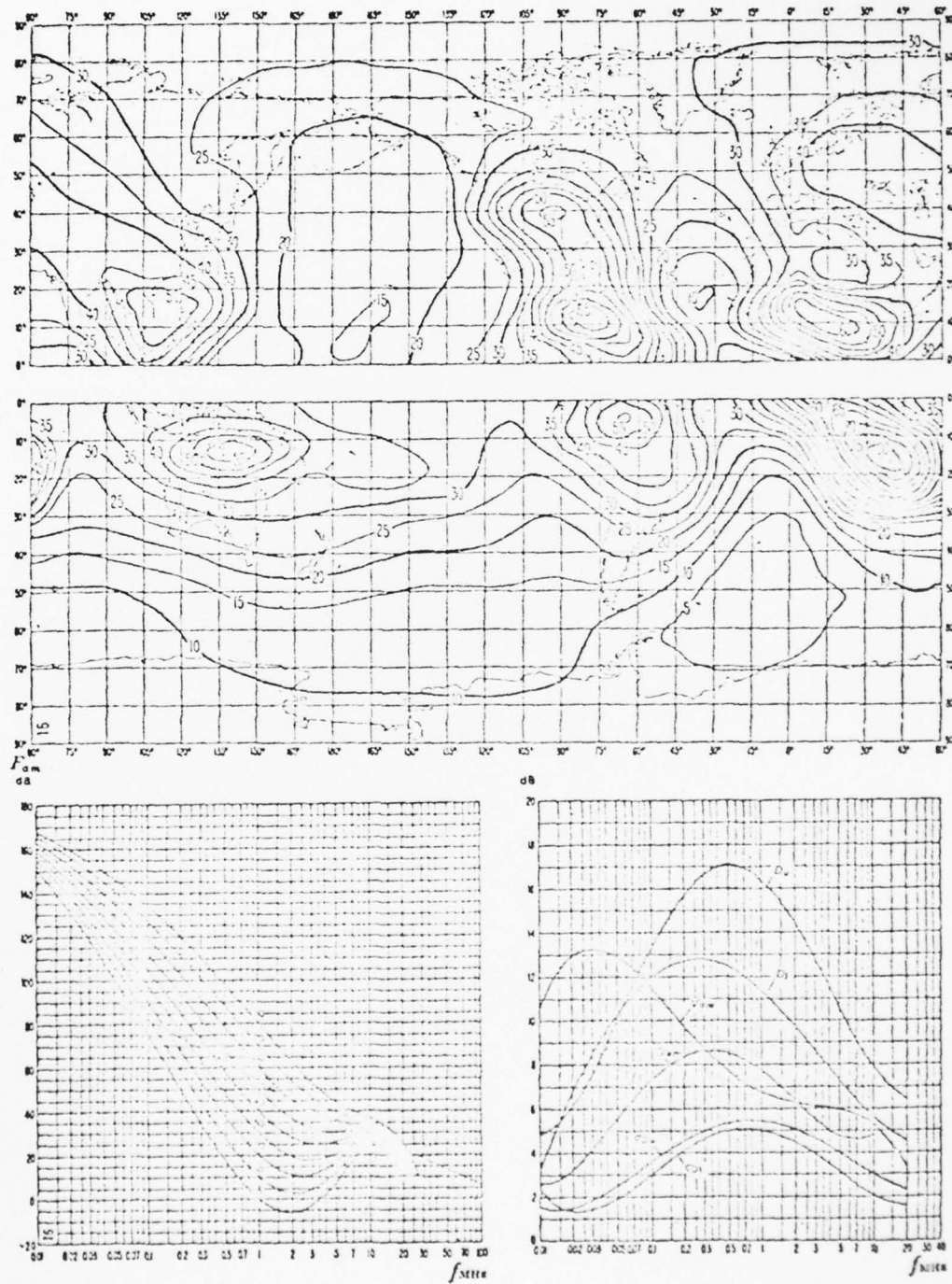


Figure 9 - Typical Noise Chart for HF
 Radio Waves on Summer Day
 Between 0800 and 1200 Hrs
 (from Picquenard p. 202)

AD-A047 096

TEXAS A AND M UNIV COLLEGE STATION DEPT OF OCEANOGRAPHY
GULF OCEANOGRAPHY-GULF STREAM STUDY (GUSS). (U)

F/G 8/3

SEP 77 A D KIRWAN

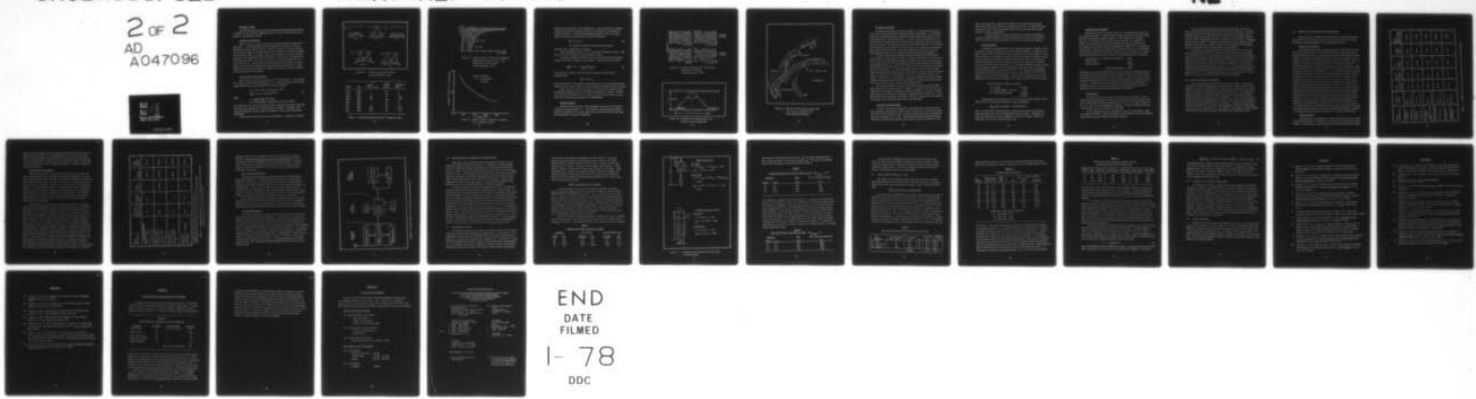
N00014-75-C-0537

UNCLASSIFIED

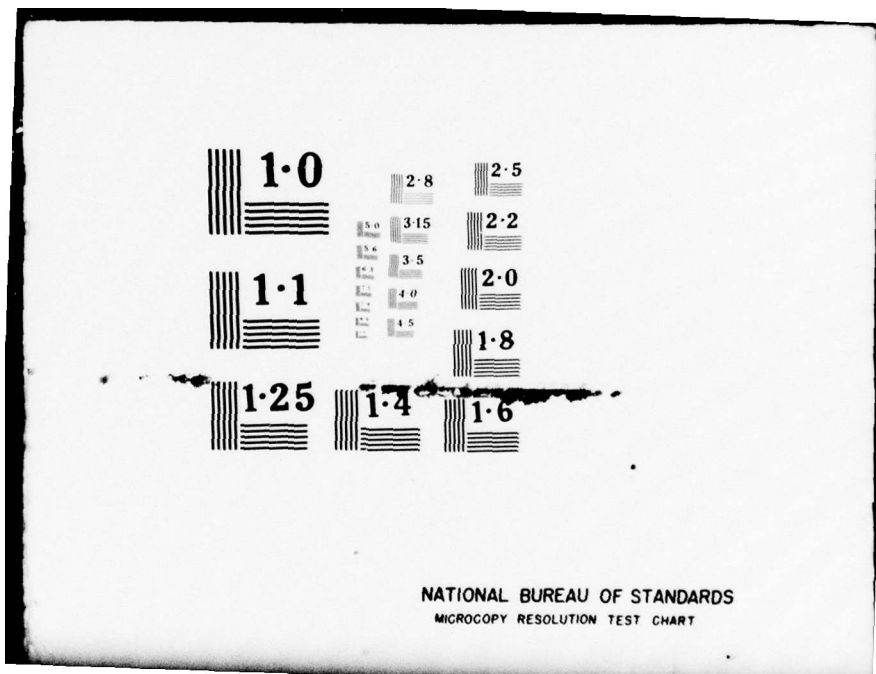
TAMU-REF-77-3-F

NL

2 of 2
AD
A047096



END
DATE
FILED
I- 78
DDC



Ionospheric Modes

The primary modes for high frequency ionospheric propagation are shown in Figure 10, with the main ionospheric layer (i.e., F_2 -layer) existing at a height of approximately 300 km.

Ionospheric Absorption

This is one of the major factors in determining signal strength over a given path. It is characterized by the absorption coefficient A , which is dependent on zenith angle of the sun, season of the year, and solar activity. The absorption index for the Gulf Stream area of interest is shown in Figure 11 for June and December at midnight and noon for extremes of the sunspot cycle. Figure 12, from Piequenard (1974), shows how the signal field is dependent on the absorption index. At 4.1 mHz, the signal field drops rapidly even for small values of A . Therefore ionospheric propagation over distances greater than those achievable by ground-wave propagation is only practical at night. Figure 13 shows field strength as a function of distance from the transmitter for the F_2 skywave mode at night.

Availability of Skywave Modes

The E and F_1 layers are not useful for our requirements. The equations for E and F_1 layer critical frequencies (i.e., frequencies above which a vertically-incident wave is not reflected) are given as follows:

$$\begin{aligned} f_0 E &= 0.9 [(180 + 1.44 R) \cos x]^{0.25} \\ f_0 F_1 &= (4.3 + 0.01R) \cos^{0.20} x \end{aligned} \quad (3)$$

where:

x = zenith angle of the sun

R = sunspot number (unimportant for this writing)

These equations show that the critical E and F_1 frequencies approach zero when the zenith angle reaches 90° (around sunrise or sunset). Therefore, when absorption decreases enough to permit propagation, the E and F_1 layers have disappeared.

The F_2 layer behaves well for this application. Propagation should be

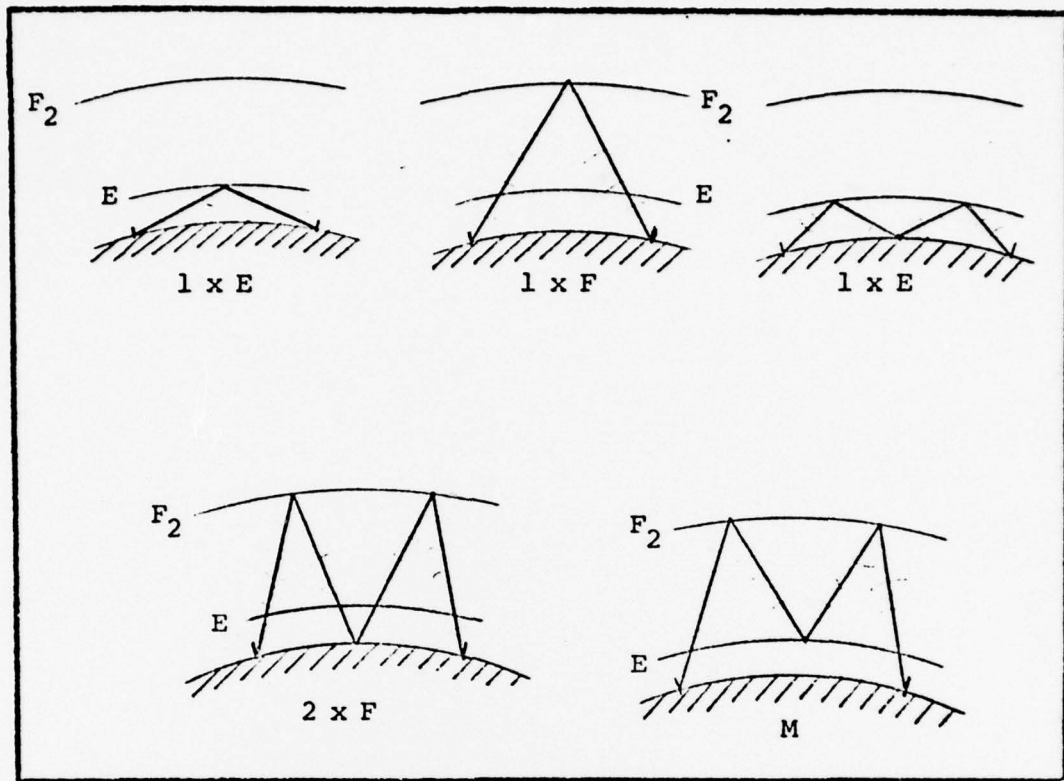


Figure 10 - HF Skywave Propagation Modes
(from Picquenard p. 133)

Month	Time	x° Solar Zenith Angle	R_{12} Sunspot Number	A Absorption Index
June	0000	-	20	0
June	0000	-	150	0
June	1200	15°	20	1.04
June	1200	15°	150	1.50
Dec	0000	-	20	0
Dec	0000	-	150	0
Dec	1200	60°	20	0.72
Dec	1200	60°	150	1.13

Figure 11 - Maximum and Minimum Values of Absorption Index

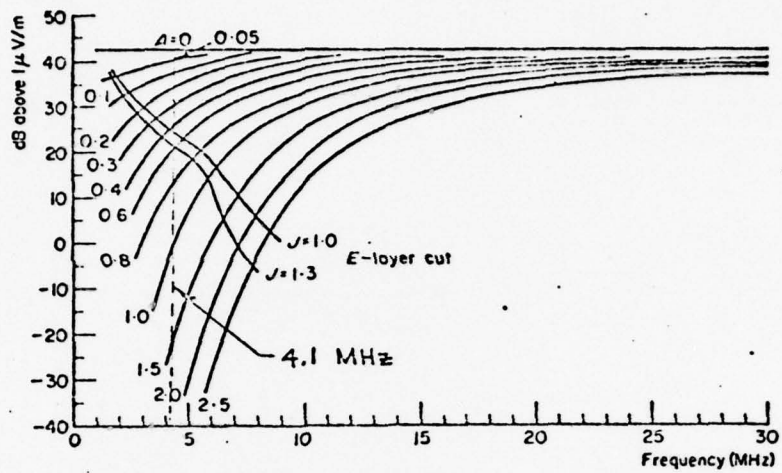


Figure 12 - Signal Field as a Function of Frequency
and Absorption Index (A) for $1 \times F_2$
Reflection at 1200 km Range
(from Picquenard p. 272)

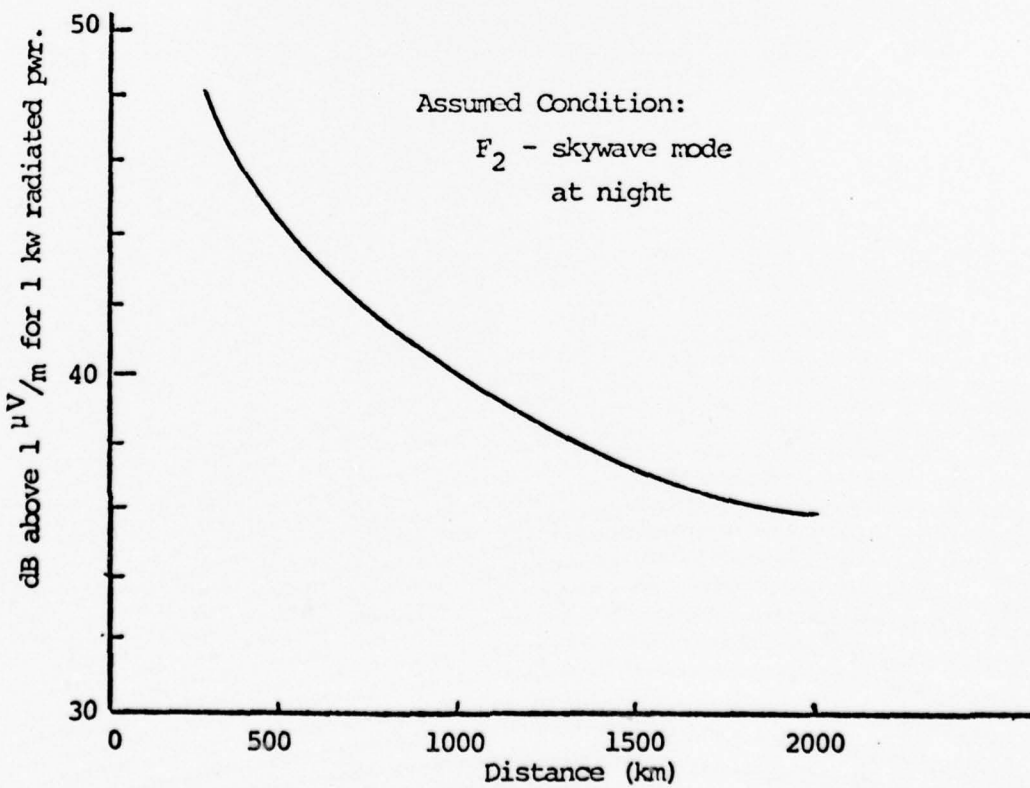


Figure 13 - Signal field as a Function of Distance
for 1 kw Radiated Power

possible at the extremes of the sunspot cycle. When the number of sunspots is high, the critical frequency exceeds 4 mHz throughout the evening, as shown in Figure 14. As the Maximum Useable Frequency (MUF) will always exceed the critical frequency (f_c) through the relation:

$$MUF = f_c \sec \phi \quad (4)$$

(ϕ = angle of incidence at the reflecting layer)

therefore the F_2 mode should be present.

When the sunspot number is low, the critical frequency is lower. However, it is still adequate for propagation at 4 mHz.

In order to explore the effect of oblique incidence on MUF, the hypothetical case shown in Figure 15 is examined. Ignoring spherical effects:

$$\frac{1}{\sec \phi} = \cos \phi = \frac{h}{[(D/2)^2 + h^2]^{1/2}} \quad (5)$$

For a distance of 600 km with an F_2 -layer height of 300 km equation indicates that:

$$MUF = 1.41 f_c$$

Along with Figure 14 this predicts that propagation will be possible throughout most of the evening (that is, when the critical frequency exceeds 3.0 mHz).

When the buoy is within about 200 to 300 km of the receiving station a different situation arises as indicated in Jenkins et al (1967). The MUF for ionospheric propagation is not raised sufficiently for reliable service and hence reliance must be placed on the ground-wave.

Combined Results

Expected signal-to-noise ratios throughout the range of Gulf Stream interest are shown in Figure 16. The available receiver signal-to-noise ratios are computed for the worst time of year at the best time of day (noon for ground-waves, evening for skywaves).

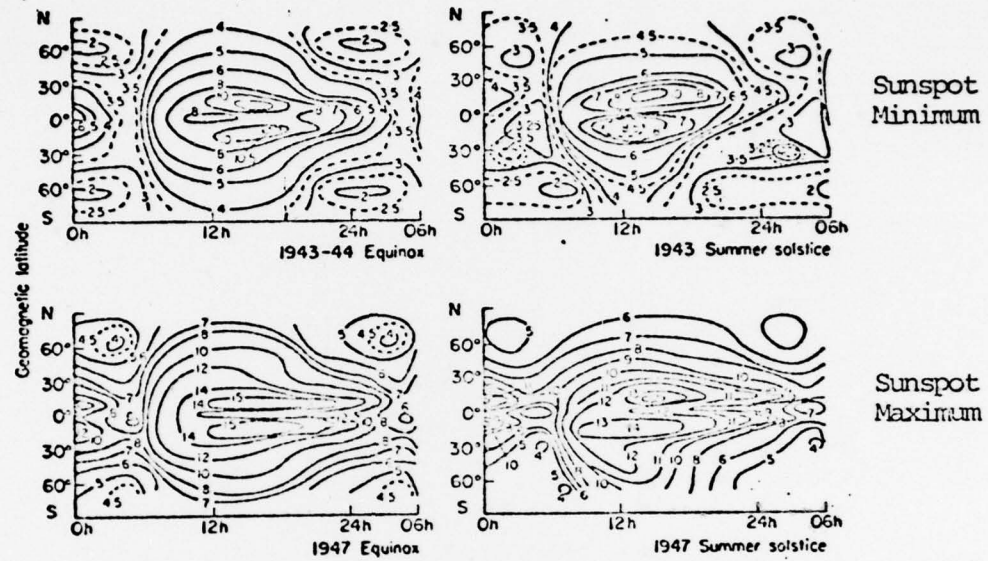


Figure 14 - Critical Frequency (MHz) for F₂-Layer
Ionospheric Reflection
(from Picquenard p. 124)

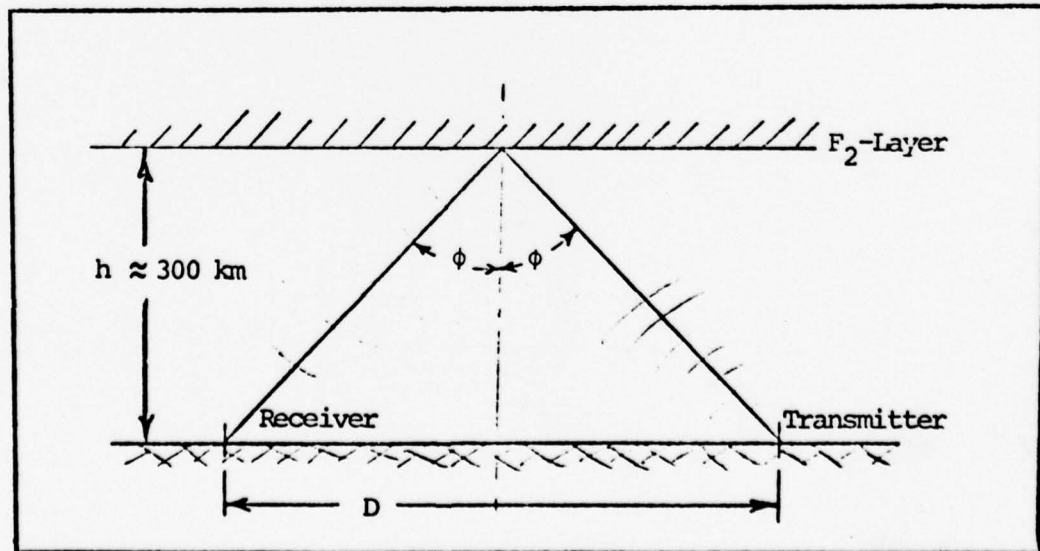


Figure 15 - Definition of Incident Angle ϕ for
One-Hop F₂-Layer Propagation

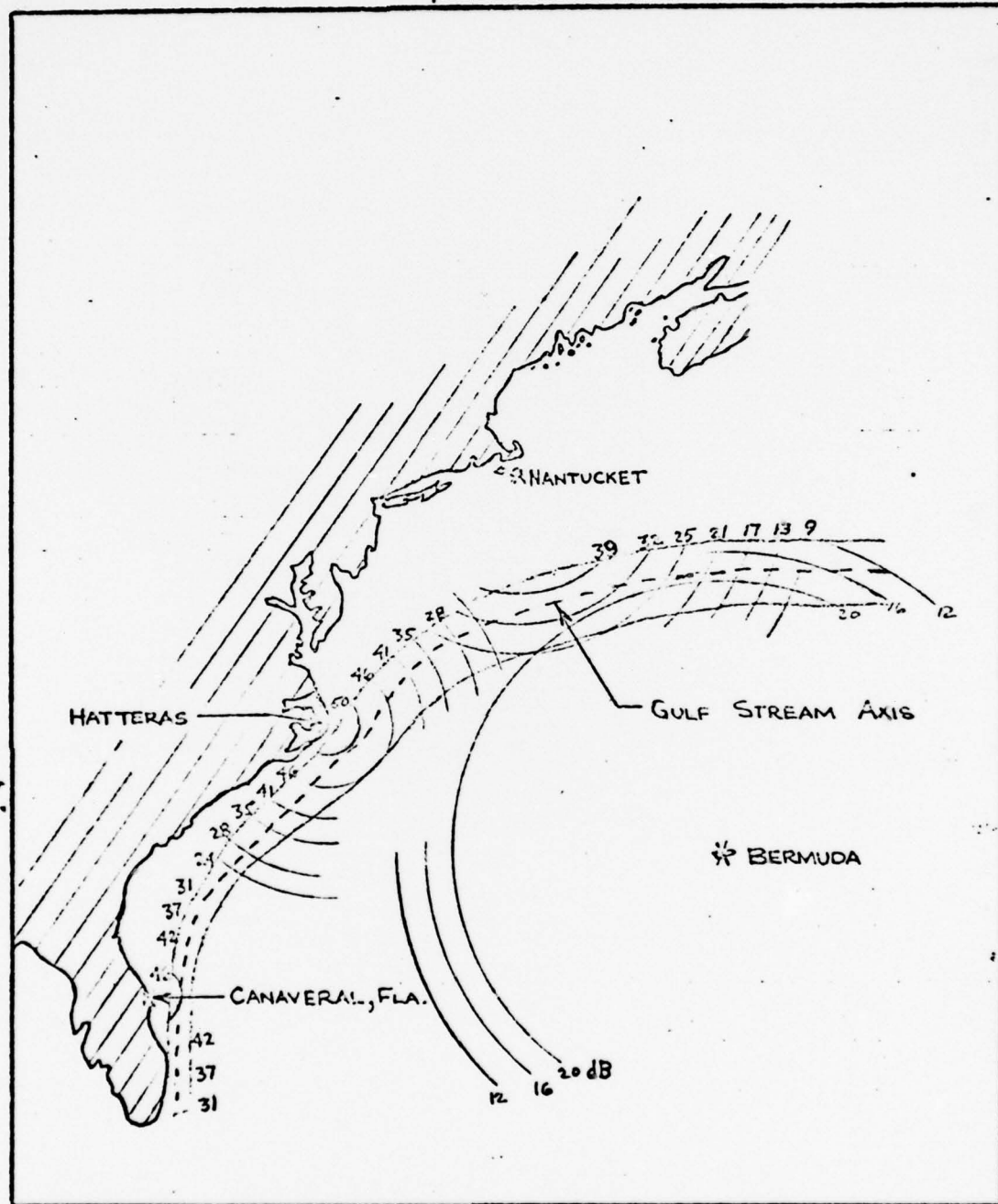


Figure 16 - Expected Signal-to-Noise Ratios (dB)
for 4.1 mHz Propagation from a
Gulf Stream Drifting Buoy

HF Receiver Stations

The receiving stations indicated in Figure 16 are assumed to exist at Canaveral, Florida; Cape Hatteras, Nantucket, Mass., and Bermuda. It has tentatively been assumed that Navy or Coast Guard bases could be employed on a non-interference basis for data acquisition. In such cases all that would be required would be to build low cost automatic data acquisition systems that turn on every 12-hours. The basic HF signal could be reinserted with the telemetered SSB suppressed carrier signal and the FSK tone put on a relatively inexpensive tape recorder along with time. The tapes could then be converted to a computer-compatible format at the laboratory where all tapes are assembled.

Because a base station receiver should be able to derive useful data from as low as a 10 db signal, or lower, it appears from Figure 16 that the full area of the Gulf Stream shown can still be tracked with the Florida, Hatteras, and Bermuda stations. If only the Hatteras and Bermuda stations are maintained the HF signal may be quite weak in the region of the Florida Straits, but afterwards very reasonable. It is not expected, however, that the type of higher frequency trajectory variability, previously found in a western boundary current such as the Gulf Stream, would exhibit itself in the confined region of the straits. Therefore, it is reasonable to initially recommend a two base station network with stations at Cape Hatteras (possibly at Diamond Light shoals tower ~20 miles offshore) and at Bermuda (possibly Tudor Hill).

The cost of building the type of base station data acquisition system described would be relatively modest (~\$1000.- replication cost) as long as a receiver and a reasonable receiving antenna are available. If such is not the case, costs per station would increase by approximately \$4000-\$12,000.- (component costs) for a receiver and antenna. Appendix B describes a few pieces of HF equipment that enable ball park system cost estimates.

Buoy Identification Coding

In order to recognize which buoy is reporting from a batch of several buoys deployed, each buoy must employ one of ten different 300 Hz bands within the 3500 Hz total bandwidth of the 4.1625 to 4.1666 mHz assigned oceanographic band (see Livingston et al, 1977). The World Administrative Radio Conference (WARC) has assigned this bandwidth which allows a 250 Hz buffer band on each

end of the total band. Therefore, a maximum of ten uniquely identifiable buoys working this band can be in the water at one time. If additional buoys are required, the 6.2445 mHz band or higher must be used and depend almost strictly on skywave propagation.

If the Teledyne 701 LORAN-C receiver with memory and FSK options is used, a standard telemetry feature would allow for 8 identifications bits such that each HF transmitter could work at the same frequency if desired.

General Comments

It should be reemphasized that the HF system suggested is somewhat costly in terms of development funds because of the memory required. In order to increase overall system reliability per transmission with a single-frequency transmission format, the candidate HF system has been programmed to transmit at noon (using groundwave) and midnight (using skywave) only. With such a timeline, calculations indicate that at least one of the transmissions will be reliable over the Gulf Stream range of interest. An alternative approach could be assumed in which periodic LORAN-C TD's were immediately radioed to shore - requiring less complicated memory and timing on the buoy. This approach would possibly require the transmittal of each of the 5 words shown in Table 4 (i.e., 52 bits) every hour at a rate of 100 bits/sec. If the words were simply assumed to be transmitted once per hour (for example) the transmit format would be as follows:

HF Hourly Transmit Format (No Memory)

(1) Warm-up	5.0 sec
(2) Carrier Enable + bit sync	7.5 sec
(3) 52 bits/100 bits/sec	<u>.5 sec</u>
	13.0 sec

If done hourly at a 200-watt level for 30 days the above transmit format would lead to the following prohibitive energy consumption:

$$E_{HF} \text{ (hourly transmit)} = 1560 \text{ watt-hours}$$

Even if the 5-second transmitter warm-up period were somehow eliminated the energy consumed would still be approximately 960 watt-hours. Therefore, the data format described in Table 4 appears to be the most energy, and by all estimates, the most cost-effective way to go.

Availability of Equipment

Transmitter costs will be much lower for a high frequency system than for a satellite system. A large number of mobile transmitters and amplifiers have been developed for amateur radio use. These systems are reliable, require a 12 vdc power supply, and cost less than \$400. (see Appendix B). Contact has been made with TPL Communications (see sheet in Appendix B), who produce suitable power amplifier equipment for about \$250. The amplifier would accept a low power HF signal from the modulated output of an oscillator. The total parts costs for an HF buoy transmitter system (exclusive of timing, memory, and antenna shown also in Figure 7) are approximately the following:

Transmitter (i.e., oscillator & modulator):	\$400.-
Power Supply	\$ 75.-
Power Amplifier	\$250.-
<hr/>	
Total Estimated Cost:	\$725.-

This total cost can be compared against a \$1500. cost for a satellite BTT, but more dollars in development and system integration costs are associated with the buoy HF transmitter and base station receiver. Because there will likely be costs associated with either a daily usage charge for the TIROS-N satellite BTT (i.e., ~ \$20/buoy day) or the purchase of a dedicated TIROS-N ground station receiver, the costs of building HF transmitters and operating two receiving stations are not overly burdensome by comparison.

Buoy Antenna

The most practical antenna for use on the buoy is the whip. Such an antenna would be typically a 2-3 meter in length with induction loading at the base. The inductive loading is necessary to make the 8 ft whip resonate at 4.1 mHz. For a 4.1 mHz transmission frequency, a vertical antenna would have to be 20-meter high if no loading coil was used.

In this application, it is necessary to use an antenna with gain that is as high as possible. Equally important, the antenna must not lose efficiency when subjected to buoy bobbing and rolling motions.

For an inductively-loaded whip, high efficiency while vertical results in poor efficiency when the antenna is inclined to vertical. Decreased efficiency when tilted occurs because the angle change with respect to the conducting plane of sea water results in a change in the resonant frequency of the antenna. Unfortunately, as the efficiency of the antenna is increased, the bandwidth decreases. Therefore, the change in resonant frequency which occurs when the antenna is tilted degrades the performance of a high efficiency antenna more than an antenna with lower efficiency.

A theoretical relationship can be developed by which it can be shown how an antenna gain varies as a function of Q for various buoy tilt angles. If an antenna, with $Q = 50$, were placed on a buoy such as the Scripps/McNally damped spar (see McNally, 1976) the loss of antenna gain due to buoy motion is expected to be less than 3 db in a sea state 5. Such would be true because the maximum tilt angle is expected to be below 20 degrees. Therefore, by selecting a 2.5-meter whip antenna, tuned to a Q of 50, the total effects due to buoy motion and antenna bending are expected to degrade its efficiency by less than 3 db. Such an antenna has a gain of -15 db when upright. For purposes of analysis a buoy antenna gain of -15 db was assumed.

4.2.3 Skywave-Groundwave Interaction

Often, signals may be received via more than one mode. As the radio wave travels different distances by different modes, the two signals will be received at slightly different times. If this delay approaches the time duration of a single bit, destructive interference may result. As a worst case, interaction between a groundwave signal and the same signal propagated by a double hop off of the F_2 -layer will be considered. If the signal originates at the edge of the groundwave range (~ 800 km), assuming an F_2 -layer height of 300 km, the time delay would be 2.1 milliseconds. If data is transmitted at 100 bits per second, or 1 bit every 10 milliseconds, the skywave would arrive late by 21% of a bit cycle period. This appears to represent no serious problem. If the FSK bit rate were increased the problem would become more acute.

5.0 SUMMARY AND RECOMMENDED SYSTEM CONFIGURATION

Table 5 presents a summary cost estimate of five possible drifting buoy system combinations which should meet the requirements of tracking the higher frequency meanders of a western boundary current.

Position Determination

The study has shown that at present the only viable means of acquiring buoy position data at the desired frequency and accuracy is with an automatic LORAN-C receiver. It has been tentatively judged that the Micrologic ML-200 receiver, although possibly not of the sophistication and reliability of the Northstar 6000 (from Digital Marine Electronics, Inc), is adequate for the job. It lowers price with an associated penalty of a few dollars worth of extra batteries seems like a reasonable choice. This is the baseline LORAN-C receiver chosen. For comparison, Table 5 indicates the use of the Northstar 6000 (config. 3). It is recommended that the system schematically shown in Figure 7 be implemented as the general design. The choice of a specific LORAN-C receiver would have to be made with all of the most recent test and evaluation data at that time. This is true because of the more recent construction and lack of test data on models such as the Northstar 6000 and the Internav IC-123. If the choice were to be made with the data presented herein it would be a difficult decision between the Micrologic ML-200, because of its low price, and the Teledyne 701, because of its widespread use and tests by the Coast Guard (Cassis and Adams, 1977) plus the low cost options which include a random access memory (RAM) and FSK output, which have already been implemented for the Department of Transportation, Automatic Vehicle Monitoring program in Philadelphia (Chambers and Stapleton, 1974). It is felt that the choice at a given point in time would depend on a very close scrutiny of available test data combined, possibly, with a few specific tests directly pertinent to performance on the buoy with a TIROS-N or HF transmitter alongside.

On-Board Sensors

The other main cost variations in Table 5 are whether or not a barometric pressure sensor is to be used on the buoy and how the data are telemetered. Configuration 1 assumes the use of the Bunker-Ramo sensor being

System Configuration	On-Board Sensors	Sensor & Electronics Costs	Battery Pack (30 day mission)	Buoy & Drogue Costs	System Ass'y Costs	Total System Costs (After Engineering)
① LORAN-C/ TIROS-N (ML-200 rcvr)	T _{water} p _{baro} drogue ind.	\$4590.	\$100.	\$1100.	\$700.	\$6490.-
② LORAN-C/ TIROS-N (ML-200 rcvr)	T _{water} drogue ind.	\$4090.	\$100.	\$1100.	\$700.	\$5990.-
③ LORAN-C/ TIROS-N (Northstar 6000 rcvr)	T _{water} drogue ind.	\$5290.	\$70.	\$1100.	\$700.	\$7160.-
④ LORAN-C/GOES (ML-200 rcvr)	T _{water} drogue indi.	\$5790.	\$100.	\$1100.	\$700.	\$7690.-
⑤ LORAN-C/1F (Teledyne 701 W. FSK option)	T _{water} drogue ind.	\$4115.	\$90.	\$1100.	\$700.	\$6005.-

Table 5 - Drifting Buoy Positioning and Data Acquisition System Cost Summary

employed by the National Center for Atmospheric Research (NCAR) at cost of approximately \$500 each. It is recommended that, in order to hold down costs, the LORAN-C/TIROS-N system eliminate the barometric pressure sensor and use configuration 2. Because of their relatively low cost (~\$100 each), it is assumed that both a water temperature sensor and drogue indicator be included on the buoy.

Data and Position Telemetry

The most cost-effective, reliable manner by which to telemeter the data to shore appears to be with TIROS-N satellite transmitter. If a user cost of \$20 per buoy per day is imposed, (at 6 buoys installed every 3 months for a 30-day lifetime each = 720 buoy-days per year) an additional cost of \$14,400 per year is expected. This represents an additional \$28,800 system cost for a 2-year monitoring program. If, on the other hand, an automatic TIROS-N ground station readout system were purchased at a cost of approximately \$20,000, more system flexibility would be achieved. Such a system would require programming for data readout, but the system costs could potentially be shared by other experimenters and used on other programs. This approach is recommended.

Configurations 4 and 5 assumed data telemetry by GOES and by HF respectively. The GOES system is deemed too costly at present. The LORAN-C/HF system suggests the use of the Teledyne 701 receiver because of the memory and FSK output which has already been used by the Department of Transportation. This combination can be purchased for approximately \$3,000. The base stations, on shore, if not already available from the Coast Guard or Navy, could be set up by erecting a reasonable antenna (~\$2,000); purchasing a good HF receiver (<\$5,000), a Teledyne FSK single sideband demodulator (~\$5,000), and a recording system (~\$1,000). A minimum of two such stations would need to be built at a total estimated shore-side component cost of \$26,000. Such a system is also competitive on buoy system costs and allows for constant buoy position determination and possible retrieval if desired. On the whole, such a system would be more cumbersome to operate and less reliable than the LORAN-C/TIROS-N system. A summary of the overall system costs for the major competing system choices is shown in Table 6. It includes not only the purchase of capital equipment which is non-expendable but also rough engineering design and service cost estimates. The overall

System Configuration	Estimated System Design &/or Data Readout Costs	Equipment Purchase Costs	User Service Fees	Cost for 48 Buoys	Total 2-Year Program Costs
<u>Recommended System</u>		*			
LORAN-C/TIROS-N (ML-200 receiver, no P _{baro} sensor, and stat. readout)	\$40K	\$20K	0	\$287.5K	\$347.5K
LORAN-C/TIROS-N (ML-200 receiver, no P _{baro} sensor, with user fee)	\$20K	0	\$28.8K	\$287.5K	\$336.3K
LORAN-C/GOES (ML-200 receiver, no P _{baro} sensor)	\$15K	0	0	\$369.1	\$384.1K
LORAN-C/HF (Teledyne 701, memory, FSK option)	+	+	+	\$288.24	\$354.2K

*Exclude such costs as test set for satellite transmitter.

+Assume that HF receiving antenna must be installed and receiver purchased.

Table 6 - Comparative Engineering Data and Hardware Cost Summary for 2-Year Program to Monitor a Western Boundary Current

summary is based on the deployment of 6 buoys per quarter for 2 years. This Table does not include overall system engineering costs, nor does it include the cost of the fabrication and test of an engineering prototype, all of which should be approximately the same for all choices. Table 6 summarizes only a best guess at the incremental costs for given choices on quantity replication.

Buoy and Drogue Selection

The buoy should be designed such that the antenna systems remain relatively upright (i.e., $< \pm 20^\circ$) under all but the most severe conditions. This is not to eliminate the potential use of a two-part or distributed buoyancy package, both of which might result in better drogue performance and survivability. The use of the Scripps-McNally spar may be a good cost-effective buoy for this program. This specific choice should be made at the time of the design. By that time more accurate and even verified math models of drogue slippage and loads may be available to help in the choice.

The choice of a drogue for the study outlined will depend very much on the state on knowledge of drogue performance at the time. If no more is known about drogues than than is known now, it is tentatively recommended that bi-planar crossed vane be employed for droguing at 30 to 50-meter depths.

Future Considerations

The system schematically shown in Figure 17 could potentially be made more flexible through the use of modularity. Figure 17 is a general block diagram of a modular drifting buoy positioning system that incorporates many of the types of positioning and data telemetry systems described herein. It can be made to function anywhere in the world in an expendable or non-expendable mode to varying degrees of accuracy by interchanging components. For example, Figure 17 encompasses the expendable system for the measurement of higher frequency changes in western boundary currents. By changing to an OMEGA receiver and an HF transmitter an experimenter is capable of monitoring large scale trajectory data anywhere in the world in a non-expendable mode as long as a radio receiver can be installed within approximately 1000-1500 km of the experiment sight.

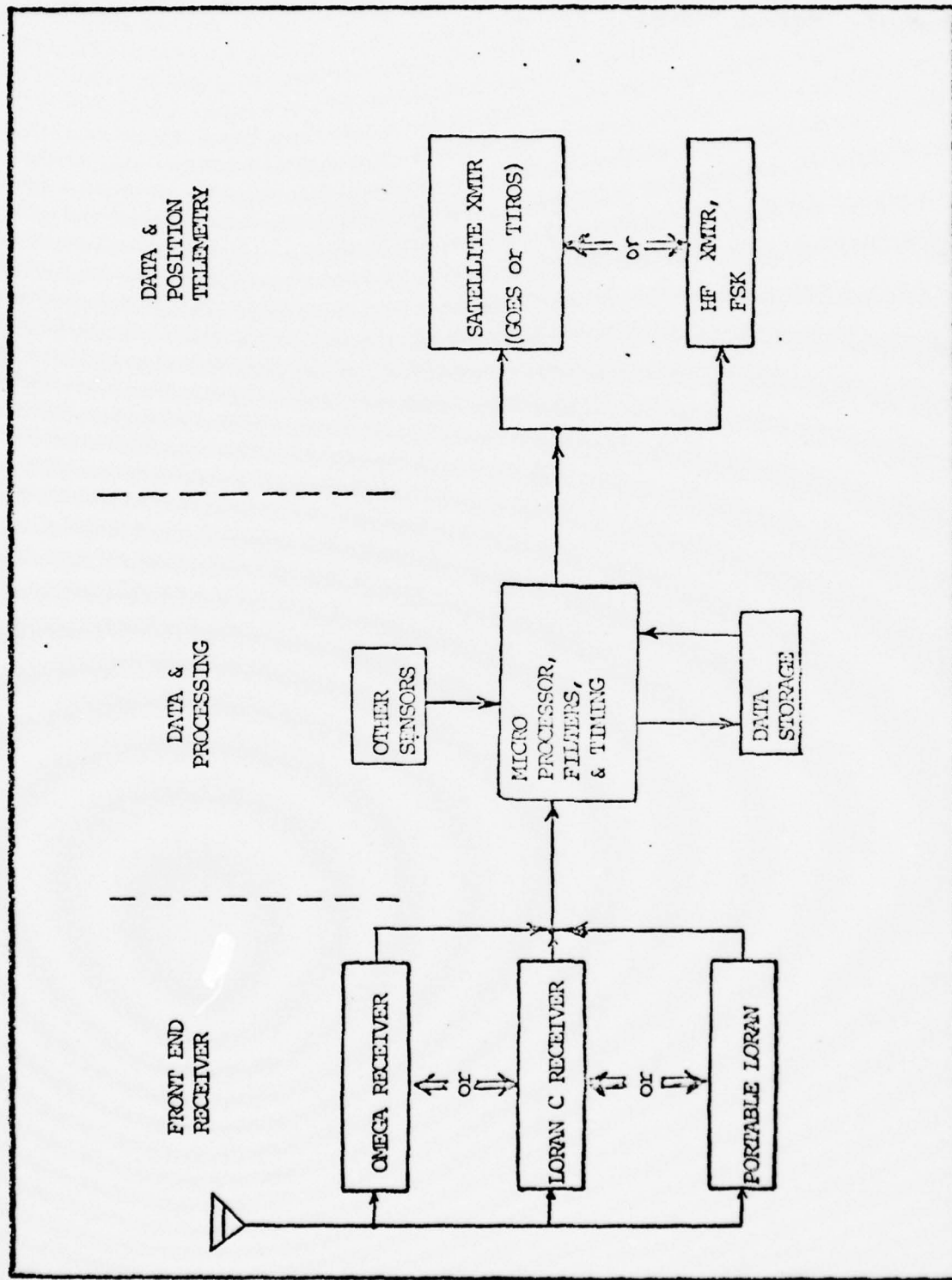


Figure 17 - Modular Concept of a Drifting Buoy Positioning System

6.0 ESTIMATED BOUNDS ON DROGUED BUOY SLIPPAGE ERRORS

This section will examine some of the current basic studies of the slippage of drogued drifters in the ocean. In addition, current research will be reviewed which permits the estimation of the wind and water drift forces on a buoy - the sum of which gives rise to the error-inducing slippage forces on a buoy. The wind force as a percent of the total error force will vary with sea state, buoy design, wind velocity, surface current velocity, shear, drogue depth, drogue size, and drogue effectiveness. With so many parameters, the problem is very complex. Only restrictive assumptions and bounds can be put on the problem to make it somewhat manageable.

It will be assumed for analysis purposes that there is no current at the drogue depth and that the drogue is shallow enough ($\sim 30-50$ m. depth) and tethered with a small enough line such that tether line horizontal drag forces can be neglected. It will be assumed for simplicity that the wind velocity can be readily determined by a single measurement at any height and related to that at the buoy by the Prandtl-von Karman universal velocity distribution. The presence of the air-water interface and waves are assumed to produce no disturbance to the wind field around the buoy such that the buoy-wind drag coefficients are those of standard cylinders for which much data is available in Hoerner (1965). The lateral dimensions of the buoy are further assumed to be those of round cylinders of diameter much less than a wavelength (i.e., $D \ll \lambda$). The NDBO Nova minibuoy design will be chosen for analysis. The assumed baseline will be the window shade supplied by NDBO which measures approximately 2.25 m. \times 9.83 m. with an area of 22 m² and a drag coefficient of 2.0.

6.1 Buoy Wind Drag Forces

It has been found by Vachon (1975) and Saunders (1976) that the predominant error force in most drifting buoy applications is that of wind. It is reasonable to assume that the rigid above-water portions of buoys do not oscillate in a wind field in the manner of a mooring line. Therefore it is felt that the standard round cylinder, open flow drag coefficient of approximately 1.1 to 1.2 applies fairly well at subcritical Reynolds numbers (cylindrical mooring lines may strum leading to much higher effective drag coefficients).

If the ratio of buoy height-to-diameter is of the order of 5 or less it appears that the cylinder drag coefficient may be as low as .73 at sub-critical Reynolds numbers (Hoerner, 1965, p. 4-3). In spite of these data, values of C_D = 1.0 and 1.1 have been used by Vachon (1975) and C_D = 1.1 by Saunders (1976) for portions of the Nova buoy subject to wind forces. These assumptions will be used in developing a maximum estimate of slippage. The analysis by Vachon (1975) found that either the values used for wind drag were too low or the value of the drogue drag coefficient was too high. The latter was generally concluded.

CASE I - Wind Force Only - No Shear

If an experimenter were to estimate drifter trajectory deviations caused only by wind influences on the non-wetted portion of a buoy, an intermediate bound can be placed on the errors. This case might well be the only type of correction that could be made based on available wind field data and a lack of knowledge of the surface current, wave influence, and drogue condition or behavior. For estimation purposes the Nova minibuoy outlined in Figure 18 will be assumed with the estimated cross-sectional areas and drag areas shown. Figure 18 also indicates the Scripps-McNally spar with estimated cross-sectional areas and drag areas given for comparison. These buoys will experience the estimated wind forces given in Table 7.

With no shear assumed between the surface and drogue depth it is possible to sum the drag areas of the wetted portion of the buoy and the drogue (i.e., $(C_D A)_{TOT} = 44.74 \text{ m}^2$). Both wetted elements of the system then act as a drogue,

TABLE 7

Estimated Wind Forces on Drifting Buoys

<u>Wind Vel.</u>		<u>Nova Forces</u>		<u>Scripps/McNally Spar</u>	
<u>knots</u>	<u>m/s</u>	<u>(Newtons)</u>	<u>lbs</u>	<u>(Newtons)</u>	<u>lbs</u>
10	5.1	7.4	1.7	5.5	1.2
20	10.3	30.2	6.8	22.3	5.0
30	15.4	67.6	12.9	49.8	11.2

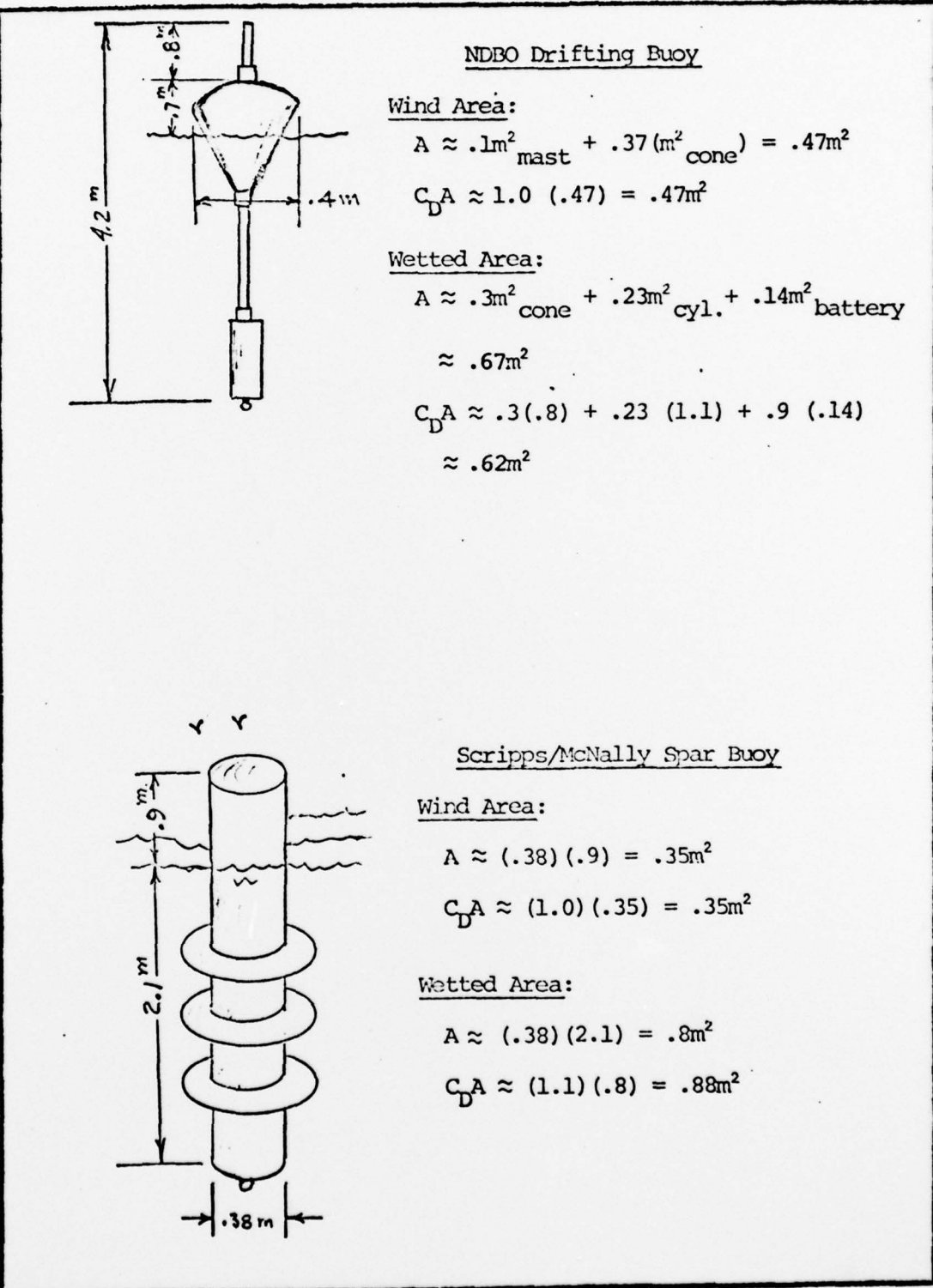


Figure 18 - Estimated Cross-Sectional and Drag Areas of Drifting Buoys

restricting the error-inducing wind force. The resultant estimated system slip is shown in Table 8 for the Nova minibuoy only. The slip of the Scripps buoy can be calculated by using values shown in Table 7.

TABLE 8

<u>Estimated Nova Buoy Slip with No Shear Present, (C_D)_{drogue} = 2.0</u>		
<u>Wind Vel.</u>	<u>Slip</u>	<u>Max. Trajectory Error/hr</u>
(knots)	(m/s)	(m)
10	.018	±65
20	.036	±130
30	.054	±195

If the drogue is working ineffectively because it is either not weathervaning properly, in the case of a window shade drogue, or is hanging downward or torn, in the case of a parachute, then its drag coefficient averaged over time may drop to approximately 0.5. This condition would lead to the slippage values shown in Table 9. It should be noted that the drag coefficient assumed has a basis in measured data. In Vachon (1973), the drag coefficient of a porous fishing net was evaluated to be approximately .2 to .3 by towing it parallel to the flow direction. It is assumed that the window shade would weathervane properly some of the time - raising the average as indicated. In addition, a parachute can still function, but at a lower level of effectiveness, even though hanging downward or torn.

TABLE 9

<u>Estimated Nova Buoy Slip with No Shear, (C_D)_{drogue} = .5</u>		
<u>Wind Vel.</u>	<u>Slip</u>	<u>Max. Trajectory Error/hr</u>
(knots)	(m/s)	(m)
10	.036	±129
20	.072	±261
30	.108	±390

It can be seen by comparing Tables 7 and 8 that the drogue could function ineffectively in moderate winds and the drifter trajectory errors will only begin to exceed the desired accuracy of the LORAN-C positioning system with 30-knot winds. Even with an effective drogue the trajectory errors can become large with over 30-knot winds.

6.2 Drag on Wetted Portions of a Buoy

The forces on the wetted portion of the buoys described, although generally estimated to be of smaller order than the wind forces, are felt to be much higher than simple calculations indicate (Vachon, 1975 and Saunders, 1976).

CASE II - Wind Driven Surface Layer

Wu (1975) has considerable data to support a claim that for the case of no major current regimes, such as the Gulf Stream, the steady wind-induced surface current will equal 3.5 percent of the wind velocity independent of fetch, at fetches greater than approximately 100 km. For shorter fetches the ratio will increase to approximately 4% at wind velocities of 20 m/s. Wave-induced Stokes drift current was estimated to constitute approximately one-seventh of this (i.e., .5%). For the analysis herein, it will be assumed that this current decays as e^{-kz} ($k = 2\pi/\lambda$) such that the current forces on the buoy can be estimated. For the purposes of analysis the Nova minibuoy will be divided into three wetted parts as described in Table 10. As the wind velocity is varied the wavelength of the seas is assumed to vary in accordance with the

TABLE 10
Nova Minibuoy Estimated Wetted Drag Characteristics

Buoy Section	Cross-Sectional Area, A (m^2)	Z_i = Depth (m)	C_D	$C_D A$ (m^2)	$K_i = \frac{1}{2} \rho (C_D A)$ ($Kg \cdot m^{-1}$)
(1) Cone	.3	.38	.8	.24	123.2
(2) Narrow Cyl.	.23	1.37	1.1	.25	128.4
(3) Battery	.14	2.44	.9	.13	66.7
Totals				.62	318.3

Pierson-Moskowitz spectrum. For the three wind velocities previously examined, Table 11 presents a summary calculation of the wind-driven current forces

TABLE 11
Current Forces on Nova Buoy

Buoy Section	Wind Velocity (knots) (m/s)	Surf. Curr., V_s (m/s)	λ (m)	$V(z) = V_s e^{-kz_i}$ (m/s)	$K_i V^2 (z)$ (Newtons)
(1)	10	5.1	.179	.17	3.4
(2)	10	5.1	.179	.14	2.5
(3)	10	5.1	.179	.12	2.5
(1)	20	10.3	.361	.35	15.1
(2)	20	10.3	.361	.33	14.0
(3)	20	10.3	.361	.31	6.4
(1)	30	15.4	.539	.53	34.6
(2)	30	15.4	.539	.52	34.7
(3)	30	15.4	.539	.51	17.5

Summation of Current Drag Forces (N)

10 - knot wind: = 6.8

20 - knot wind: = 35.5

30 - knot wind: = 86.8

on the buoy. The sum of these forces over the three buoy sections is listed at the bottom of Table 11. In the most extreme case, these forces are assumed to always act colinear and sum with the wind forces given in Table 7. Table 12 presents the new buoy force sum as well as the expected slip and trajectory deviation for a drogue with drag coefficients of 2.0 and .5. It is apparent in this analysis that, if no trajectory corrections are made based on wind data, the hourly trajectory error will be of the same order as the LORAN-C position error in the presence of up to 20 knot winds. Above this value, wind field data must be acquired and corrections made in order to hold down the errors. If the drogue is assumed to be working properly (i.e., $C_D \approx 2.0$), but in reality

TABLE 12

Maximum Buoy Forces and Drogue Slippage for Sum
of Wind and Wind-Induced Current Forces

Wind Velocity (knots)	Force Sum (Newtons)	Drogue Slip ($C_D = 2.0$) (m/s)	Trajectory Error/hr (m)	Drogue Slip ($C_D = .5$) (m/s)	Trajectory Error/hr (m)
10	5.1	14.2	.024	± 90	± 179
20	10.3	65.7	.053	± 193	± 385
30	15.4	154.4	.082	± 295	± 590

it is not (i.e., $C_D \approx .5$), the error in the trajectory correction itself will vary from 89 m. (at 10 knots) to 295 m. (at 30 knots). For this analysis, the error in drogue drag coefficient gives rise to trajectory correction errors equal to the first order trajectory correction itself if the drogue was working properly.

The works of Keulegan and Carpenter (1958) and Sarpkaya (1976) were employed in order to analyze how the estimates of wetted drag coefficients might vary in wave-induced oscillatory flow compared to those values in Table 10 derived under steady flow conditions. This analysis lead to approximately a 10% increase in $C_D A$ because the C_D in the cylinder area was raised to 1.35 while the others were unchanged. The additional trajectory correction required is minimal. If, however, one is beginning to estimate the various C_D 's for wetted portions of a buoy these analyses should be employed rather than values derived under steady flow conditions.

The work of Saunders (1977) could also be employed in the case of oscillatory flow in order to get an estimate of wetted forces. His work applies to forces in the presence of non-zero currents for which $|aw| \gg |\bar{U}|$ (a = wave amplitude, w = frequency, $|\bar{U}|$ = average surf. current). His main conclusion is that for many applications the average drag on a wetted body in oscillatory flow may be written with sufficient accuracy by the expression:

$$\bar{F} = (\frac{1}{2} \rho C_D A) aw \bar{U} \quad (6)$$

He is mainly addressing the problem of averaging a velocity relative to the buoy which is composed of a steady and an oscillatory flow component as follows:

$$\vec{v}_{\text{rel}} |\vec{v}_{\text{rel}}| = [\vec{U} + a w \cos(kx - wt)] |\vec{U} + a w \cos(kx - wt)| \quad (7)$$

This relation can be simply averaged by integration as long as $|\vec{U}| > |aw|$. When such is not the case it must be done numerically or use equation (3) as an approximation. The value of C_D employed in (6) should come from the work of Keulegan and Carpenter (1958) and Sarpkaya (1976). The data presented in Tables 11 and 12 were not redone using equation (6) because the general results of this chapter would change little.

6.3 Comparison with Measured Slippage Data

Two instrumented slippage experiments have been conducted on drifting buoys in recent years. Both Vachon (1975) and Saunders (1976) have indicated an inability to get closure on a force balance on a drifting buoy unless either the drogue is of a drastically lower drag coefficient than derived under steady flow tests or wave forces are greater. In Vachon (1975) there are indications that a window shade drogue may not weathervane properly which supports the former contention. Furthermore, James McCullough at Woods Hole (personal contact) has demonstrated a strong correlation between measured slip and wind velocity. In both experiments insufficient ground truth data were available by which to ascertain true current at the drogue depth or true shear forces on the buoys. As a result there is at present no firm slippage data which is fully correlatable to the forcing on the buoy.

6.4 Drogue Performance

Because of present questions regarding the performance of both parachutes and window shade drogues, it seems reasonable to mount a bi-planar crossed vane drogue to a buoy for the study of western boundary currents. This drogue, with a scale model drag coefficient of $C_D \approx 1.18$ (Vachon, 1973) should behave in a more predictable fashion allowing adequate trajectory corrections from wind field data. As more positive performance data are derived on the other drogues - they should be used where feasible.

REFERENCES-1

- 1) Beukers, J. M., 1973, "Accuracy Limitations of the OMEGA Navigation System Employed in the Differential Mode", Navigation, Vol. 20, No. 1, pp. 81-92.
- 2) Cassis, R. H. Jr. and R. J. Adams, 1977, "An Operational Test and Evaluation of an Airborne LORAN-C Navigator System", Proc. Offshore Technology Conference 1977, Paper No. OTC 2816.
- 3) Chambers, F. J., and R. S. Stapleton, 1974, "A Comparison of Automatic Vehicle Tracking Systems", Jour. of Institute of Navigation, Vol. 21, No. 3, pp. 208-222.
- 4) Fried, W. R., 1977, "A Comparative Performance Analysis of Modern Ground-Based, Air-Based, and Satellite-Based Radio Navigation Systems", Jour. of Institute of Navigation, Vol. 24, No. 1, pp. 48-58.
- 5) Hoerner, S. F., 1965, "Fluid-Dynamic Drag, Theoretical, Experimental, and Statistical Information", published by the Author, Midland Park, N. J.
- 6) Intergovernmental Oceanographic Commission (IOC), 1967, "Radio Communication Requirements for Oceanography", UNESCO Publication, Paris, France.
- 7) International Telephone and Telegraph Co., 1975, Reference Data for Radio Engineers, Howard W. Sams & Co., Indianapolis, Ind.
- 8) Jenkins, C. F., E. J. Aubert, W. R. Brian Caruth, L. H. Clem, and R. G. Walden, 1967, "A Cost Effectiveness Evaluation of Buoy and Non-Buoy Systems to Meet the National Requirements for Marine Data", Travelers Research Center, Inc. Report No. 7484-274 to U. S. Coast Guard.
- 9) Keulegan, G. H. and L. H. Carpenter, 1958, "Forces on Cylinders and Plates in an Oscillating Fluid", Jour. of Research of the National Bureau of Standards, Research Paper No. 2857, Vol. 60, No. 5.
- 10) Kirwan, A. D. and G. McNally, 1975, "A Note on Observations of Long-Term Trajectories of the North Pacific Current", J. Phys. Oceanog., Vol. 5, No. 1, pp. 188-191.

REFERENCES-2

- 11) Livingston, T. L., G. Haas, and R. Mueller, 1977, "Data Buoy Communications Experiences: HF vs UHF", 1977 Radio Technical Commission for Marine Services (RTCM) Assembly Meeting, Valley Forge, Pennsylvania.
- 12) Micrologic Inc., 1975, "Micrologic ML-200 LORAN-C Receiver Operator's Manual."
- 13) Picquenard, A., 1974, Radio Wave Propagation, John Wiley & Sons, New York
- 14) Pierce, J. A., 1972, "Lane Identification in OMEGA", AD 746 503, Harvard University.
- 15) Richardson, P. L., R. E. Cheney, and L. A. Mantini, 1977, "Tracking a Gulf Stream Ring with a Free Drifting Surface Buoy", J. Phys. of Oceanog. (in press).
- 16) Robinson, A. R., J. R. Luyten, and F. C. Fuglister, 1974, "Transient Gulf Stream Meandering, Part I: An Observational Experiment", J. Phys. Oceanog., Vol. 4, No. 2, pp. 237-255.
- 17) Roland, W. F., and Board of Directors of the Wild Goose Assoc., 1973, "LORAN-C - A Decade of Maturity", Proc. of National Radio Navigation Symposium, pp. 125-130.
- 18) Research Triangle Institute, 1973, "Investigation into the Propagation of OMEGA Very Low Frequency Signals and Techniques for Improvement of Navigation Accuracy Including Differential and Composite OMEGA", Final Report to N.A.S.A. under Contract No. NAS1-11298.
- 19) Sarpkaya, T., 1976, "In-Line and Transverse Forces on Cylinders in Oscillatory Flow at High Reynolds Numbers", Proc. of Offshore Technology Conference 1976, Paper No. OTC 2533, pp. 95-108.
20. Saunders, P. M., 1976, "Drifting Buoy Lagrangian Test", Final Report of Woods Hole Contract NAS 13-5 with NOAA Data Buoy Office.

REFERENCES-3

- 21) Saunders, P. M., 1977, "Average Drag in Oscillatory Flow", Deep-Sea Research, Vol. 24, pp. 381-384.
- 22) Swanson, E. R. and M. L. Tibbals, 1965, "The OMEGA Navigation System", Navigation, Vol. 12, No. 1, pp. 24-35.
- 23) Vachon, W., 1975, "Instrumented Full Scale Tests of a Drifting Buoy and Drogue", C. S. Draper Laboratory Report No. R-947.
- 24) Vachon, W., 1973, "Scale Model Tests of DRogues for Free Drifting Buoys", C. S. Draper Laboratory Report R-769.
- 25) Westerfield, E. E., 1972, "Determination of Position of a Drifting Buoy by Means of the Navy Navigation Satellite System", Proc. of Ocean '72, pp. 443-446.
- 26) Whelan, W. T., H. G. Tornatore, S. P. Murray, H. H. Roberts, and W. J. Wiseman, 1975, "An Over-the-Horizon Radio Direction-Finding System for Tracking Coastal and Shelf Currents", AGU Geophysical Research Letters, Vol. 2, No. 6, pp. 211-213.
- 27) Wu, J., 1975, "Sea Surface DRift Currents", Proc. of Offshore Technology Conference 1975, Paper No. OTC 2294, pp. 478-484.

APPENDIX A

TIROS-N Word Structure and Data Rate Description

For purposes of estimation it will be assumed that every 12 hours the satellite transmitter dumps the previous 12-hours of LORAN-C data. At these times it will be assumed that it transmits a 256-bit word stream for the parameters shown in Table A-1. In order to code the LORAN-C time-difference

Table A-1

TIROS-N Satellite Transmitter Data Word Structure

<u>Parameter</u>	<u>Bits/Word</u>	<u>Max. Words/XMSN</u>	<u>Total Bits</u>
LORAN-C, TD ₁	12	9 (i.e., 1 pt./80')	108
LORAN-C, TD ₂	12	9	108
Water Temperature	12	1	12
Barometric Pressure	12	1	12
Drogue Indicator	4	1	4
Total useful bits/12 hrs:			224

words (TD's) into a 12-bit format, the first two digits of the normal 6-digit array (i.e., 5-digits plus single decimal digit) must be dropped. In other words if the normal TD were to be 69,046.2 (microseconds), the first two digits could be easily dropped while still retaining position knowledge. This is possible as long as it is known which station pair is being tracked and there are no long periods during which the buoy position is not approximately known.

The 244-bits of data being transmitted every 12-hours to the TIROS-N satellite represents a pair of buoy TD's every 80 minutes. The standard TIROS-N format is expected to be 32, 8-bit words (i.e., 256 bits) with every transmission. The extra 12 bits capable of being added to the 244-bit format

in Table A-1 could represent a designation of LORAN Station pairs or another data word such as battery voltage or a LORAN-C signal monitoring function. Besides the 256-bits per transmission, the buoy satellite transmitter would send up additional bits for synchronization and platform identification. As with the NIMBUS-6 satellite, the TIROS-N buoy transmitters can be multiplexed such that the first 256-bits could represent one set of data and approximately one minute later the next 256 bits represents the remainder of the data. With such a feature, a full 24-hours of data can be theoretically stored in the suggested 1024 bit random access memory (RAM) and dumped every 12-hours - allowing a double redundancy in data transmission.

APPENDIX B

HF Transmission Equipment

There is a limited amount of HF transmission equipment available for the purposes described in this writing. The following are examples of ham-type equipment that might be employed for transmitting data from the buoy and commercial-type equipment that could be purchased for the receiving station.

Buoy HF Transmitter Equipment

- (1) TEN-TEC Triton IV transceiver
 - 200 watts input
 - freq. 3.5 to 29.7 MHz
 - SSB with 12 VDC drive @ \$699.
- (2) TPL Solid State Linear amplifier
 - 1 watt-in, 70 watts-out.
 - SSB @ ~ \$170.-
- (3) Heathkit Model HW-104 SSB 5 band transceiver (3.5 - 29 MHz) - \$490.-

Base Station Receiving Equipment

- (1) HF Receivers -
 - National Radio Corp. ~ \$5,000.
 - Collins Radio ~ \$8,000 - \$11,000.
 - Others ~ \$8,000 - \$12,000.
- (2) Demodulators:
Teledyne: \$5,000.

MANDATORY DISTRIBUTION LIST

FOR UNCLASSIFIED TECHNICAL REPORTS, REPRINTS, & FINAL REPORTS
PUBLISHED BY OCEANOGRAPHIC CONTRACTORS
OF THE OCEAN SCIENCE AND TECHNOLOGY DIVISION
OF THE OFFICE OF NAVAL RESEARCH
(REVISED JAN 1975)

1 Director of Defense Research and Engineering
Office of the Secretary of Defense
Washington, D. C. 20301
ATTN: Office, Assistant Director
(Research) 12** Defense Documentation Center
Cameron Station
Alexandria, Virginia
22314

NOTE: 1 Office of Naval Research
Arlington, Virginia 22217 Commander
3 ATTN: (Code 480)* Naval Oceanographic
1 ATTN: (Code 460) Office
1 ATTN: (Code 102-OS) Washington, D. C. 20390
6 ATTN: (Code 102IP) 1 ATTN: Code 1640
1 ATTN: Code 200 1 ATTN: Code 70
1 ONR ResRep (if any) 1 NODC/NOAA
Rockville, MD 20882

Director
Naval Research Laboratory
Washington, D. C. 20375
6 ATTN: Library, Code 2620

TOTAL REQUIRED - 35 copies

* Add one separate copy of
Form DD-1473

** Send with these 12 copies
two completed forms DDC-50,
one self addressed back to
contractor, the other ad-
dressed to ONR, Code 480